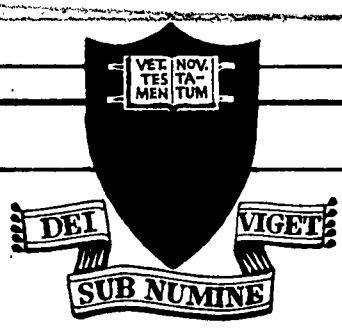

PRINCETON UNIVERSITY

DEPARTMENT OF AERONAUTICAL ENGINEERING

U.S. Army Transporation Research Command
Fort Eustis, Virginia

Project Number: 9-38-01-000,TK902
Contract Number: DA44-177-TC-524

AN ANALYTICAL STUDY OF THE LONGITUDINAL DYNAMICS OF A TILT-WING VTOL

by

Charles R. Hargraves

Department of Aeronautical Engineering
Princeton University

Report No. 561 June 1961

Approved by:

A. A. Nikolsky
Project Leader

FOREWORD

The research in this report was conducted by the Department of Aeronautical Engineering of Princeton University under the sponsorship of the United States Army Transportation Research Command, as Phase 1 of work under the ALART Program.

The work was performed under the supervision of Professor A. A. Nikolsky, Department of Aeronautical Engineering, Princeton University.

This work was administered for the United States Army by Mr. John Yeates.

ACKNOWLEDGEMENT

The author wishes to express his appreciation to Mr. H. C. Curtiss, Jr. and Mr. W. F. Putman for their helpful discussions and criticism of the material presented in this report.

TABLE OF CONTENTS

TABLE OF CONTENTS (contd)

LIST OF FIGURES

LIST OF FIGURES (cont)

NOTATION

Linear Dimensions & Areas

C	Chord of blade
C_w	Chord of wing
D	Diameter of rotor
e	Rotor blade flapping hinge offset
l_a, l_p, r	Distances defined in Figure 3
r	Radial distance along rotor blade
R	Rotor radius
S	Wing Area
x, y, z	Non-dimensionalized distances in $X-Y-Z$ directions (See list of subscripts below)
x_{cp}	Distance of center of pressure of wing behind rotor
X, Y, Z	Distances in $X-Y-Z$ directions (See list of subscripts below)

Angular Measurement

α	Rotor angle of attack
α'	Wing angle of attack
α_f	Fuselage angle of attack
β	Angle defined in Figure 8
ϵ	Angle of downwash due to wing
θ	Effective blade pitch at 0.75 R
θ_f	Aircraft pitch attitude
i_w	Wing incidence measured from fuselage reference line
ϕ	Angle between lift vector with and without slipstream (See Figure 1)
ψ	Blade azimuth position

FORCES AND MOMENTS

C_H	H-force coefficient
C_T	Thrust coefficient
CF	Centrifugal force per blade
δ	Blade sectional profile drag coefficient
F	Force (See list of subscripts below)
L	Lift (See list of subscripts below)
M	Moment (See list of subscripts below)
T	Thrust
μ_x	Non-dimensional velocity $\frac{V}{\Omega R}$

COEFFICIENTS AND CONSTANTS

a	Rotor blade lift curve slope
a_o	Wing lift curve slope without slipstream; Rotor constant flapping
a_1	Rotor longitudinal flapping
AR	Wing aspect ratio
A,B,C,D,E	Quartic coefficients (Equation 194)
b_1	Rotor lateral flapping
C	Non-dimensional coefficient (See list of subscripts below)
K	Aspect-ratio-dependent constant
$\overline{K}$	Constant defined by equation 116
λ	Inflow ratio defined by equation 11
λ_o	$\sqrt{C_T/2}$
λ_1	Constant defined on page 8

λ_s Inflow based on induced velocity in slipstream

μ Velocity ratio defined by equation 12

ς Defined by equation 4

σ Blade solidity factor $\equiv \frac{bc}{\pi R}$

γ Locke's Number $\equiv \frac{\rho a c}{I_1}$

VELOCITIES

u Body axis system longitudinal velocity

v Induced velocity

V Free stream velocity along flight path

V_R Resultant velocity at wing

w Body axis system vertical velocity

Ω Rotor rotational velocity

μ_x Velocity ratio $\frac{V}{\Omega R}$

MISCELLANEOUS PARAMETERS

b Number of blades

$\Delta t = l_T/V_T$

fn Symbol for "a function of"

I_y Moment of inertia of aircraft about Y-axis

m Aircraft mass

N Number of rotors

ρ Density of air

t_c Characteristic time (See Figure 19)

W Aircraft weight

I_1 Blade moment of inertia about flapping hinge

SUBSCRIPTS

a	Aerodynamic
D	Drag
F	Fuselage
g	Gravity
H	Hub
I	Inertia
L	Lift
o	Initial
R	Rotor
S	Slipstream, static
T	Tail
W	Wing

DERIVATIVE CONVENTIONS

1. $\frac{\partial}{\partial V}$ indicates the derivative with respect to V with α and C_T both held constant.
2. $\frac{\partial}{\partial V}\Big|_\alpha$ indicates the derivative with respect to V with only α held constant and C_T free to vary. This is related to derivatives of the first type by a relation of the form

$$\frac{\partial}{\partial V}\Big|_\alpha = \frac{\partial}{\partial V} + \frac{\partial}{\partial C_T}\frac{\partial C_T}{\partial V}\Big|_\alpha$$

3. $\frac{d}{dV}$ indicates the derivative with respect to V with both α and C_T free to vary, e.g.,

$$\frac{d}{dV} = \frac{\partial}{\partial V}\Big|_{\alpha} + \frac{\partial}{\partial \alpha}\Big|_{V} \frac{d\alpha}{dV}$$

In order to find $\frac{d\alpha}{dV}$ some flight condition must be specified. For instance, if it is specified that the force in the Z - direction be held constant, then

$$\frac{\partial C_Z}{\partial V}\Big|_{\alpha} dV + \frac{\partial C_Z}{\partial \alpha}\Big|_{V} d\alpha = 0$$

and

$$\frac{d\alpha}{dV} = - \frac{\frac{\partial C_Z}{\partial V}\Big|_{\alpha}}{\frac{\partial C_Z}{\partial \alpha}\Big|_{V}}$$

SUMMARY

An analysis of the stability characteristics of a tilt-wing VTOL aircraft is made. The stability derivatives associated with the wing-rotor combination are estimated on the basis of the assumption that for the purpose of stability analysis, the forces acting on the wing in the slipstream can be assumed to depend on the vector sum of the free-stream velocity and the induced velocity of the rotor. The wing derivatives are presented in the form of general charts which can be used for the evaluation of the derivatives for any wing-rotor combination. Numerical calculations are made for a typical tilt-wing VTOL (the Vertol 76) transition. From these calculations a curve is obtained showing the variation of the stability characteristics with wing tilt angle. On the basis of these numerical results and the general expressions for the derivatives, an extensive discussion is given concerning the effects of important physical parameters on values of the derivatives and of the effect of these derivatives on the stability characteristics of the aircraft.

INTRODUCTION

It is probably well to set forth at the offset the purpose of this investigation. It is not to analyze the stability of a tilt-wing VTOL aircraft but rather to study the factors which effect the stability characteristics. In order to obtain useful information of this type it is necessary to simplify the governing equations to such a point that the stability characteristics, e.g. the periods and damping ratios or time constants of the various modes of motion as a function of the tilt angle, can only be relied upon to give a rather qualitative picture of the aircrafts response to a disturbance. Certainly, at the present time, it is necessary to resort to experimental means if one wishes to obtain accurate information on the stability characteristics of a proposed design.

There are numerous reasons why the stability prediction problem is more difficult than the similar problem for low speed, conventional aircraft. Probably two of the most difficult problems, however, are due to the high velocity of the slipstream at low forward speeds and to the rotation of the wing during conversion. The effect of the former will be the main subject of the present report and only little will be said about the latter, albeit it could easily prove to be of equal importance.

The scope of this report is quite limited. Consideration will be given only to VTOL aircraft of the tilt-wing type with articulated rotors fixed rigidly to the wing. The results obtained should, however, give some insight into the characteristics of similar types of VTOL

such as the tilt-wing with conventional propellers or the fixed-wing, tilting-rotor aircraft. Also, only the longitudinal dynamics will be considered although the lateral dynamics present similar problems and are equally worthy of consideration.

This investigation will be concerned only with stability of VTOL aircraft. The quality sought by aircraft designers, which is usually called "flying qualities" is not the same thing as stability although it bears a definite relation to it. Thus, for instance an airplane can be unstable in the mathematical sense, i.e. have a response to an initially small disturbance which grows without limit as time increases, and still have satisfactory flying qualities. This occurs in a conventional aircraft with a very long period but slightly unstable mode or for the helicopter which has a slightly unstable short period mode near the hovering flight condition. Flying qualities are also intimately involved with the concept of control since an aircraft could be so stable as to be impossible to control. Although these other aspects of aircraft flying qualities are equally important, we will be concerned here only with mathematical stability.

Consideration of aircraft stability in the above sense ultimately reduces to the consideration of the stability of solutions of a set of differential equations in the neighborhood of some equilibrium point. The degree of difficulty encountered in determining whether or not a system of differential equations possesses an unstable solution depends on the nature of the equations obtained. The types of systems which may be obtained are:

1. Linear with constant coefficients.

2. Linear with time varying coefficients.

3. Non-linear

For systems of equations of the first type the determination of the stability is easily reduced to an algebraic problem. Although in the present report only linear systems with constant coefficients are obtained, a more accurate analysis of the VTOL conversion maneuver could easily lead to equations of either of the other types. Thus, in the present discussion the question asked is: If the rotation of the wing were stopped at any point in the conversion maneuver and the aircraft allowed to come to equilibrium what would be the stability of this equilibrium point? This is in effect assuming that the conversion takes place over a very long time interval. In the practical VTOL aircraft, however, the conversion time may be relatively short, e.g. less than half a minute, and it would be reasonable to ask what the effect of this acceleration would be. If a constant acceleration is assumed, the equations which describe a conversion will be linear with time varying coefficients. General solutions of systems of equations of this type can not in general be found although there are methods for obtaining approximate solutions if the coefficients do not vary too rapidly.

In general it is desirable to have more information than just knowing whether the motion is stable or not. Although it is desirable to have explicit expressions for frequency and damping in terms of the physical parameters of the aircraft, this is seldom possible and even if possible may lead to expressions of such complexity that

the dependence on a particular parameter is difficult to see. In the case of linear equations with constant coefficients, information of this type is easily obtained by means of the root locus method. Using this method the movement of the roots of the characteristic equation in the complex plane with variation of any desired parameter is easily found.

The main problem in determining the stability characteristics for VTOL aircraft is the prediction of the forces and moments acting on that section of the aircraft which is in the slipstream of the rotor or propeller and in particular those acting on the wing. In most VTOL with tilting rotors, nearly the entire wing is in the slipstream as well as part of the fuselage and the tail over a large part of the conversion.

The problem of predicting the forces and moments on an airfoil in a slipstream has been considered by a number of authors (Ref. 1, 2, 3, 4, 5).

Koning considered the effect of the propeller slipstream on the wing forces and moments. His theory is however, valid when the induced velocity of the propeller is small compared to the free stream velocity and thus can not be of any use for VTOL aircraft where the free stream velocity may be zero or very small and the induced velocity quite large.

The more recent analysis of Rethorst was particularly carried out for VTOL aircraft and is hence not limited by velocity ratio. These calculations were carried out for a large number of wing planforms (Ref. 6) and may be useful in selecting optimum planforms for

a specific design. An adequate comparison of these results with experiment is not possible due to the lack of experimental work in this area. Some comparison is made in Reference 21.

The experimental work of Stuper is quite extensive but was unfortunately done before the interest in VTOL aircraft and hence does not include tests at high induced velocities.

In the experimental work of Brenkmann it is interesting to note the effect of the slipstream rotation. For the condition of small angle of attack and large induced velocity the lift coefficient becomes negative over part of the span. It is concluded by Brenkmann that this effect on the total lift of the span is small since the increase over one half of the span and the decrease over the other average out to that given by an average angle of attack. This conclusion is probably valid as long as the wing is not stalled. If part of the wing is stalled, the actual lift may be considerably less than that based on an average angle of attack. Since present tilt-wing VTOL aircraft often operate with the wing at very high angles of attack, this could lead to considerable error in computing the lift on the wing. See Reference 20 for a more complete discussion of this effect. Brenkmann also found that the slipstream over the entire wing had a destalling effect which gave a significant additional lift.

In order to make a qualitative analysis of the effects of the slipstream on the stability characteristics it is almost essential to have a fairly simple expression for the lift on the wing in the slipstream which accounts for the most important effects. In order to obtain an expression of sufficient simplicity to be useful for stability

analysis purposes, it is necessary to neglect many of the effects which might be important.

For the purpose of the present investigation the following method of estimating the wing forces and moments and their derivatives will be employed:

We assume that the wing forces are dependent on an "effective" angle of attack and a "resultant" velocity which are determined by the vector sum of the free stream and rotor induced velocities. The value for the induced velocity to be used is not that at the rotor disc but somewhat greater than this. Simple momentum theory shows that the induced velocity far downstream must be twice that at the rotor disc, and in fact experimental evidence (Ref. 7) shows that a velocity nearly twice that at the rotor disc is reached within a very short (less than one diameter) distance behind it. Thus in computing the general expressions for the resultant velocity and its derivatives we take the induced velocity to be $\lambda' v$, where λ' is a constant between one and two and v is the induced velocity at the rotor disc.

The lift curve slope to be used in computing the lift is obtained from the work of Smelt and Davies (Ref. 8). These investigators derive a correction to the power off lift curve slope which is dependent on the thrust coefficient and the aspect ratio of that portion of the wing which is covered by the slipstream. This correction is based on the following considerations: Since the effect of the rotor will be to increase the velocity over that part of the wing in its wake, the lift will be increased over this portion of the wing and hence there will be a spanwise change in the lift at the outer edge of the rotor which

will give rise to a trailing vortex. The effect of this vortex will be to decrease the angle of attack of the airfoil. If the aspect ratio of that portion of the wing in the slipstream is very large the effect of the trailing vortices will be negligible and the lift will simply be proportional to the resultant dynamic pressure and the effective angle of attack of the airfoil. For smaller values of the aspect ratio, however, the trailing vortices will decrease the angle of attack, the magnitude of this reduction depending on the strength of the vortex which will be dependent on the magnitude of the spanwise discontinuity in the lift which is in turn proportional to the induced velocity or the thrust coefficient. Smelt and Davies simply compute the two limiting cases and include a constant which depends on the aspect ratio and is to be found by some experimental means. Using the procedure outlined above, the lift on the wing can then be expressed as,

$$L = \frac{1}{2}\rho S V_R^2 a_c \alpha' \left[1 + K\left(\frac{1}{1+S} - 1\right)\right] \tag{1}$$

where the above symbols have the following meaning:

$$\vec{V}_R = \vec{V} + \lambda' \vec{v} \tag{2}$$

$$\alpha' = \cos^{-1} \frac{\vec{V}_R \cdot \lambda' \vec{v}}{|\vec{V}_R|\,|\lambda \vec{v}|} \tag{3}$$

$\vec{V}$ is the free stream velocity and $\vec{v}$ the induced velocity (See Fig. 1).

a_c -slope of the lift curve of the wing section without the

presence of the slipstream.

S - area of wing in slipstream.

$$S = \frac{\sigma}{V}\left(1 + \frac{x_{cp}}{\sqrt{D^2/4 + x_{cp}^2}}\right) \tag{4}$$

where x_{cp} -distance of center of pressure of wing behind rotors.

K - aspect-ratio-dependent constant mentioned above having value between 0 ($AR \to \infty$) and 1 ($AR = 0$).

λ' as mentioned above has value between 1 and 2.

The particular values of these two constants in an analysis are to be determined in one of the following ways:

1. Experiment; either from models or full scale aircraft of the configuration being analyzed or by extrapolation from experimental data obtained from similar wing-rotor arrangements.

2. Rough estimates based on physical reasoning, e.g. if on the particular aircraft under consideration, the wing center of pressure was greater than one rotor diameter behind the rotor, it would be reasonable to assume that λ' could be considered to have the value 2.

3. Choose values so as to give a best possible fit to more accurate theoretical calculations if available.

The value of σ, the velocity induced at the rotor disc, is obtained by equating the thrust of the rotor to the change of momentum of the slipstream, i.e.

$$T = (2\sigma)(\rho S V_f) \tag{5}$$

It is assumed here that the mass flow is that flowing through a stream tube of the same diameter as the rotor disc at the resultant velocity.

The process of taking the required derivatives of the resultant velocity based on the above assumptions becomes quite laborious. However, it was found that they could be computed in a general manner and expressed in the form of charts so that their values can be found immediately if all the trim conditions are known.

An approximate expression for the resultant velocity can be found, which under certain conditions introduces only a small amount of error, by assuming that the thrust can be equated to the change in momentum of the fluid based on only the component of the freestream velocity which is normal to the rotor plane. This expression leads to large errors when the angle of attack of the rotor plane is small at appreciable forward velocities. Also the error involved increases in inverse proportion to the disc loading. Thus the assumption leads to the greatest error for "helicopter-like" configurations and to the least error for "airplane-like" configurations.

The remainder to this report will be conducted in the following manner:

First, we will derive the controls-fixed, small disturbance equations for the longitudinal modes of motion. These equations will be applied to a sample aircraft (Vertol model 76) and the roots of the characteristic equation obtained for a number of tilt angles through the conversion. The effect of the various stability derivatives on these roots will be determined by means of the root locus

method. Then all of the important derivatives will be investigated to see the relative magnitudes of the contributions of the various parts of the aircraft such as the tail, rotor, wing, etc. and how these are influenced by changes in the various physical parameters of the aircraft such as the lift-curve slope, center of gravity location, tail size, etc.

Finally, an attempt will be made to draw some general conclusions from the important results of the investigation and to outline some of the important areas which will have to be investigated further either analytically or experimentally in order to obtain a sufficient understanding of VTOL dynamics to enable the designer to proceed systematically to the optimum design.

The dynamics of VTOL aircraft have been considered previously in References 18, 19, and 20. The approach in 19 and 20 is essentially experimental. The analysis given in Reference 18 is somewhat similar to that given here although little consideration was given in that report to the effects of the various physical parameters on the dynamic characteristics of the aircraft.

ANALYSIS

Assumptions

We now proceed to develop equations for the longitudinal motion of a tilt-wing VTOL aircraft. As the general development of small disturbance equations of aircraft has been given many times before (See e.g. Ref. 9), we will be mainly concerned here with those parts of the development which differ because of the presence of the rotors and the tilting of the wing. As many simplifying assumptions as possible will be made so that the important effects of the rotors on the stability characteristics can be seen without being obscured by the multitude of small effects which would have to be included to obtain a precise description of the aircraft's dynamic behavior. Thus we make the following assumptions:

1. Airframe is a rigid body.

2. There is no coupling between the lateral and longitudinal modes of motion. This is normally true for conventional aircraft if all disturbances are sufficiently small, the aircraft is initially in level flight, and any gyroscopic effects due to the engines are small enough to be neglected. The only other forces acting on the VTOL which might give a coupling are the lateral rotor forces and these cancel for two rotors which rotate in opposite directions.

3. All disturbance quantities are small enough that their products and squares can be neglected.

4. Aircraft performs a constant altitude conversion and initially all velocity components are zero except along the X-axis.

5. The wing tilt angle is fixed during the analysis as well as all other controls. This assumption could very well be untenable except when the conversion takes place over a long period of time.

6. The rotor satisfies the following relations:

$$v = \frac{T}{2\rho N \pi R^2 \Omega R \sqrt{\lambda^2+\mu^2}} \tag{6}$$

$$\frac{2C_T}{a\sigma} = \frac{\lambda}{2} + \frac{\theta}{3} \tag{7}$$

$$\frac{2C_H}{a\sigma} = \frac{\mu\delta}{2a} + \frac{\theta a_1}{3} - \frac{\lambda\theta}{2} + \frac{3\lambda a_1}{4} + \frac{\mu a_1^2}{4} - \frac{a_0 b_1}{6} + \frac{\mu a_0^2}{4} \tag{8}$$

where v is the induced velocity at the rotor; T is the total thrust produced by both rotors; N the number of rotors; R the radius of the rotor; Ω the angular speed of rotation of the rotor; θ the collective pitch at $0.75R$; δ the profile drag coefficient of the blades and C_T, C_H, λ, and μ are defined by:

$$C_T = \frac{T}{\rho N \pi R^2 (\Omega R)^2} \tag{9}$$

$$C_H = \frac{H}{\rho N \pi R^2 (\Omega R)^2} \tag{10}$$

$$\lambda = \frac{V \sin \alpha - v}{\Omega R} \tag{11}$$

$$\mu = \frac{V \cos \alpha}{\Omega R} \tag{12}$$

where V is the free stream velocity and α is defined in Figure 1. The directions of T and H are also defined there. For the derivation of the expressions for C_T and C_H see References 10 and 11. A number of terms were dropped from the expressions given in these books due to the fact that μ is much less than one for most tilt-wing configurations. It is also assumed that Ω is constant in all of the above expressions.

7. All force and moment derivatives are constant at each trim point.

8. Effects of rotor on wing forces can be described by the expressions given in the first section of this report. (Expressions 1, 2, and 3).

Non-dimensionalization

Non-dimensionalizing the equations of motion for this type of VTOL aircraft does not lead to the degree of simplification found in the case of conventional aircraft. This is due to the fact that the rotor forces are proportional to the square of the rotor tip speed rather than the dynamic pressure. When the force equations are divided through by the wing area times the dynamic pressure, the wing and tail forces are simplified to the usual lift and drag coefficients;

the rotor forces, however, are preceded by the factor $\frac{\pi R^2}{S}\left(\frac{\Omega R}{V_R}\right)^2$ which remains nearly constant through a transition since ΩR is constant and the resultant velocity does not vary much. All of the force terms are never-the-less made independent of the size of the aircraft which is probably the most important reason for the non-dimensionalization. The moment equation was also divided by the wing chord.

Equations of Motion

A body axis system will be used in which the fuselage reference line is initially horizontal and pointing into the wind. The variables, however, will be expressed in terms of the familiar wind axes variables, i.e. V, α_f, θ_f instead of u, w, θ_f where V is the magnitude of the free stream velocity, α_f is the angle between the fuselage reference line and the free stream, θ_f is the angle between the horizontal and the fuselage reference line, u and w are the velocity components along the body axes. For hovering flight u and w must be retained. The relations between these variables are:

$$u = V\cos\alpha_f$$
$$w = V\sin\alpha_f \qquad (13)$$

The inertia forces for the longitudinal motion only are then:

$$F_{x_I} = -m\left[\dot{V}\cos\alpha_f + V\sin\alpha_f\,(\dot{\theta}_f - \dot{\alpha}_f)\right] \qquad (14)$$

$$F_{z_I} = -m\left[\dot{V}\sin\alpha_f + V\cos\alpha_f\,(\dot{\theta}_f - \dot{\alpha}_f)\right] \tag{15}$$

$$M_{y_I} = -I_y\,\ddot{\theta}_f \tag{16}$$

For the derivation of these expressions see e.g. Reference 9.

Using the relation $\alpha_f = 90 + \alpha - i_w$ (α & i_w are defined in Figure 1), we obtain:

$$F_{x_I} = -m\left[-\dot{V}\sin(\alpha - i_w) - V\cos(\alpha - i_w)(\dot{\alpha} - \dot{\theta}_f)\right] \tag{17}$$

$$F_{z_I} = -m\left[\dot{V}\cos(\alpha - i_w) - V\sin(\alpha - i_w)(\dot{\alpha} - \dot{\theta}_f)\right] \tag{18}$$

$$M_{y_I} = -\ddot{\theta}_f\, I_y \tag{19}$$

$\dot{\alpha}_f = \dot{\alpha}$ since i_w is constant at each trim point.

The forces acting on the aircraft due to gravity are:

$$F_{x_g} = -W\sin\theta_f \tag{20}$$

$$F_{z_g} = W\cos\theta_f \tag{21}$$

$$M_{y_g} = 0 \tag{22}$$

From Figure 2 we see that the aerodynamic forces are:

$$F_{x_a} = F_{x_S} + F_{x_R} + F_{x_T} + F_{x_W} + F_{x_F} \tag{23}$$

$$F_{z_a} = F_{z_S} + F_{z_R} + F_{z_T} + F_{z_W} + F_{z_F} \tag{24}$$

$$M_{ya} = -X_a F_{zs} - Z_a F_{xs} - N X_R F_{zR} - N Z_R F_{xR}$$
$$+ X_T F_{zT} - Z_T F_{xT} - X_a F_{zw} - Z_a F_{xw}$$
$$- X_F F_{zF} - Z_F F + M_{cF} + M_{ac} + M_{ac_T} \qquad (25)$$

(The subscripts S , R , T , W , F indicate slipsteam, rotor, tail, wing, and fuselage respectively; see Figure 2) where,

$$F_{xS} = D_S \sin(\alpha - i_W - \phi) + L_S \cos(\alpha - i_W - \phi) \qquad (26)$$

$$F_{xR} = T \cos i_W - H \sin i_W \qquad (27)$$

$$F_{xT} = L_T \cos(\alpha - i_W - \epsilon) + D_T \sin(\alpha - i_W - \epsilon) \qquad (28)$$

$$F_{xw} = D_W \sin(\alpha - i_W) + L_W \cos(\alpha - i_W) \qquad (29)$$

$$F_{xF} = D_F \sin(\alpha - i_W) + L_F \cos(\alpha - i_W) \qquad (30)$$

$$F_{zS} = -D_S \cos(\alpha - i_W - \phi) + L_S (\alpha - i_W - \phi) \qquad (31)$$

$$F_{zR} = -T \sin i_W - H \cos i_W \qquad (32)$$

$$F_{zT} = L_T \sin(\alpha - i_W - \epsilon) - D_T \cos(\alpha - i_W - \epsilon) \qquad (33)$$

$$F_{zw} = L_W \sin(\alpha - i_W) - D_W \cos(\alpha - i_W) \qquad (34)$$

$$F_{zF} = L_F \sin(\alpha - i_W) - D_F \cos(\alpha - i_W) \qquad (35)$$

The distances X_A, X_R, Z_A, Z_R are not constant but depend on the angle of tilt i_W. They are given by the expressions:

$$X_A = X_g + (r + l_p)\cos i_W \tag{36}$$

$$X_R = X_g + (r + l_p + l_a)\cos i_W \tag{37}$$

$$Z_A = Z_g + (-r + l_p)\sin i_W \tag{38}$$

$$Z_R = Z_g + (-r + l_p + l_a)\sin i_W \tag{39}$$

where X_g, Z_g, r, l_p, l_a are constants and are shown in Figure 3. These distances have also been computed for various tilt angles and are shown plotted as a function of i_W in Figure 4.

Thus the sum of the forces and moments acting on the aircraft may be expressed:

$$F_X = F_{XI} + F_{Xg} + F_{Xs} + F_{XR} + F_{XT} + F_{Xw} + F_{XF} \tag{40}$$

$$F_Z = F_{ZI} + F_{Zg} + F_{Zs} + F_{ZR} + F_{ZT} + F_{Zw} + F_{ZF} \tag{41}$$

$$\begin{aligned} M = {} & M_{yI} - X_a F_{Zs} - Z_a F_{Xs} - X_R F_{ZR} - Z_R F_{XR} \\ & + X_T F_{ZT} - Z_T F_{XT} - X_a F_{Zw} - Z_a F_{Xw} \\ & + X_F F_{ZF} + Z_F F_{XF} + M_{cF} + M_{ac} + M_{acT} \end{aligned} \tag{42}$$

Since we are considering only the longitudinal equations of motion with controls fixed, we have three degrees of freedom. The three variables will be taken as V, α, θ_f. As already noted, derivatives with respect to α are the same as with respect to α_f.

If we expand all the forces in Taylor series, retain only the first order terms, neglect products of the perturbation quantities, and write for simplicity the variables themselves for their perturbations, we obtain the equations in the form given below. The process of taking the first term of the Taylor series for the inertia and gravity forces along with the aerodynamic forces eliminates the necessity of subtracting the steady state solution from the perturbation equations and also gives rise to the convenient symbols such as $C_{m_{\ddot{\theta}}}$ for the non-dimensional form of the moment of inertia about the Y-axis. The derivatives are constant for a given trim condition but vary with the variable i_w. The perturbation equations are thus given by:

$$\frac{\partial F_x}{\partial V} V + \frac{\partial F_x}{\partial \dot{V}} \dot{V} + \frac{\partial F_x}{\partial \alpha} \alpha + \frac{\partial F_x}{\partial \dot{\alpha}} \dot{\alpha} + \frac{\partial F_x}{\partial \theta_f} \theta_f + \frac{\partial F_x}{\partial \dot{\theta}_f} \dot{\theta}_f = 0 \quad (43)$$

$$\frac{\partial F_z}{\partial V} V + \frac{\partial F_z}{\partial \dot{V}} \dot{V} + \frac{\partial F_z}{\partial \alpha} \alpha + \frac{\partial F_z}{\partial \dot{\alpha}} \dot{\alpha} + \frac{\partial F_z}{\partial \theta_f} \theta_f + \frac{\partial F_z}{\partial \dot{\theta}_f} \dot{\theta}_f = 0 \quad (44)$$

$$\frac{\partial M}{\partial V} V + \frac{\partial M}{\partial \dot{V}} \dot{V} + \frac{\partial M}{\partial \alpha} \alpha + \frac{\partial M}{\partial \dot{\alpha}} \dot{\alpha} + \frac{\partial M}{\partial \dot{\theta}_f} \dot{\theta}_f + \frac{\partial M}{\partial \ddot{\theta}_f} \ddot{\theta}_f = 0 \quad (45)$$

Evaluation of stability derivatives

Due to the influence of the induced velocity on the magnitude and direction of the resultant velocity at the wing section in the slipstream, most of the stability derivatives will be functions of

the rotor thrust T . In order to separate the effect of the change due to rotor thrust variation from that due to variation with the thrust held constant, the derivatives will be taken in the following manner:

$$\frac{\partial(\ )}{\partial\alpha}\Big|_V = \frac{\partial(\ )}{\partial\alpha}\Big|_{V,C_T} + \frac{\partial(\ )}{\partial C_T}\Big|_{\alpha,V} \frac{\partial C_T}{\partial\alpha}\Big|_V \tag{46}$$

$$\frac{\partial(\ )}{\partial V}\Big|_\alpha = \frac{\partial(\ )}{\partial V}\Big|_{\alpha,C_T} + \frac{\partial(\ )}{\partial C_T}\Big|_{\alpha,V} \frac{\partial C_T}{\partial V}\Big|_\alpha \tag{47}$$

Where C_T is the thrust coefficient defined by,

$$T = \rho N \pi R^2 (\Omega R)^2 C_T \tag{48}$$

and the subscripts beside the vertical line indicate the variable or variables held constant while taking the derivative. The two derivatives $\frac{\partial C_T}{\partial\alpha}\Big|_V$ and $\frac{\partial C_T}{\partial V}\Big|_\alpha$ are obtained in the following manner:

The expression for C_T is,

$$\frac{2C_T}{a\sigma} = \frac{\lambda}{2} + \frac{\theta}{3} \tag{49}$$

which is sufficiently accurate as long as $\mu_x = \frac{V}{\Omega R}$ is small compared to unity; which is nearly always true for VTOL aircraft. The definition of λ is,

$$\lambda = \mu_x \sin\alpha - \frac{v}{\Omega R} = fn(V, \alpha, C_T) \tag{50}$$

Thus,

$$\left.\frac{\partial C_T}{\partial \alpha}\right|_V = \frac{a\sigma}{4}\left[\left.\frac{\partial \lambda}{\partial \alpha}\right|_{V,C_T} + \left.\frac{\partial \lambda}{\partial C_T}\right|_{V,\alpha}\left.\frac{\partial C_T}{\partial \alpha}\right|_V\right]$$

or,

$$\left.\frac{\partial C_T}{\partial \alpha}\right|_V = \frac{\frac{a\sigma}{4}\left.\frac{\partial \lambda}{\partial \alpha}\right|_{V,C_T}}{1-\frac{a\sigma}{4}\left.\frac{\partial \lambda}{\partial C_T}\right|_{V,\alpha}} \tag{51}$$

In a similar manner,

$$\left.\frac{\partial C_T}{\partial V}\right|_a = \frac{\frac{a\sigma}{4\Omega R}\left.\frac{\partial \lambda}{\partial \mu_x}\right|_{\alpha,C_T}}{1-\frac{a\sigma}{4}\left.\frac{\partial \lambda}{\partial C_T}\right|_{V,\alpha}} \tag{52}$$

The derivatives $\frac{\partial \lambda}{\partial \mu_x}$, $\frac{\partial \lambda}{\partial C_T}$ can be calculated and plotted in a general manner so that they may be applied to any rotor at any operating condition. This has been done in Reference 12. Expressions for and plots of these derivatives are given in Appendix A.

Thus we see that expressions for the derivatives of the X, Z -forces and Y-moments with respect to the three variables α, V, C_T are needed. These will be discussed in two sections; first the static derivatives and then the dynamic derivatives.

Static derivatives

The static derivatives which are required are the derivatives of the forces F_X and F_Z and the moment M with respect to velocity, angle of attack and pitch angle. These derivatives in

$$\frac{\partial C_X}{\partial V}\Big|_\alpha = \frac{1}{\frac{1}{2}\rho S V_{R_0}^2}\frac{\partial F_X}{\partial V}\Big|_\alpha = \frac{\partial C_{X_i}}{\partial V}\Big|_\alpha + \frac{\partial C_{X_q}}{\partial V}\Big|_\alpha + \frac{\partial C_{X_\beta}}{\partial V}\Big|_\alpha$$

$$+ \frac{\partial C_{X_T}}{\partial V}\Big|_\alpha + \frac{\partial C_{X_W}}{\partial V}\Big|_\alpha + \frac{\partial C_{X_F}}{\partial V}\Big|_\alpha + \frac{\partial C_{X_S}}{\partial V}\Big|_\alpha \qquad (53)$$

$$\frac{\partial C_X}{\partial \alpha}\Big|_V = \frac{1}{\frac{1}{2}\rho S V_{R_0}^2}\frac{\partial F_X}{\partial \alpha}\Big|_V = \frac{\partial C_{X_i}}{\partial \alpha}\Big|_V + \frac{\partial C_{X_q}}{\partial \alpha}\Big|_V + \frac{\partial C_{X_\beta}}{\partial \alpha}\Big|_V$$

$$+ \frac{\partial C_{X_T}}{\partial \alpha}\Big|_V + \frac{\partial C_{X_W}}{\partial \alpha}\Big|_V + \frac{\partial C_{X_F}}{\partial \alpha}\Big|_V + \frac{\partial C_{X_S}}{\partial \alpha}\Big|_V \qquad (54)$$

$$\frac{\partial C_Z}{\partial V}\Big|_\alpha = \frac{1}{\frac{1}{2}\rho S V_{R_0}^2}\frac{\partial F_Z}{\partial V}\Big|_\alpha = \frac{\partial C_{Z_i}}{\partial V}\Big|_\alpha + \frac{\partial C_{Z_q}}{\partial V}\Big|_\alpha + \frac{\partial C_{Z_\beta}}{\partial V}\Big|_\alpha$$

$$+ \frac{\partial C_{Z_T}}{\partial V}\Big|_\alpha + \frac{\partial C_{Z_W}}{\partial V}\Big|_\alpha + \frac{\partial C_{Z_F}}{\partial V}\Big|_\alpha + \frac{\partial C_{Z_S}}{\partial V}\Big|_\alpha \qquad (55)$$

$$\frac{\partial C_Z}{\partial \alpha}\Big|_V = \frac{1}{\frac{1}{2}\rho S V_{R_0}^2}\frac{\partial F_Z}{\partial \alpha}\Big|_V = \frac{\partial C_{Z_i}}{\partial \alpha}\Big|_V + \frac{\partial C_{Z_q}}{\partial \alpha}\Big|_V + \frac{\partial C_{Z_\beta}}{\partial \alpha}\Big|_V$$

$$+ \frac{\partial C_{Z_T}}{\partial \alpha}\Big|_V + \frac{\partial C_{Z_W}}{\partial \alpha}\Big|_V + \frac{\partial C_{Z_F}}{\partial \alpha}\Big|_V + \frac{\partial C_{Z_S}}{\partial \alpha}\Big|_V \qquad (56)$$

(Θ_f is held constant in each of these derivatives also, but this is not indicated by a subscript since no confusion is likely to result over this point)

$$\frac{\partial C_X}{\partial \Theta_f} = \frac{2}{\rho S V_{R_0}^2}\frac{\partial F_X}{\partial \Theta_f} = \frac{-2}{\rho S V_{R_0}^2} W \cos\Theta_{f_0} = \frac{-2W}{\rho S V_{R_0}^2} \qquad (57)$$

$$\frac{\partial C_z}{\partial \theta_f} = \frac{2}{\rho S V_{R_0}^2} \frac{\partial F_z}{\partial \theta_f} = \frac{-2}{\rho S V_{R_0}^2} W \mu n \theta_{f_0} = 0 \qquad (58)$$

The derivatives of the moment about the Y-axis with respect to V and α are given below. The lower case letters x , z , are the various distances given previously non-dimensionalized with respect to the wing chord.

$$\frac{\partial C_m}{\partial \alpha}\Big|_V = \frac{2}{\rho S V_{R_0}^2 C_w} \frac{\partial M}{\partial \alpha}\Big|_V = -x_a \frac{\partial C_{z_s}}{\partial \alpha}\Big|_V - z_a \frac{\partial C_{x_s}}{\partial \alpha}\Big|_V$$
$$- N x_R \frac{\partial C_{z_R}}{\partial \alpha}\Big|_V - N z_R \frac{\partial C_{x_R}}{\partial \alpha}\Big|_V + x_T \frac{\partial C_{z_T}}{\partial \alpha}\Big|_V$$
$$- z_T \frac{\partial C_{x_T}}{\partial \alpha}\Big|_V - x_a \frac{\partial C_{z_w}}{\partial \alpha}\Big|_V - z_a \frac{\partial C_{x_w}}{\partial \alpha}\Big|_V + x_F \frac{\partial C_{z_F}}{\partial \alpha}\Big|_V$$
$$+ z_F \frac{\partial C_{x_F}}{\partial \alpha}\Big|_V + \frac{\partial C_{m_{CF}}}{\partial \alpha}\Big|_V + \frac{\partial C_{m_{ac}}}{\partial \alpha}\Big|_V + \frac{\partial C_{m_{ac_T}}}{\partial \alpha}\Big|_V$$

(59)

$$\frac{\partial C_m}{\partial V}\Big|_\alpha = \frac{2}{\rho S V_{R_0}^2 C_w} \frac{\partial M}{\partial V}\Big|_\alpha = -x_a \frac{\partial C_{z_s}}{\partial V}\Big|_\alpha - z_a \frac{\partial C_{x_s}}{\partial V}\Big|_\alpha$$
$$- N x_R \frac{\partial C_{z_R}}{\partial V}\Big|_\alpha - N z_R \frac{\partial C_{x_R}}{\partial V}\Big|_\alpha + x_T \frac{\partial C_{z_T}}{\partial V}\Big|_\alpha$$
$$- z_T \frac{\partial C_{x_T}}{\partial V}\Big|_\alpha - x_a \frac{\partial C_{z_w}}{\partial V}\Big|_\alpha - z_a \frac{\partial C_{x_w}}{\partial V}\Big|_\alpha + x_F \frac{\partial C_{z_F}}{\partial V}\Big|_\alpha$$
$$+ z_F \frac{\partial C_{x_F}}{\partial V}\Big|_\alpha + \frac{\partial C_{m_{CF}}}{\partial V}\Big|_\alpha + \frac{\partial C_{m_{ac}}}{\partial V}\Big|_\alpha + \frac{\partial C_{m_{ac_T}}}{\partial V}\Big|_\alpha$$

(60)

We must now find expressions for the derivatives of the forces acting on the various components of the aircraft with respect to the free stream velocity and angle of attack. We note that the derivatives of the inertia and gravity forces are zero since each term of the inertia forces contains a perturbation quantity which is zero when evaluated at the trim condition and the gravity forces do not contain the variables α and V. The fuselage force derivatives can be carried no further since there is no theoretical method available for treating the odd shaped fuselages which are likely to be present on VTOL aircraft. These will normally have to be found by a wind tunnel test on a model unless the fuselage is similar to that of a conventional aircraft, in which case it can be estimated by analytical means. However, if part of the fuselage is in the wake of the rotor, any type of analytical estimate will probably be very difficult. The expressions for the various forces acting on the aircraft in terms of the appropriate velocities and coefficients are:

$$D_S = \frac{1}{2} \rho S V_R^2 C_{DS} \tag{61}$$

$$L_S = \frac{1}{2} \rho S V_R^2 C_{LS} \tag{62}$$

$$D_W = \frac{1}{2} \rho S_W V^2 C_{DW} \tag{63}$$

$$L_W = \frac{1}{2} \rho S_W V^2 C_{LW} \tag{64}$$

$$D_T = \frac{1}{2} \rho S_T V_T^2 C_{DT} \tag{65}$$

$$L_T = \frac{1}{2} \rho S_T V_T^2 C_{LT} \tag{66}$$

$$T = \rho \pi R^2 (\Omega R)^2 C_T \tag{67}$$

$$H = \rho \pi R^2 (\Omega R)^2 C_H \tag{68}$$

Substituting these expressions into the equations and carrying out the differentiation, we easily obtain the following expressions for the required derivatives:

$$\frac{\partial C_{ZS}}{\partial V}\Big|_\alpha = \left[\frac{2C_{DS}}{V_R}\frac{\partial V_R}{V}\Big|_\alpha + \left(-\frac{\partial C_{DS}}{\partial \alpha'} + C_{LS}\right)\frac{\partial \phi}{\partial V}\Big|_\alpha\right]\sin\phi$$
$$-\left[\frac{2C_{LS}}{V_R}\frac{\partial V_R}{\partial V}\Big|_\alpha - \left(\frac{\partial C_{LS}}{\partial \alpha'} + C_{DS}\right)\frac{\partial \phi}{\partial V}\Big|_\alpha\right]\cos\phi \tag{69}$$

$$\frac{\partial C_{XS}}{\partial V}\Big|_\alpha = -\left[\frac{2C_{LS}}{V_R}\frac{\partial V_R}{\partial V}\Big|_\alpha - \left(\frac{\partial C_{LS}}{\partial \alpha'} + C_{DS}\right)\frac{\partial \phi}{\partial V}\Big|_\alpha\right]\sin\phi$$
$$-\left[\frac{2C_{DS}}{V_R}\frac{\partial V_R}{\partial V}\Big|_\alpha - \left(\frac{\partial C_{DS}}{\partial \alpha'} - C_{LS}\right)\frac{\partial \phi}{\partial V}\Big|_\alpha\right]\cos\phi \tag{70}$$

$$\frac{\partial C_{ZS}}{\partial \alpha}\Big|_V = \left[\frac{2C_{DS}}{V_R}\frac{\partial V_R}{\partial \alpha}\Big|_V + \left(\frac{\partial C_{DS}}{\partial \alpha'} + C_{LS}\right)\left(1 - \frac{\partial \phi}{\partial \alpha}\Big|_V\right)\right]\sin\phi$$
$$-\left[\frac{2C_{LS}}{V_R}\frac{\partial V_R}{\partial \alpha}\Big|_V + \left(\frac{\partial C_{LS}}{\partial \alpha'} + C_{DS}\right)\left(1 - \frac{\partial \phi}{\partial \alpha}\Big|_V\right)\right]\cos\phi \tag{71}$$

$$\frac{\partial C_{XS}}{\partial \alpha}\Big|_V = -\left[\frac{2C_{LS}}{V_R}\frac{\partial V_R}{\partial \alpha}\Big|_V + \left(\frac{\partial C_{LS}}{\partial \alpha'} + C_{DS}\right)\left(1 - \frac{\partial \phi}{\partial \alpha}\Big|_V\right)\right]\sin\phi$$
$$-\left[\frac{2C_{DS}}{V_R}\frac{\partial V_R}{\partial \alpha}\Big|_V + \left(\frac{\partial C_{DS}}{\partial \alpha'} + C_{LS}\right)\left(1 - \frac{\partial \phi}{\partial \alpha}\Big|_V\right)\right]\cos\phi \tag{72}$$

$$\frac{\partial C_{ZR}}{\partial V}\Big|_\alpha = -2N\frac{\pi R^2}{S}\left(\frac{\Omega R}{V_R}\right)^2\left[\frac{\partial C_H}{\partial V}\Big|_\alpha \cos i_W + \sin i_W \frac{\partial C_T}{\partial V}\Big|_\alpha\right] \tag{73}$$

$$\frac{\partial C_{XR}}{\partial V}\Big|_\alpha = -2N\frac{\pi R^2}{S}\left(\frac{\Omega R}{V_R}\right)^2\left[\frac{\partial C_H}{\partial V}\Big|_\alpha \sin i_W - \cos i_W \frac{\partial C_T}{\partial V}\Big|_\alpha\right] \tag{74}$$

$$\frac{\partial C_{ZR}}{\partial \alpha}\Big|_V = -2N\frac{\pi R^2}{S}\left(\frac{\Omega R}{V_R}\right)^2\left[\frac{\partial C_H}{\partial \alpha}\Big|_V \cos i_W + \sin i_W \frac{\partial C_T}{\partial \alpha}\Big|_V\right] \tag{75}$$

$$\frac{\partial C_{XR}}{\partial \alpha}\Big|_V = -2N\frac{\pi R^2}{S}\left(\frac{\Omega R}{V_R}\right)^2\left[\frac{\partial C_H}{\partial \alpha}\Big|_V \sin i_W - \cos i_W \frac{\partial C_T}{\partial \alpha}\Big|_V\right] \tag{76}$$

$$\frac{\partial C_{ZW}}{\partial V}\Big|_{\alpha} = -\frac{S_W}{S}\frac{V}{V_R^2} C_{LW} \tag{77}$$

$$\frac{\partial C_{XW}}{\partial V}\Big|_{\alpha} = -\frac{S_W}{S}\frac{V}{V_R^2} C_{DW} \tag{78}$$

$$\frac{\partial C_{ZW}}{\partial \alpha}\Big|_{V} = -\frac{S_W}{S}\left(\frac{V}{V_R}\right)^2\left(\frac{\partial C_{LW}}{\partial \alpha} + C_{DW}\right) \tag{79}$$

$$\frac{\partial C_{XW}}{\partial \alpha}\Big|_{V} = -\frac{S_W}{S}\left(\frac{V}{V_R}\right)^2\left(\frac{\partial C_{DW}}{\partial \alpha} - C_{LW}\right) \tag{80}$$

$$\frac{\partial C_{ZT}}{\partial V}\Big|_{\alpha} = 2\frac{S_T}{S}\frac{V_T}{V_R^2}\left\{\left[C_{D_T}\frac{\partial V_T}{\partial V}\Big|_{\alpha} + \frac{V_T}{2\Omega R}\frac{\partial \epsilon}{\partial \alpha'}\frac{\partial \phi}{\partial \mu_x}\Big|_{\alpha}\left(\frac{\partial C_{D_T}}{\partial \alpha_T} - C_{L_T}\right)\right]\sin\epsilon - \left[C_{L_T}\frac{\partial V_T}{\partial V}\Big|_{\alpha} + \frac{V_T}{2\Omega R}\frac{\partial \epsilon}{\partial \alpha'}\frac{\partial \phi}{\partial \mu_x}\Big|_{\alpha}\left(\frac{\partial C_{L_T}}{\partial \alpha_T} - C_{D_T}\right)\right]\cos\epsilon\right\} \tag{81}$$

$$\frac{\partial C_{XT}}{\partial V}\Big|_{\alpha} = -2\frac{S_T}{S}\frac{V_T}{V_R^2}\left\{\left[C_{L_T}\frac{\partial V_T}{\partial V}\Big|_{\alpha} + \frac{V_T}{2\Omega R}\frac{\partial \epsilon}{\partial \alpha'}\frac{\partial \phi}{\partial \mu_x}\Big|_{\alpha}\left(\frac{\partial C_{L_T}}{\partial \alpha_T} + C_{D_T}\right)\right]\sin\epsilon + \left[C_{D_T}\frac{\partial V_T}{\partial V}\Big|_{\alpha} + \frac{V_T}{2\Omega R}\frac{\partial \epsilon}{\partial \alpha'}\frac{\partial \phi}{\partial \mu_x}\Big|_{\alpha}\left(\frac{\partial C_{D_T}}{\partial \alpha_T} + C_{L_T}\right)\right]\cos\epsilon\right\} \tag{82}$$

$$\frac{\partial C_{ZT}}{\partial \alpha}\Big|_{V} = 2\frac{S_T}{S}\frac{V_T}{V_R^2}\left\{\left[C_{D_T}\frac{\partial V_T}{\partial \alpha}\Big|_{V} + \frac{V_T}{2}\left(\frac{\partial C_{D_T}}{\partial \alpha_T} - C_{L_T}\right)\left\{1 - \frac{\partial \epsilon}{\partial \alpha'}\left(1 - \frac{\partial \phi}{\partial \alpha}\Big|_{V}\right)\right\}\right]\sin\epsilon - \left[C_{L_T}\frac{\partial V_T}{\partial \alpha}\Big|_{V} + \frac{V_T}{2}\left(\frac{\partial C_{L_T}}{\partial \alpha_T} - C_{D_T}\right)\left\{1 - \frac{\partial \epsilon}{\partial \alpha'}\left(1 - \frac{\partial \phi}{\partial \alpha}\Big|_{V}\right)\right\}\right]\cos\epsilon\right\} \tag{83}$$

$$\frac{\partial C_{XT}}{\partial \alpha}\Big|_{V} = -2\frac{S_T}{S}\frac{V_T}{V_R^2}\left\{\left[C_{L_T}\frac{\partial V_T}{\partial \alpha}\Big|_{V} + \frac{V_T}{2}\left(\frac{\partial C_{L_T}}{\partial \alpha_T} + C_{D_T}\right)\left\{1 - \frac{\partial \epsilon}{\partial \alpha'}\left(1 - \frac{\partial \phi}{\partial \alpha}\Big|_{V}\right)\right\}\right]\sin\epsilon + \left[C_{D_T}\frac{\partial V_T}{\partial \alpha}\Big|_{V} + \frac{V_T}{2}\right.$$

$$\left(\frac{\partial C_{D_T}}{\partial \alpha_T} - C_{L_T}\right)\left\{1 - \frac{\partial \epsilon}{\partial \alpha'}\left(1 - \frac{\partial \Phi}{\partial \alpha}\Big|_V\right)\right\}\Big] \cos\epsilon \Bigg\} \tag{84}$$

The only point which might need some explanation in obtaining these expressions is the evaluation of the derivatives $\frac{\partial \alpha_T}{\partial V}$, $\frac{\partial \alpha_T}{\partial \alpha}$. The angle α_T is obtained from Figure 2 and is,

$$\alpha_T = 90 + \alpha - \iota_W + \iota_T - \epsilon \tag{85}$$

Thus,
$$\frac{\partial \alpha_T}{\partial V} = -\frac{\partial \epsilon}{\partial V} = -\frac{\partial \epsilon}{\partial \alpha'}\frac{\partial \alpha'}{\partial V} \tag{86}$$

$$\frac{\partial \alpha_T}{\partial \alpha} = 1 - \frac{\partial \epsilon}{\partial \alpha} = 1 - \frac{\partial \epsilon}{\partial \alpha'}\frac{\partial \alpha'}{\partial \alpha} \tag{87}$$

since the downwash at the tail is a function of the angle of attack of the wing. The angle of attack of the wing is,

$$\alpha' = 90 + \alpha - \Phi \tag{88}$$

Thus,
$$\frac{\partial \alpha'}{\partial V} = -\frac{\partial \Phi}{\partial V}\Big|_\alpha \tag{89}$$

$$\frac{\partial \alpha'}{\partial \alpha} = 1 - \frac{\partial \Phi}{\partial \alpha}\Big|_V \tag{90}$$

This finally gives,

$$\frac{\partial \alpha_T}{\partial V} = \frac{\partial \epsilon}{\partial \alpha'}\frac{\partial \Phi}{\partial V}\Big|_\alpha \tag{91}$$

$$\frac{\partial \alpha_T}{\partial \alpha} = 1 - \frac{\partial \epsilon}{\partial \alpha'}\left(1 - \frac{\partial \Phi}{\partial \alpha}\Big|_V\right) \tag{92}$$

The only derivatives which we have left to evaluate in terms of known physical parameters are derivatives of C_H, V_R, Φ, C_{D_S}, C_{L_S}, V_T with respect to α, V. We will now consider the evaluation of these derivatives.

In order to find the C_H derivatives we need an expression for C_H in terms of C_T, μ, λ. This is obtained from the expression given previously by substituting the expressions for a_1, b_1, and a_0 given in Reference 11 into it. The result is:

$$\frac{2C_H}{a\sigma} = \frac{\delta}{2a}\mu + 8\mu\left[\frac{4}{a^2\sigma^2}C_T^2\left(1-\frac{\mu^2}{2}\right) - \frac{3}{8a\sigma}C_T\lambda\right.$$
$$\left.\left(1-\frac{2}{3\pi}\mu-\frac{7}{6}\mu^2\right) - \frac{\lambda^2\mu}{16\pi}\left(1-\frac{5\pi}{8}\mu\right)\right] \qquad (93)$$

Taking the derivative of this expression with respect to α, $\checkmark$, C_T, and neglecting powers of μ greater than or equal to two as compared with unity, we obtain the following:

$$\frac{2\Omega R}{a\sigma}\frac{\partial C_H}{\partial V}\Big|_{\alpha,C_T} = \cos\alpha\left[\frac{\delta}{2a} + 8\left(\frac{2C_T}{a\sigma}\right)^2 - \frac{3}{2}\lambda\left(\frac{2C_T}{a\sigma}\right)\left(1-\frac{2\mu}{3\pi}\right)\right.$$
$$\left.-\mu\frac{\lambda^2}{4}\left(\frac{1}{\pi}-\frac{15}{8}\mu\right)\right] - \mu\frac{\partial\lambda}{\partial\mu_x}\left[\frac{3}{2}\left(\frac{2C_T}{a\sigma}\right)\left(1-\frac{2\mu}{3\pi}\right)\right.$$
$$\left.-\frac{\lambda\mu}{\pi}\left(1-\frac{5\pi}{8}\mu\right)\right] \qquad (94)$$

$$\frac{2}{a\sigma}\frac{\partial C_H}{\partial\alpha}\Big|_{V,C_T} = -\mu_x\sin\alpha\left[\frac{\delta}{2a}+8\left(\frac{2C_T}{a\sigma}\right)^2\right] + \left(\frac{2C_T}{a\sigma}\right)\left[\mu\frac{\partial\lambda}{\partial\alpha}\right.$$
$$\left.\left(\frac{\mu}{\pi}-\frac{3}{2}\right) - \mu_x\lambda\sin\alpha\left(-3+2.636\mu+7\mu^2\right)\right]$$
$$+\lambda\mu^2\frac{\partial\lambda}{\partial\alpha}\left(\frac{5}{8}\mu-.318\right) - \mu_x\mu\lambda^2\sin\alpha$$
$$\left(\frac{15}{16}\mu-.318\right) \qquad (95)$$

$$\frac{2}{a\sigma}\frac{\partial C_H}{\partial C_T}\Big|_{\alpha,V} = \left(\frac{2C_T}{a\sigma}\right)\mu\left[\frac{32}{a\sigma} - \frac{3}{2}\frac{\partial\lambda}{\partial C_T}\left(1-\frac{2}{3\pi}\mu\right)\right] - \lambda\mu$$
$$\left[\frac{3}{a\sigma}\left(1-\frac{2}{3\pi}\mu\right) + \frac{1}{\pi}\frac{\partial\lambda}{\partial C_T}\left(1-\frac{5\pi}{8}\mu\right)\right] \qquad (96)$$

The derivatives $\frac{\partial C_H}{\partial V}\Big|_\alpha$ and $\frac{\partial C_H}{\partial \alpha}\Big|_V$ are then obtained from,

$$\frac{\partial C_H}{\partial V}\Big|_\alpha = \frac{\partial C_H}{\partial V}\Big|_{\alpha, C_T} + \frac{\partial C_H}{\partial C_T}\Big|_{\alpha, V} \frac{\partial C_T}{\partial V}\Big|_\alpha \tag{97}$$

$$\frac{\partial C_H}{\partial \alpha}\Big|_V = \frac{\partial C_H}{\partial \alpha}\Big|_{V, C_T} + \frac{\partial C_H}{\partial C_T}\Big|_{\alpha, V} \frac{\partial C_T}{\partial \alpha}\Big|_V \tag{98}$$

The C_T derivatives were given previously.

The values of the resultant velocity V_R and the angle between the resultant and free stream velocities, ϕ, depend upon the value of the induced velocity of the rotor. Simple momentum considerations show that the induced velocity far downstream approaches a value twice that at the rotor plane in the absence of dissipation. Since experimental evidence shows (See Ref. 7) that the induced velocity approaches a value twice that at the disc at a rather short distance behind the disc, using the induced velocity at the disc to compute the resultant velocity acting on an airfoil behind the disc could lead to considerable error. In order to account for this effect we will use for the induced velocity the value $\lambda' \nu$ where λ' may have any value between 1 and 2 to be chosen later and ν is the value of the induced velocity at the disc which is given by:

$$\nu = \frac{T}{2\rho \pi R^2 \Omega R \sqrt{\lambda^2 + \mu^2}} \tag{99}$$

Consideration of Figure 1 shows that the resultant velocity is given by:

$$V_R^2 = [\lambda_N + V\sin(-\alpha)]^2 + [V\cos(-\alpha)]^2$$

$$= (\Omega R)^2 \left\{ \left[-\frac{(V\sin\alpha - \lambda_N)}{\Omega R} \right]^2 + \left[\frac{V\cos\alpha}{\Omega R} \right]^2 \right\}$$

$$= (\Omega R)^2 [\lambda_s^2 + \mu^2] \tag{100}$$

which defines λ_s and μ. Thus,

$$V_R = \Omega R \sqrt{\lambda_s^2 + \mu^2} \tag{101}$$

The relation between λ_s and λ is,

$$\lambda_s - \lambda = -\frac{\lambda_N}{\Omega R} \tag{102}$$

Taking the derivatives of V_R with respect to α, $\mu_x = V/\Omega R$, and C_T, we obtain the following expressions:

$$\frac{V_R}{(\Omega R)^2} \frac{\partial V_R}{\partial \mu_x}\Big|_{\alpha, C_T} = 2(2\lambda - \mu_x \sin\alpha) \frac{\partial \lambda}{\partial \mu_x} - 2\lambda \sin\alpha + \mu_x \tag{103}$$

$$\frac{V_R}{(\Omega R)^2} \frac{\partial V_R}{\partial C_T}\Big|_{\alpha, V} = 2(2\lambda - \mu_x \sin\alpha) \frac{\partial \lambda}{\partial C_T} \tag{104}$$

$$\frac{V_R}{(\Omega R)^2} \frac{\partial V_R}{\partial \alpha}\Big|_{V, C_T} = 2(2\lambda - \mu_x \sin\alpha) \frac{\partial \lambda}{\partial \alpha} - 2\lambda \mu_x \cos\alpha \tag{105}$$

Using the charts of Reference 12 (See Appendix A) for λ and its derivatives, we may plot the derivatives of V_R in general charts for a given value of λ'. This has been done for the two extreme values of λ' and the results are shown in Figure 5. It may be

noted that in some cases the charts for the two different values of λ' differ considerably. Using these charts with the trim conditions we easily evaluate the derivatives $\frac{\partial V_R}{\partial V}\Big|_\alpha$ and $\frac{\partial V_R}{\partial \alpha}\Big|_V$ from the expressions:

$$\frac{\partial V_R}{\partial V}\Big|_\alpha = \left[\frac{\partial V_R}{\partial \mu_x}\Big|_{\alpha, C_T} + \frac{\partial V_R}{\partial C_T}\Big|_{\alpha, V} \frac{\partial C_T}{\partial \mu_x}\Big|_\alpha\right] \frac{1}{\Omega R} \tag{106}$$

$$\frac{\partial V_R}{\partial \alpha}\Big|_V = \frac{\partial V_R}{\partial \alpha}\Big|_{V, C_T} + \frac{\partial V_R}{\partial C_T}\Big|_{\alpha, V} \frac{\partial C_T}{\partial \alpha}\Big|_V \tag{107}$$

From Figure 1, ϕ may be expressed as,

$$\mu \sin\phi = \frac{\lambda' V}{V_R} \cos\alpha \tag{108}$$

Taking the derivatives of this expression with respect to α , μ_x and C_T we obtain the expressions:

$$\cos\phi \frac{V_R}{\Omega R} \frac{\partial \phi}{\partial \alpha}\Big|_{V, C_T} = 2\Big\{\mu_x \cos 2\alpha + \lambda \mu \sin\alpha - \cos\alpha \frac{\partial \lambda}{\partial \alpha} - \lambda_s \cos\alpha \left(\frac{\Omega R}{V_R}\right)^2 \Big[(\mu_x \mu \sin\alpha - \lambda_s)\frac{\partial \lambda}{\partial \alpha} + \mu(\lambda_s - \lambda)\Big]\Big\} \tag{109}$$

$$\cos\phi \frac{V_R}{\Omega R} \frac{\partial \phi}{\partial \mu_x}\Big|_{\alpha, C_T} = 2\cos\alpha \Big[\mu \sin\alpha - \frac{\partial \lambda}{\partial \mu_x} - \left(\frac{\Omega R}{V_R}\right)^2 (\mu_x \mu \sin\alpha - \lambda_s)\Big(\lambda_s \frac{\partial \lambda}{\partial \mu_x} - \lambda \mu \sin\alpha + \frac{\mu_x}{2}\Big)\Big] \tag{110}$$

$$\cos\phi \frac{V_R}{\Omega R} \frac{\partial \phi}{\partial C_T}\Big|_{\alpha, V} = -2\cos\alpha \Big[1 + 2\left(\frac{\Omega R}{V_R}\right)^2 \lambda_s (\lambda - \lambda_s)\Big] \frac{\partial \lambda}{\partial C_T} \tag{111}$$

The derivatives were also plotted in the form of charts and are shown in Figure 6. All of the derivatives are functions of the parameter, $\bar{\mu}_x = \mu_x / \lambda_o$ and α, where $\lambda_o = -\sqrt{\frac{C_T}{2}}$ is the value of λ for $V = 0$. Also included with these charts are charts giving V_R, Φ, λ_s, λ and the derivatives of the induced velocity w.

Using these charts and the trim conditions, one can easily obtain the derivatives $\frac{\partial V_R}{\partial V}|_\alpha$, $\frac{\partial V_R}{\partial \alpha}|_V$, $\frac{\partial \Phi}{\partial V}|_\alpha$, $\frac{\partial \Phi}{\partial \alpha}|_V$ from the expressions:

$$\frac{\partial V_R}{\partial V}|_\alpha = \left[\frac{\partial V_R}{\partial \mu_x}|_{\alpha, C_T} + \frac{\partial V_R}{\partial C_T}|_{\alpha, V} \frac{\partial C_T}{\partial \mu_x}|_\alpha \right] \frac{1}{\Omega R} \tag{112}$$

$$\frac{\partial V_R}{\partial \alpha}|_V = \frac{\partial V_R}{\partial \alpha}|_{V, C_T} + \frac{\partial V_R}{\partial C_T}|_{\alpha, V} \frac{\partial C_T}{\partial \alpha}|_V \tag{113}$$

$$\frac{\partial \Phi}{\partial V}|_\alpha = \left[\frac{\partial \Phi}{\partial \mu_x}|_{\alpha, C_T} + \frac{\partial \Phi}{\partial C_T}|_{\alpha, V} \frac{\partial C_T}{\partial \mu_x}|_\alpha \right] \frac{1}{\Omega R} \tag{114}$$

$$\frac{\partial \Phi}{\partial \alpha}|_V = \frac{\partial \Phi}{\partial \alpha}|_{V, C_T} + \frac{\partial \Phi}{\partial C_T}|_{\alpha, V} \frac{\partial C_T}{\partial \alpha}|_V \tag{115}$$

As mentioned previously, the lift coefficient of the wing in the slipstream is represented by the expression,

$$C_{L_S} = C_{L_o}(\alpha') \left[1 + K \left(\frac{1}{1 + w/V} - 1 \right) \right] = C_{L_o} \bar{K} \tag{116}$$

where C_{L_O} is the lift curve slope of the airfoil for the power-off condition, i.e. for $N = 0$ in the above expression.

Thus,

$$\frac{\partial C_{L_S}}{\partial \alpha}\Big|_V = \frac{\partial C_{L_O}}{\partial \alpha'} \frac{\partial \alpha'}{\partial \alpha}\Big|_V \bar{K} + C_{L_O} \frac{\partial \bar{K}}{\partial \alpha}\Big|_V \tag{117}$$

and since,

$$\alpha' = 90 + \alpha - \Phi$$

we obtain,

$$\frac{\partial \alpha'}{\partial \alpha}\Big|_V = \left(1 - \frac{\partial \Phi}{\partial \alpha}\Big|_V\right) \tag{118}$$

giving for $\frac{\partial \bar{K}}{\partial \alpha}\Big|_V$ the expression,

$$\frac{\partial \bar{K}}{\partial \alpha}\Big|_V = -K \frac{1}{(1 + N/V)^2} \frac{1}{V} \frac{\partial N}{\partial \alpha} \tag{119}$$

An estimate of the magnitude of the second term in the expression for $\frac{\partial C_{L_S}}{\partial \alpha}\Big|_V$ shows that it is much smaller than the first term and thus we take,

$$\frac{\partial C_{L_S}}{\partial \alpha}\Big|_V = \frac{\partial C_{L_O}}{\partial \alpha'} \bar{K} \left(1 - \frac{\partial \Phi}{\partial \alpha}\Big|_V\right) \tag{120}$$

In a similar way we find,

$$\frac{\partial C_{L_S}}{\partial V}\Big|_\alpha = - \frac{\partial C_{L_O}}{\partial \alpha'} \bar{K} \frac{\partial \Phi}{\partial V}\Big|_\alpha \tag{121}$$

The C_{D_S} derivatives are simply given by:

$$\frac{\partial C_{D_S}}{\partial \alpha}\Big|_V = \frac{\partial C_{D_S}}{\partial \alpha'} \frac{\partial \alpha'}{\partial \alpha}\Big|_V = \frac{\partial C_{D_S}}{\partial \alpha'} \left(1 - \frac{\partial \Phi}{\partial \alpha}\Big|_V\right) \tag{122}$$

$$\frac{\partial C_{D_S}}{\partial V}\Big|_\alpha = \frac{\partial C_{D_S}}{\partial \alpha'} \frac{\partial \alpha'}{\partial V}\Big|_\alpha = - \frac{\partial C_{D_S}}{\partial \alpha'} \frac{\partial \Phi}{\partial V}\Big|_\alpha \tag{123}$$

In order to make an estimate of V_T and its derivatives, two separate cases must be considered. The first is for the tail not in the slipstream. This case will be valid for hovering and all high tilt angles up to some angle which will have to be determined from the geometry of a particular tail-rotor arrangement. Although the rotor disturbs the flow somewhat even outside of the slipstream, the disturbance is quite small (See Ref. 13), and can probably be neglected. For this case then we have,

$$V_T = V \qquad \frac{\partial V_T}{\partial V}\Big|_\alpha = 1 \qquad \frac{\partial V_T}{\partial \alpha}\Big|_V = 0$$

When the tail is in the slipstream the velocity can as a first approximation be taken as V_R computed for $\lambda' = \lambda$ and the derivatives are those given previously for V_R .

We will now consider the derivatives of the rotor pitching moment. In order to do this we must first have an expression for the pitching moment acting on the aircraft due to the rotor. This expression is obtained in the following analysis:

Figure 7 shows the forces acting at the flapping hinge which may cause a pitching moment if offset hinges are present. If the angle β is small, the resultant force on the blade is approximately equal to the centrifugal force and we may approximate the vertical force by,

$$F_{z_a} \cong CF \sin\beta \tag{124}$$

where,

$$\beta = \beta_0 - a_1 \cos\psi - b_1 \sin\psi \tag{125}$$

The moment acting at the hub is thus approximately,

$$M_H = F_{za}\, e \cong CF\, \beta\, e \tag{126}$$

where e is the amount of hinge offset. The pitching moment about the Y-axis is then,

$$M_{y_0} = -M_H \cos\psi \tag{127}$$

We are only interested in the value obtained by averaging this expression over the angle ψ. This is for b blades,

$$M_{y_0} = -\frac{b}{2\pi}\int_0^{2\pi} CF\, e \cos\psi\,(\beta_0 - a_1\cos\psi - b_1 \sin\psi)\,d\psi$$

$$= \frac{b}{2} CF\, e\, a_1 \tag{128}$$

The centrifugal force is,

$$CF = \Omega^2 \int_0^R m r\, dr = \Omega^2 M_S \tag{129}$$

where M_S is the static moment. Thus,

$$M_{y_0} = \frac{b}{2}\Omega^2 M_S\, e\, a_1 \tag{130}$$

For small μ,

$$a_1 = \mu_x \cos\alpha \left(\frac{8}{3}\theta + 2\lambda\right) \tag{131}$$

A more complete analysis of this moment valid for any μ and β is given in Reference 10.

The required derivatives are given by,

$$\frac{\partial C_{MCF}}{\partial V}\Big|_{\alpha} = \frac{\partial C_{MCF}}{\partial V}\Big|_{\alpha, C_T} + \frac{\partial C_{MCF}}{\partial C_T}\Big|_{\alpha, V} \frac{\partial C_T}{\partial V}\Big|_{\alpha} \tag{132}$$

$$\frac{\partial C_{MCF}}{\partial \alpha}\Big|_{V} = \frac{\partial C_{MCF}}{\partial \alpha}\Big|_{V, C_T} + \frac{\partial C_{MCF}}{\partial C_T}\Big|_{\alpha, V} \frac{\partial C_T}{\partial \alpha}\Big|_{V} \tag{133}$$

The terms on the right are easily obtained from the above expression for the moment as,

$$\frac{\partial C_{MCF}}{\partial V}\Big|_{\alpha, C_T} = \left(\frac{\Omega R}{V_R}\right)^2 K_{CF} \frac{\cos\alpha}{\Omega R}\left(\frac{8}{3}\theta + 2\lambda + 2\mu_x \frac{\partial \lambda}{\partial \mu_x}\right) \tag{134}$$

$$\frac{\partial C_{MCF}}{\partial \alpha}\Big|_{V, C_T} = -\left(\frac{\Omega R}{V_R}\right)^2 K_{CF} \mu_x \left[\left(\frac{8}{3}\theta + 2\lambda\right)\mu \sin\alpha - 2\frac{\partial \lambda}{\partial \alpha}\cos\alpha\right] \tag{135}$$

$$\frac{\partial C_{MCF}}{\partial C_T}\Big|_{\alpha, V} = 2\left(\frac{\Omega R}{V_R}\right)^2 K_{CF} \mu_x \cos\alpha \frac{\partial \lambda}{\partial C_T} \tag{136}$$

where, $$K_{CF} = \frac{N b e M_5}{\rho S_c R^2} \tag{137}$$

Dynamic Derivatives

Probably the most important dynamic derivatives are those which arise due to a pitch rate, or the $\dot{\theta}_f$ derivatives. Contributions to these derivatives arise from the tail and the rotors. There is also a small contribution due to the main wing but this is usually

negligible since the wing is so near the center of gravity of the aircraft. The damping due to the offset hinges of the rotor is very important since it does not depend upon the free stream velocity and hence provides damping while the aircraft is hovering.

Taking the derivatives of the moment equation with respect to $\dot{\theta}_f$ we obtain,

$$\frac{\partial C_M}{\partial \dot{\theta}_f} = -X_R \frac{\partial C_{ZR}}{\partial \dot{\theta}_f} - Z_R \frac{\partial C_{XR}}{\partial \dot{\theta}_f} - Z_T \frac{\partial C_{XT}}{\partial \dot{\theta}_f} + X_T \frac{\partial C_{ZT}}{\partial \dot{\theta}_f} + \frac{\partial C_{MCE}}{\partial \dot{\theta}_f} \tag{138}$$

The force derivatives appearing in this expression are given by,

$$\frac{\partial C_{ZR}}{\partial \dot{\theta}_f} = -2 \frac{\pi R^2}{S} \left(\frac{\Omega R}{V_R}\right)^2 \left[\frac{\partial C_T}{\partial \dot{\theta}_f} \sin i_w + \frac{\partial C_H}{\partial \dot{\theta}_f} \cos i_w \right] \tag{139}$$

$$\frac{\partial C_{XP}}{\partial \dot{\theta}_f} = 2 \frac{\pi R^2}{S} \left(\frac{\Omega R}{V_R}\right)^2 \left[\frac{\partial C_T}{\partial \dot{\theta}_f} \cos i_w - \frac{\partial C_H}{\partial \dot{\theta}_f} \sin i_w \right] \tag{140}$$

$$\frac{\partial C_{ZT}}{\partial \dot{\theta}_f} = \frac{2}{\rho S V_R^2} \left[-\frac{\partial L_T}{\partial \dot{\theta}_f} \cos \epsilon + \frac{\partial D_T}{\partial \dot{\theta}_f} \sin \epsilon \right] \tag{141}$$

$$\frac{\partial C_{XT}}{\partial \dot{\theta}_f} = \frac{2}{\rho S V_R^2} \left[-\frac{\partial L_T}{\partial \dot{\theta}_f} \sin \epsilon - \frac{\partial D_T}{\partial \dot{\theta}_f} \cos \epsilon \right] \tag{142}$$

Since C_T is given by the expression,

$$\frac{2C_T}{a\sigma} = \frac{\lambda}{2} + \frac{\theta}{3}$$

we obtain,

$$\frac{\partial C_T}{\partial \dot{\theta}_f} = \frac{a\sigma}{4} \frac{\partial \lambda}{\partial \dot{\theta}_f} \tag{143}$$

From Figure 8 we may calculate the change in the velocity at the rotor plane due to the pitch rate $\dot{\Theta}_f$. Using simple trigonometric relations we find,

$$\sin\beta = \frac{Z_p}{l_a + l_p} \quad \frac{\sin\left[\tan^{-1}\frac{Z_p}{X_p} - \tan^{-1}\frac{Z_R}{X_R}\right]}{\sin\left[\tan^{-1}\frac{Z_p}{X_p}\right]} \tag{144}$$

$$l = \frac{Z_R}{\sin\left[\tan^{-1}\frac{Z_R}{X_R}\right]} \tag{145}$$

Since we are only interested in the product of these two relations we may multiply them together and simplify considerably the resulting expression. Thus,

$$l\sin\beta = \frac{Z_p Z_R}{l_a + l_p} \quad \frac{\sin\left[\tan^{-1}\frac{Z_f}{X_p} - \tan^{-1}\frac{Z_R}{X_R}\right]}{\sin\left[\tan^{-1}\frac{Z_p}{X_p}\right]\sin\left[\tan^{-1}\frac{Z_R}{X_R}\right]} \tag{146}$$

Using the double angle relations this is readily seen to reduce to,

$$l\sin\beta = \frac{Z_p X_R - Z_R X_p}{l_a + l_p} \tag{147}$$

Expression for the distances in the above expression were given earlier.

The expression for λ in terms of $\dot{\Theta}_f$ then becomes,

$$\lambda = \frac{V\sin\alpha - v + l\dot{\Theta}_f \sin\beta}{\Omega R} \tag{148}$$

and,

$$\frac{\partial \lambda}{\partial \dot{\theta}_f} = \frac{\ell \sin\beta}{\Omega R} \tag{149}$$

Thus,

$$\frac{\partial C_T}{\partial \dot{\theta}_f} = \frac{a\sigma}{4} \frac{\ell \sin\beta}{\Omega R} \tag{150}$$

Using the expression given in Reference 11 for C_H ,

$$C_H = \frac{a\sigma}{2}\left[\frac{\delta\mu}{2a} + \frac{\theta a_1}{3} - \frac{\mu\lambda\theta}{2} + \frac{3\lambda a_1}{4} + \frac{\mu a_1^2}{4} - \frac{a_0 b_1}{6} + \frac{\mu a_2^2}{4}\right] \tag{151}$$

we can obtain an expression for $\frac{\partial C_H}{\partial \dot{\theta}_f}$. The parameters λ , a_1 , μ change with pitch rate. Thus,

$$\frac{\partial C_H}{\partial \dot{\theta}_f} = \frac{\partial C_H}{\partial a_1}\frac{\partial a_1}{\partial \dot{\theta}_f} + \frac{\partial C_H}{\partial \mu}\frac{\partial \mu}{\partial \dot{\theta}_f} + \frac{\partial C_H}{\partial \lambda}\frac{\partial \lambda}{\partial \dot{\theta}_f} \tag{152}$$

Taking the derivatives of expression 151 and neglecting the small terms, we obtain,

$$\frac{\partial C_H}{\partial a_1} = \frac{a\sigma}{2}\left[\frac{\theta}{3} + \frac{3\lambda}{4}\right] \tag{153}$$

$$\frac{\partial C_H}{\partial \mu} = \frac{a\sigma}{2}\left[-\frac{1}{2}\lambda\theta\right] \tag{154}$$

$$\frac{\partial C_H}{\partial \lambda} = \frac{a\sigma}{2}\left[-\frac{1}{2}\mu\theta + \frac{3}{4}a_1\right] \tag{155}$$

The derivative $\frac{\partial a_1}{\partial \dot{\theta}_f}$ is just the rotor lag,

$$\frac{\partial a_1}{\partial \dot{\theta}_f} = \frac{\partial a_1}{\partial \dot{\theta}_f}\Big|_{a,\mu_x} + \frac{\partial a_1}{\partial a}\Big|_{\mu_x,a_1}\frac{\partial \alpha}{\partial \dot{\theta}_f} + \frac{\partial a_1}{\partial \mu_x}\Big|_{a,a_1}\frac{\partial \mu_x}{\partial \dot{\theta}_f} \tag{156}$$

where

$$\frac{\partial a_1}{\partial \dot{\theta}_f}\Big|_{\alpha,\mu_x} = -\frac{16}{\gamma\Omega}$$

The last two terms of $\frac{\partial a_1}{\partial \dot{\theta}_f}$ are found to be negligible. (For derivation of this expression see Ref. 10) $\frac{\partial \lambda}{\partial \dot{\theta}_f}$ was evaluated before. From Fig. 8 we see that,

$$\frac{\partial M}{\partial \dot{\theta}_f} = \frac{\ell \cos(\alpha+\beta)\cos\alpha}{\Omega R} \tag{158}$$

Combining these expressions we obtain,

$$\frac{\partial C_H}{\partial \dot{\theta}_f} = -\frac{a\sigma}{2}\left[\left(\frac{\theta}{3}+\frac{3\lambda}{4}\right)\frac{16}{\gamma\Omega} + \frac{\lambda\theta\,\ell\sin\beta}{2\Omega R} + \left(\frac{3a_1}{4}-\frac{\mu\theta}{2}\right)\frac{\ell\cos^2\alpha}{\Omega R}\right] \tag{159}$$

The derivation of this expression was also carried out using the more accurate expression of Ref. 10 and the additional terms obtained were found to be quite small.

The lift at the tail is given by,

$$L_T = \frac{1}{2}\rho S_T V_T^2 a_T \alpha_T + T_T \tag{160}$$

When the aircraft is pitching at the rate $\dot{\theta}_f$, the angle of attack of the tail is,

$$\alpha_T = i_T + \varepsilon_0 + \alpha - i_W + \frac{\ell_T \dot{\theta}_f}{V_T} \tag{161}$$

Thus,

$$\frac{\partial L_T}{\partial \dot{\theta}_f} = \frac{1}{2}\rho S_T V_T a_T \ell_T + \frac{\partial T_T}{\partial \dot{\theta}_f} \tag{162}$$

Also,

$$\frac{\partial D_T}{\partial \dot{\theta}_f} = \frac{1}{2}\rho S_T V_T \frac{\partial C_{D_T}}{\partial \alpha_T}\ell_T \tag{163}$$

We find the contribution due to the tail fan in the following manner,

$$\frac{\partial T_T}{\partial \dot{\theta}_f} = \rho \pi R_T^2 (\Omega R)_T^2 \left[\frac{\partial C_{T_T}}{\partial \dot{\theta}_f}\Big|_\alpha + \frac{\partial C_{T_T}}{\partial \alpha_T}\Big|_{\dot{\theta}_f} \frac{\partial \alpha_T}{\partial \dot{\theta}_f} \right]$$

$$= \rho \pi R_T^2 (\Omega R)_T^2 \left[\frac{a_T \sigma_T}{4} \frac{\partial \lambda_T}{\partial \dot{\theta}_f} + \frac{a_T \sigma_T}{4} \frac{\partial \lambda_T}{\partial \alpha_T} \frac{l_T}{V_T} \right] \quad (164)$$

From Figure 9 we see that,

$$\lambda_T = \frac{V_T \sin \alpha_T + l_T \dot{\theta}_f \cos \alpha_T - v_T}{(\Omega R)_T} \quad (165)$$

Then,

$$\frac{\partial \lambda_T}{\partial \dot{\theta}_f} = \frac{l_T \cos \alpha_T}{(\Omega R)_T} \quad (166)$$

$$\frac{\partial \lambda_T}{\partial \alpha_T} = \frac{V_T \cos \alpha_T - l_T \cancel{\dot{\theta}_f}^{\,0} \sin \alpha_T - \frac{\partial v_T}{\partial \alpha_T}}{(\Omega R)_T} \quad \text{neg} \quad (167)$$

Thus,

$$\frac{\partial T_T}{\partial \dot{\theta}_f} = \rho \pi R_T^2 (\Omega R)_T \frac{a_T \sigma_T}{2} l_T \cos \alpha_T \quad (168)$$

The pitching moment derivative $\frac{\partial C_{MCF}}{\partial \dot{\theta}_f}$ is computed in the following manner:

The expression for the moment was given earlier as,

$$M_{y_0} = \frac{Nb}{2} M_s \Omega^2 e a_1$$

Thus,

$$\frac{\partial C_{MCF}}{\partial \dot{\theta}_f} = \frac{\partial C_{MCF}}{\partial a_1} \frac{\partial a_1}{\partial \dot{\theta}_f} = \frac{Nbe}{\rho s c} \left(\frac{\Omega R}{V_R}\right)^2 \frac{M_s}{R^2} \left(\frac{-16}{\gamma \Omega}\right) \quad (169)$$

The derivative of the X-force equation with respect to $\dot{\theta}_f$ is given by,

$$\frac{\partial C_X}{\partial \dot{\theta}_f} = \frac{2}{\rho S V_R^2} \frac{\partial X}{\partial \dot{\theta}_f} = \frac{2}{\rho S V_R^2} \left[- m V \cos(\alpha - i_w) + \frac{\partial F_{X_I}}{\partial \dot{\theta}_f} + N \frac{\partial F_{X_R}}{\partial \dot{\theta}_f} \right] \tag{170}$$

These terms have been evaluated previously. The derivative of the Z-force equation with respect to $\dot{\theta}_f$ is likewise,

$$\frac{\partial C_Z}{\partial \dot{\theta}_f} = \frac{2}{\rho S V_R^2} \left[- m V \sin(\alpha - i_w) + \frac{\partial F_{Z_I}}{\partial \dot{\theta}_f} + N \frac{\partial F_{Z_R}}{\partial \dot{\theta}_f} \right] \tag{171}$$

These terms were also evaluated while finding the moment derivatives.

The derivative $C_{M_{\ddot{\theta}_f}}$

From equation 42 we obtain,

$$\frac{\partial C_M}{\partial \ddot{\theta}_f} = \frac{2}{\rho S V_R^2} \frac{\partial M}{\partial \ddot{\theta}_f} = \frac{-2 I_y}{\rho S V_R^2 c} \tag{172}$$

where I_y is the moment of inertia of the aircraft about the Y-axis. This is not constant but varies with the wing tilt angle i_w. However, the amount of variation is quite small and may usually be neglected.

Derivatives with respect to $\dot{V}$

$$\frac{\partial C_X}{\partial \dot{V}} = \frac{2}{\rho S V_{R_0}^2} \frac{\partial X}{\partial \dot{V}} = \frac{2}{\rho S V_{R_0}^2} m \sin(\alpha - i_w)_0 \tag{173}$$

$$\frac{\partial C_Z}{\partial \dot{V}} = \frac{2}{\rho S V_{R_0}^2} \frac{\partial Z}{\partial \dot{V}} = -\frac{2}{\rho S V_{R_0}^2} m \cos(\alpha - i_w)_0 \tag{174}$$

$$\frac{\partial C_M}{\partial \dot{V}} = \frac{2}{\rho S V_{R_0}^2} \frac{\partial M}{\partial \dot{V}} = 0 \tag{175}$$

Derivatives with respect to rate of change of angle of attack $\dot{\alpha}$

$$\frac{\partial C_X}{\partial \dot{\alpha}} = \frac{2}{\rho S V_{R_0}^2} \frac{\partial X}{\partial \dot{\alpha}} = \frac{2}{\rho S V_R^2} \left[-m V \cos(\alpha - i_w)_0 \right] + \frac{\partial C_{X_T}}{\partial \dot{\alpha}} \tag{176}$$

$$\frac{\partial C_Z}{\partial \dot{\alpha}} = \frac{2}{\rho S V_{R_0}^2} \frac{\partial Z}{\partial \dot{\alpha}} = \frac{2}{\rho S V_{R_0}^2} \left[-m V \sin(\alpha - i_w)_0 \right] + \frac{\partial C_{Z_T}}{\partial \dot{\alpha}} \tag{177}$$

$$\frac{\partial C_M}{\partial \dot{\alpha}} = \frac{2}{\rho S V_R^2 c} \frac{\partial M}{\partial \dot{\alpha}} = x_T \frac{\partial C_{Z_T}}{\partial \dot{\alpha}} - z_T \frac{\partial C_{X_T}}{\partial \dot{\alpha}} \tag{178}$$

These derivatives arise due to the fact that there is a time lag between a change in the angle α and its effect on the downwash angle at the tail ϵ. This time lag is the amount of time required for the flow to move from the wing to the tail and is given approximately by, $\Delta t = \frac{l_T}{V_T}$. The contribution to the angle of attack of the tail due to this effect is then,

$$\frac{\partial \epsilon}{\partial \alpha} \frac{\partial \alpha}{\partial t} \Delta t = \frac{\partial \epsilon}{\partial \alpha} \dot{\alpha} \frac{l_T}{V_T} \tag{179}$$

and the angle of attack of the tail is,

$$\alpha_T = i_T + 90 + \alpha - i_w - \frac{\partial \epsilon}{\partial \alpha} \left(\alpha - \dot{\alpha} \frac{l_T}{V_T} \right) \tag{180}$$

The derivative of this with respect to $\dot{\alpha}$ is,

$$\frac{\partial \alpha_T}{\partial \dot{\alpha}} = \frac{\partial \epsilon}{\partial \alpha} \frac{l_T}{V_T} \tag{181}$$

The derivatives of C_{X_T} and C_{Z_T} are given by,

$$\frac{\partial C_{X_T}}{\partial \dot{\alpha}} = \frac{-2}{\rho S V_{R_0}^2} \left[\frac{\partial L_T}{\partial \dot{\alpha}} \sin\epsilon + \frac{\partial D_T}{\partial \dot{\alpha}} \cos\epsilon \right] \tag{182}$$

$$\frac{\partial C_{ZT}}{\partial \dot{\alpha}} = -\frac{2}{\rho S V_{R_0}^2}\left[\frac{\partial L_T}{\partial \dot{\alpha}}\cos\epsilon - \frac{\partial D_T}{\partial \dot{\alpha}}\sin\epsilon\right] \tag{183}$$

The lift and drag derivatives are,

$$\frac{\partial L_T}{\partial \dot{\alpha}} = \frac{1}{2}\rho S_T V_T^2 a_T \frac{\partial \alpha_T}{\partial \dot{\alpha}} + \frac{\partial T_T}{\partial \dot{\alpha}} \tag{184}$$

$$\frac{\partial D_T}{\partial \dot{\alpha}} = \frac{1}{2}\rho S_T V_T^2 \frac{\partial C_{D_T}}{\partial \alpha_T}\frac{\partial \alpha_T}{\partial \dot{\alpha}} \tag{185}$$

We may evaluate the derivative of the tail rotor thrust in the following way,

$$\frac{\partial T_T}{\partial \dot{\alpha}} = \rho \pi R_T^2 (\Omega R)_T^2 \frac{\partial C_{T_T}}{\partial \dot{\alpha}} \tag{186}$$

The thrust coefficient is given by,

$$\frac{2 C_{T_T}}{a_T \sigma_T} = \frac{\theta_T}{2} + \frac{\lambda_T}{2} \tag{187}$$

Considering the collective pitch θ_T constant, we obtain,

$$\frac{\partial C_{T_T}}{\partial \dot{\alpha}} = \frac{a_T \sigma_T}{4}\frac{\partial \lambda_T}{\partial \dot{\alpha}} \tag{188}$$

The inflow factor for the tail rotor is,

$$\lambda_T = \frac{V_T \sin\alpha_T - N_T}{(\Omega R)_T} \tag{189}$$

Thus,

$$\frac{\partial \lambda_T}{\partial \dot{\alpha}} = \frac{V_T}{(\Omega R)_T} \cos \alpha_T \frac{\partial \alpha_T}{\partial \dot{\alpha}} \tag{190}$$

Combining all of the above expressions, we obtain,

$$\frac{\partial C_{XT}}{\partial \dot{\alpha}} = -\frac{\ell_T}{S V_R^2} \frac{\partial \epsilon}{\partial \alpha} \left[a_T \left(S_T V_T + R_T C_T \cos \alpha_T (\Omega R_T) \right) \right.$$
$$\left. \sin \epsilon + S_T V_T \frac{\partial C_{DT}}{\partial \alpha_T} \cos \epsilon \right] \tag{191}$$

$$\frac{\partial C_{ZT}}{\partial \dot{\alpha}} = -\frac{\ell_T}{S V_R^2} \frac{\partial \epsilon}{\partial \alpha} \left[a_T S_T V_T \cos \epsilon \right.$$
$$\left. - S_T V_T \frac{\partial C_{DT}}{\partial \alpha_T} \sin \epsilon \right] \tag{192}$$

The most important parameters needed in order to evaluate these expressions are the downwash angle at the tail ϵ and its derivative with respect to angle of attack α . These derivatives are very difficult to evaluate with accuracy, since the flow at the tail is effected considerably by both the wing and the rotor and the effect of these change with the wing tilt angle i_w .

Evaluation of Coefficients to Stability Quartic

The non-dimensional derivatives developed in the previous section can be used in place of the dimensional derivatives in equations 43-45 since all of the force derivatives were non-dimensionalized with respect to the same force and all of the moment derivatives with respect to the same moment. We wish to determine the stability characteristics of the solutions to this set of homogeneous, linear, constant-coefficient differential equations. To do this we assume solutions for each of the variables of the form $V = V_1 e^{\lambda t}$, etc. In order for non-zero solutions to exist for the three constants V, α, θ, the determinant of their coefficients must be zero. Thus,

$$\begin{vmatrix} (C_{X_V} + C_{X_{\dot{V}}}\lambda) & (C_{X_\alpha} + C_{X_{\dot{\alpha}}}\lambda) & (C_{X_\theta} + C_{X_{\dot{\theta}}}\lambda) \\ (C_{Z_V} + C_{Z_{\dot{V}}}\lambda) & (C_{Z_\alpha} + C_{Z_{\dot{\alpha}}}\lambda) & (C_{Z_\theta} + C_{Z_{\dot{\theta}}}\lambda) \\ (C_{M_V} + C_{M_{\dot{V}}}\lambda) & (C_{M_\alpha} + C_{M_{\dot{\alpha}}}\lambda) & (C_{M_{\dot{\theta}}}\lambda + C_{M_{\ddot{\theta}}}\lambda^2) \end{vmatrix} = 0 \qquad (193)$$

where the lower subscript indicates the derivative with respect to a variable with the other variables held constant.

Expansion of this determinant gives a quartic equation in λ. These four solutions for λ determine the character of the motion of the aircraft in response to a small disturbance. We write the quartic in the form,

$$A\lambda^4 + B\lambda^3 + C\lambda^2 + D\lambda + E = 0 \tag{194}$$

Expansion of the above determinant gives the coefficients of this equation in terms of the stability derivatives. Eliminating the derivatives C_{Z_θ}, $C_{Z_{\dot{V}}}$, $C_{M_{\dot{V}}}$ which are zero for $\theta_{f_0} = 0$, i.e. for the aircraft initially trimmed level, we obtain the following expressions for the coefficients:

$$A = C_{M_{\ddot{\theta}}} C_{X_{\dot{V}}} C_{Z_{\dot{\alpha}}} \tag{195}$$

$$B = C_{M_{\ddot{\theta}}} \left(C_{X_V} C_{Z_{\dot{\alpha}}} - C_{Z_V} C_{X_{\dot{\alpha}}} + C_{X_{\dot{V}}} C_{Z_\alpha}\right) + C_{M_{\dot{\theta}}} C_{Z_{\dot{\alpha}}} C_{X_{\dot{V}}} - C_{M_{\dot{\alpha}}} C_{X_{\dot{V}}} C_{Z_{\dot{\theta}}} \tag{196}$$

$$C = C_{M_{\ddot{\theta}}} \left(C_{X_V} C_{Z_\alpha} - C_{Z_V} C_{X_\alpha}\right) + C_{M_{\dot{\theta}}} \left(C_{X_V} C_{Z_{\dot{\alpha}}} + C_{X_{\dot{V}}} C_{Z_\alpha} - C_{Z_V} C_{X_{\dot{\alpha}}}\right) + C_{M_{\dot{\alpha}}} \left(C_{Z_V} C_{X_{\dot{\theta}}} - C_{X_V} C_{Z_{\dot{\theta}}}\right) - C_{M_\alpha} C_{X_{\dot{V}}} C_{Z_{\dot{\theta}}} + C_{M_V} \left(C_{X_{\dot{\alpha}}} C_{Z_{\dot{\theta}}} - C_{Z_{\dot{\alpha}}} C_{X_{\dot{\theta}}}\right) \tag{197}$$

$$D = C_{M\ddot{\theta}}\left(C_{X_V}C_{Z_\alpha} - C_{Z_V}C_{X_\alpha}\right) + \underline{C_{M\dot{\alpha}}C_{Z_V}C_{X_\theta}}$$

$$+ \underline{C_{M_\alpha}\left(C_{Z_V}C_{X_{\dot{\theta}}} - C_{X_{\dot{V}}}C_{Z_\theta}\right)} + C_{M_V}\left(C_{X_\alpha}C_{Z_{\dot{\theta}}}\right.$$

$$\left. - \underline{C_{Z_\alpha}C_{X_{\dot{\theta}}}} - C_{Z_{\dot{\alpha}}}C_{X_\theta}\right) \tag{198}$$

$$E = C_{X_\theta}\left(C_{Z_V}C_{M_\alpha} - C_{M_V}C_{Z_\alpha}\right) \tag{199}$$

The underlined terms are generally smaller than the others and in many cases can be neglected.

These expressions for the coefficients can be considerably simplified and made more physically understandable by introducing the concept of the static and maneuver "Margins".

Consider first the airplane in trimmed level flight. If the velocity is changed by a small amount, the change in the moment about the Y-axis with the angle of attack free to change but with the restriction that constant vertical force be maintained, i.e. $C_Z = C'_{ST}$, is given by the total derivative,

$$\left.\frac{dC_M}{dV}\right|_{C_Z} = \left.\frac{\partial C_M}{\partial V}\right|_\alpha + \left.\frac{\partial C_M}{\partial \alpha}\right|_V \left.\frac{d\alpha}{dV}\right|_{C_Z} \tag{200}$$

Taking the derivative of the equation,

$$C_Z = C'_{ST} \tag{201}$$

we obtain,

$$\frac{\partial C_z}{\partial \alpha}\Big|_V d\alpha + \frac{\partial C_z}{\partial V}\Big|_\alpha dV = 0 \tag{202}$$

Solving this for the total derivative $\frac{d\alpha}{dV}\Big|_{C_z}$,

$$\frac{d\alpha}{dV}\Big|_{C_z} = -\frac{\partial C_z}{\partial V}\Big|_\alpha \Big/ \frac{\partial C_z}{\partial \alpha}\Big|_V \tag{203}$$

Thus we obtain,

$$\frac{dC_M}{dV} = \frac{\partial C_M}{\partial V}\Big|_\alpha - \frac{\partial C_M}{\partial \alpha}\Big|_V \frac{\frac{\partial C_z}{\partial V}\Big|_\alpha}{\frac{\partial C_z}{\partial \alpha}\Big|_V} \tag{204}$$

or,

$$\frac{\partial C_z}{\partial \alpha}\Big|_V \frac{dC_M}{dV}\Big|_{C_z} = -\frac{\partial C_z}{\partial V}\Big|_\alpha \frac{dC_M}{d\alpha}\Big|_{C_z}$$

$$= \frac{\partial C_z}{\partial \alpha}\Big|_V \frac{\partial C_M}{\partial V}\Big|_\alpha - \frac{\partial C_M}{\partial \alpha}\Big|_V \frac{\partial C_z}{\partial V}\Big|_\alpha = (S.M.) \tag{205}$$

This grouping of derivatives is called the static margin, and the E coefficient can be expressed in terms of it as,

$$E = -C_{x_\theta}(S.M.) \tag{206}$$

Now consider the aircraft in a steady pull-up (See Fig. 10). The change in the moment about the Y-axis due to the rate of rotation of the aircraft is given by the total derivative,

$$\frac{dC_M}{d\dot{\theta}}\Big|_{C_z} = \frac{\partial C_M}{\partial \dot{\theta}}\Big|_\alpha + \frac{\partial C_M}{\partial \alpha}\Big|_{\dot{\theta}} \frac{d\alpha}{d\dot{\theta}}\Big|_{C_z} \tag{207}$$

From Figure 10 we see that the Z-force in a steady pull-up is,

$$F_z = F_{z_\alpha} - mg\cos\theta - mV\dot{\theta} = 0 \tag{208}$$

and its derivative with respect to $\dot{\theta}$ is,

$$\frac{\partial F_z}{\partial \dot{\theta}} = -mV \tag{209}$$

or in non-dimensional form,

$$\frac{\partial C_z}{\partial \dot{\theta}} = \frac{-2mV}{\rho S V_R^2} \tag{210}$$

This gives a physical picture of the derivative and is seen to be the first term of the expression obtained previously for this derivative. The other terms are due to change in the velocity at the tail and rotor and are usually smaller than the term obtained above. For $C_z = c'st$. we obtain,

$$\frac{\partial C_z}{\partial \dot{\theta}}\Big|_{\alpha,V} d\dot{\theta} + \frac{\partial C_z}{\partial \alpha}\Big|_{\dot{\theta},V} d\alpha = 0 \tag{211}$$

from which we can obtain the total derivative,

$$\frac{d\alpha}{d\dot{\theta}}\Big|_{C_z} = -\frac{\partial C_z}{\partial \dot{\theta}} \Big/ \frac{\partial C_z}{\partial \alpha}\Big|_V \tag{212}$$

Thus,

$$\frac{dC_M}{d\dot{\theta}} = \frac{\partial C_M}{\partial \dot{\theta}} - \frac{\partial C_M}{\partial \alpha}\Big|_V \frac{\frac{\partial C_z}{\partial \dot{\theta}}}{\frac{\partial C_z}{\partial \alpha}\Big|_V} \tag{213}$$

Multiplying by $\frac{\partial C_z}{\partial \alpha}\Big|_V$ we obtain,

$$\frac{\partial C_z}{\partial \alpha}\Big|_V \frac{dC_M}{d\dot{\theta}} = \frac{\partial C_z}{\partial \alpha}\Big|_V \frac{\partial C_M}{\partial \dot{\theta}} - \frac{\partial C_z}{\partial \dot{\theta}} \frac{\partial C_M}{\partial \alpha}\Big|_V = (M.M.) \tag{214}$$

This group of terms is usually called the maneuver margin and appears in the C coefficient and in the D coefficient.

If we make these substitutions in the expressions for the coefficients and omit the terms which are small compared to the others, we obtain the following expressions:

$$A = C_{M\ddot{\theta}} C_{X\dot{v}} C_{Z\dot{\alpha}} \tag{215}$$

$$B = C_{Z\dot{\alpha}} \left[C_{M\ddot{\theta}} C_{X_v} + C_{M\dot{\theta}} C_{X\dot{v}} \right] + C_{M\ddot{\theta}} C_{X\dot{v}} C_{Z_\alpha} \tag{216}$$

$$C = C_{X\dot{v}} (M.M.) + C_{M\dot{\theta}} C_{X_v} C_{Z\dot{\alpha}} \tag{217}$$

$$D = C_{X_v} (M.M.) - C_{M\dot{\theta}} C_{Z_v} C_{X_\alpha} + C_{M_v} (C_{X_\alpha} C_{Z\dot{\theta}} - C_{Z\dot{\alpha}} C_{X_\theta}) \tag{218}$$

$$E = -C_{X_\theta} (S.M.) \tag{219}$$

Characteristic Equation in Hovering

When the aircraft is hovering the variable α is no longer defined since the free stream velocity is zero. The equations can be considerably simplified due to the fact that the coupling between the vertical degree of freedom and the other degrees of freedom is very weak, i.e. small forward velocities or angular rotations do not cause any appreciable change in the Z-force and small perturbations in the vertical velocity cause only negligibly small changes in the X-force and the moment about the Y-axis. Thus the motion can be approximated by the following two equations:

$$\begin{aligned} (C_{X_v} + C_{X\dot{v}} \lambda) v + (C_{X_\theta} + C_{X\dot{\theta}} \lambda) \theta &= 0 \\ C_{M_v} v + (C_{M\dot{\theta}} \lambda + C_{M\ddot{\theta}} \lambda^2) \theta &= 0 \end{aligned} \tag{220}$$

Setting the determinant of the coefficients equal to zero gives a cubic equation in λ with the following coefficients:

$$B = C_{X_{\dot{V}}} C_{M_{\ddot{\theta}}} \tag{221}$$

$$C = C_{X_V} C_{M_{\ddot{\theta}}} + C_{X_{\dot{V}}} C_{M_{\dot{\theta}}} \tag{222}$$

$$D = C_{X_V} C_{M_{\dot{\theta}}} - C_{M_V} C_{X_{\ddot{\theta}}} \tag{223}$$

$$E = -C_{M_V} C_{X_\theta} \tag{224}$$

Calculation of roots to the Quartic and Cubic Equations for Various Flight Configurations

In order to evaluate the stability for the various flight configurations it is necessary to have trim conditions at each tilt angle at which the roots of the characteristic equation are desired. These have been evaluated with the aid of a digital computer for the Vertol 76 (Ref. 14), and are shown plotted as a function of α and V in Figure 11. The velocities on these charts are for a 1:5.2 scale model. The full scale velocity is thus 2.28 times the velocities on this scale. Given these conditions, values for the wing and rotor derivatives are easily obtained by using the charts in the appendix and these derivatives allow calculation of the required force and moment derivatives. These calculations were carried out for hovering and at intervals of 10 degrees down to 15 degrees and also for 7 degrees which is approximately the forward flight angle of attack.

(In forward flight the wing tilt angle is approximately equal to the angle of attack.) The values obtained for the derivatives and for the coefficients of the stability quartic are given in the appendix. Using these coefficients the quartics were solved and the results are shown in Figure 12. Values of the various parameters for the Vertol 76 and the lift curve slope assumed are given in Appendix B. The values obtained for all of the derivatives and variables at each of the tilt angles are given in Appendix D.

It should be borne in mind that these calculations were intended merely to provide a qualitative picture of how the stability changes while the aircraft moves through transition and consequently they can not be expected to give accurate values for the period and damping of the actual aircraft. Inspection of the various contributions to the coefficients of the quartic allows one to see which are the main terms and which can usually be neglected.

Approximate Factorization of Quartic

Often much useful information can be obtained by an approximate factorization of the quartic. This gives an expression for each of the roots in terms of the stability derivatives. If such an approximation is sufficiently accurate and results in expressions which are not too complicated, it will enable one to determine very easily the effect of any derivative on the quartic roots.

Since the roots which represent the short-period oscillation are usually much larger than the other two for conventional airplanes, we assume that an approximation to the short period oscillation can be

obtained by dropping the last two terms of the quartic. Doing this and retaining only the largest terms of the first three coefficients, we obtain the following quadratic:

$$C_{M\ddot{\theta}}\lambda^2 + C_{M\dot{\theta}}\lambda + \frac{(M.M.)}{C_{Z\dot{\alpha}}} = 0 \tag{225}$$

To obtain an approximation to the other two roots we assume a quadratic of the form $a\lambda^2+b\lambda+c$, and multiply it times the short-period approximation. Then, equating coefficients of like powers of λ , gives five equations relating a , b , c , to known coefficients. Using the first, fourth and fifth of these we obtain the following expressions for the coefficients of the quadratic which should approximate the remaining roots of the quartic:

$$a = C_{X_{\dot{V}}} \tag{226}$$

$$b = \frac{C_{X_\theta} C_{Z_{\dot{\alpha}}} C_{M_\alpha}}{(M.M.)^2}\left[C_{M_V} C_{Z_{\dot{\theta}}} - C_{M_{\dot{\theta}}} C_{Z_V}\right] + C_{X_V} \tag{227}$$

$$c = -C_{X_\theta}\frac{(S.M.)}{(M.M.)} \tag{228}$$

In the short period approximation the constant term is directly proportional to (MM) whereas in the second quadratic both the constant and λ terms are inversely proportional to (MM). We thus might expect that the larger (MM), the better the approximation.

To determine the accuracy of the approximation, these two quadratics were solved for a number of tilt angles and compared with solutions of the complete quartic. This comparison is illustrated in Figure 13. We see that for the lower tilt angles the approximation

is fairly good and breaks down when the roots become smaller as would be expected. We may also note that the approximation did not predict the increased damping of the 7 degree tilt angle.

Variation of quartic roots with tilt angle

In order to discuss VTOL aircraft stability it is necessary to know what types of response are considered desirable and also since the desirable type can not always be attained, we would like to know what is acceptable.

The stability criterion is most conveniently expressed by specifying the regions on the complex plane into which the roots of the quartic which determine the nature of the motion should fall. It is known, of course, that the roots should fall into the left half plane; however, as is shown by the hovering helicopter, this condition is not necessary in order that an aircraft be capable of being flown. An instability similar to that which exists in most hovering helicopters would, of course, never be tolerated in a conventional airplane. We thus see that any criterion for desirable or acceptable stability will depend on the type of aircraft which is being considered. It is also true, as mentioned before, that handling qualities depend on more than the values of the complex frequencies. The amount of control available to the pilot is also very important. Several criteria have recently been established for VTOL handling qualities by means of simulators (See e.g. Ref. 15). Although such results will have to be examined more closely by actual flight test, they do give some indication of the type of response which is acceptable to the pilot. When the VTOL has developed considerable velocity in the conversion, then handling quality criteria established for

conventional subsonic aircraft can be used as a basis for establishing desirable VTOL handling qualities. Some of the results of these two criteria are shown in Figure 12.

In order to obtain some indication of how the stability characteristics change as the VTOL aircraft goes through a constant altitude conversion, a sample calculation for a typical aircraft was carried out using the equations developed in Section I. The results of these calculations for the Vertol 76 are shown in Figure 12. Typical roots for an airplane and hovering helicopter are also shown. These results serve only as an indication of how the roots vary with tilt angle and should not be thought of as giving an accurate picture of the stability of the Vertol 76 since the effects of the fuselage were omitted from the calculations and a large number of simplifying assumptions were made in order that approximate results might be obtained without recourse to experimental data.

In the discusssion which follows the effect of the important stability derivatives will be considered as well as the effect of various physical parameters on these derivatives. Whenever possible, root locus plots are used to show the effect of increasing or decreasing the value of the important derivatives starting from the value which was estimated for the sample aircraft.

From Figure 12 we see that the hovering roots are quite similar to those of the typical hovering helicopter shown; i.e., there is an unstable oscillation and a real convergence. The oscillation for the hovering VTOL doubles amplitude in about 1.5 seconds while the helicopter takes 3.5 seconds to double amplitude. According to the

criteria of A'Harrah and Kwiatkowski which is shown in Figure 12, the VTOL is unflyable in hovering while the helicopter roots shown fall into the acceptable region. It will be noticed that the damping ratios of the two oscillations are nearly the same. It thus appears that in this regime damping ratio is not a significant measure of the handling qualities.

The real convergence shown for the VTOL is quite rapid, having a time to half amplitude of only 0.5 seconds. This is seen to be considerably more rapid than the helicopter.

It is interesting to see how these hovering roots may be altered by changing the various derivatives which appear in the coefficients of the cubic equation which determines the roots. The constant coefficient of the hovering cubic is,

$$E = -C_{m_w} C_{x_\theta} \tag{229}$$

Since C_{x_θ} is always negative, the static stability is determined by the sign of the derivative C_{M_w} . The following root locus sketch for variation of C_{M_w} shows how the stability characteristics of the aircraft change as this derivative is changed:

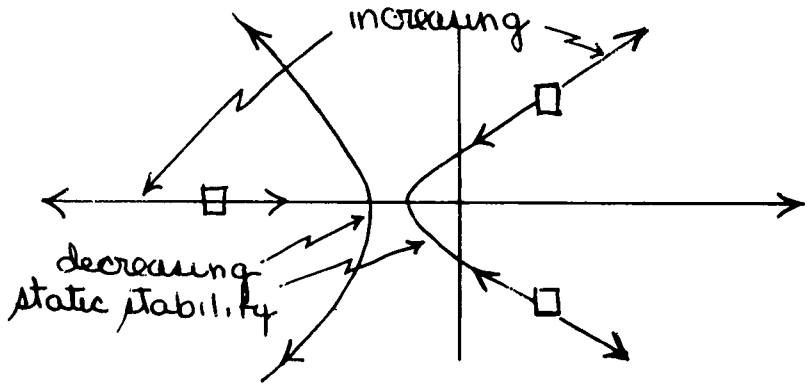

We see from this diagram that although the time to reach half amplitude of the aperiodic mode is decreased by increasing the static stability, the time to double amplitude of the oscillation is also decreased. Thus, making the aircraft statically more stable makes it dynamically more unstable. Decreasing the static stability has just the opposite effect. The dynamic stability improves until it reaches the real axis where the roots combine to give two real convergences, one of which soon becomes unstable. The point at which it crosses the axis is where $C_{m_{NP}} = 0$.

Probably the most important derivative in the determination of the stability characteristics of the hovering VTOL is the pitch damping $C_{m_{\dot{\theta}}}$. The next sketch shows how the cubic roots are effected by variation of this derivative:

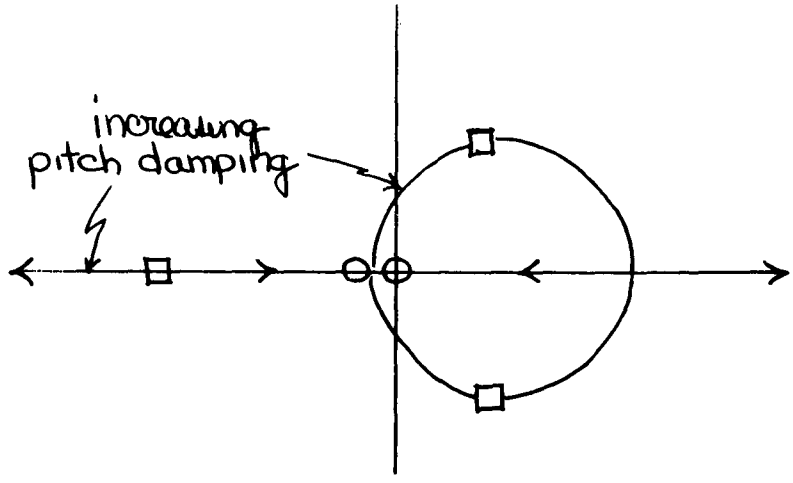

We see from this that a definite improvement in the hovering roots can be obtained by increasing the pitch damping. The time to half amplitude of the real convergence is further decreased

while at the same time the damping characteristics of the oscillation are improved. This derivative in hovering is mainly due to the offset hinges of the rotor and can be increased by increasing the amount of offset.

The effect of changing the moment of inertia about the Y-axis is shown below:

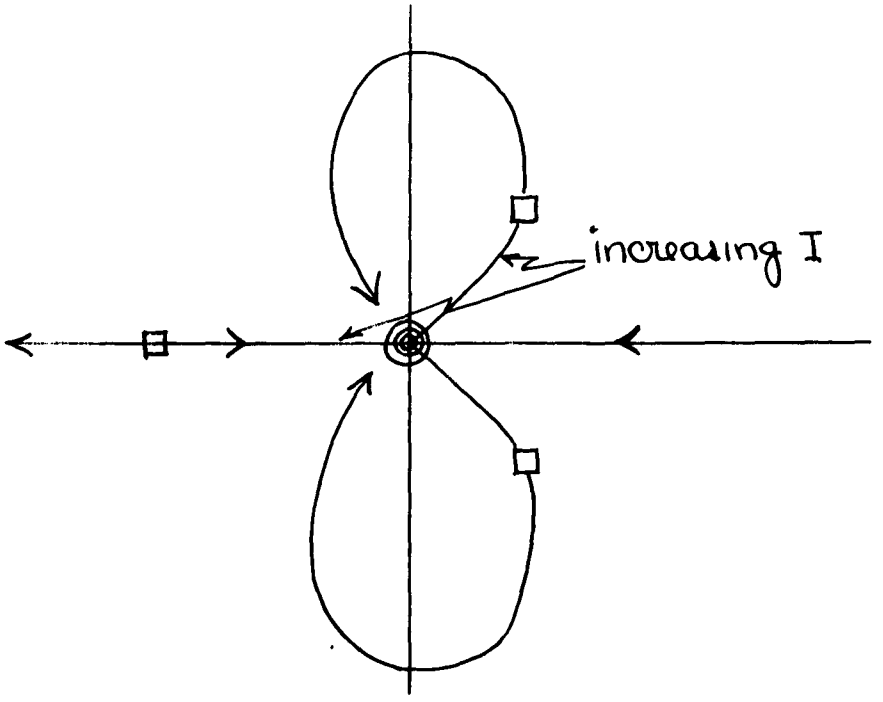

Increasing the moment of inertia causes all of the roots to move toward the origin. By comparing this sketch with Figure 12 we see that increasing the moment of inertia of the VTOL a sufficient amount makes them quite similar to those of the hovering helicopter shown in the drawing.

We now consider what happens as the wing is tilted forward from the hovering position. The first fact which can be noticed from an examination of Figure 12 is that the stability characteristics change quite rapidly as the aircraft begins to move forward. This is due to

the fact that as soon as the aircraft has some forward velocity the tail has an important effect on the derivatives whereas in hovering it had practically no effect at all.

With ten degrees of tilt angle the short period oscillation changes period only slightly, but the damping characteristics are improved considerably. As the wing is tilted down another 10 degrees the real part of the root changes from positive to negative while the period decreases to about four seconds.

It is worth mentioning here that there is no definite reason why the loci sketched through the points in Figure 12 should be drawn as they are. Thus, it is possible that the mode which becomes similar to the airplane short period could be associated with the mode which is represented by the two real convergences near hovering. Thus, the locus through the roots could appear as in the following sketch:

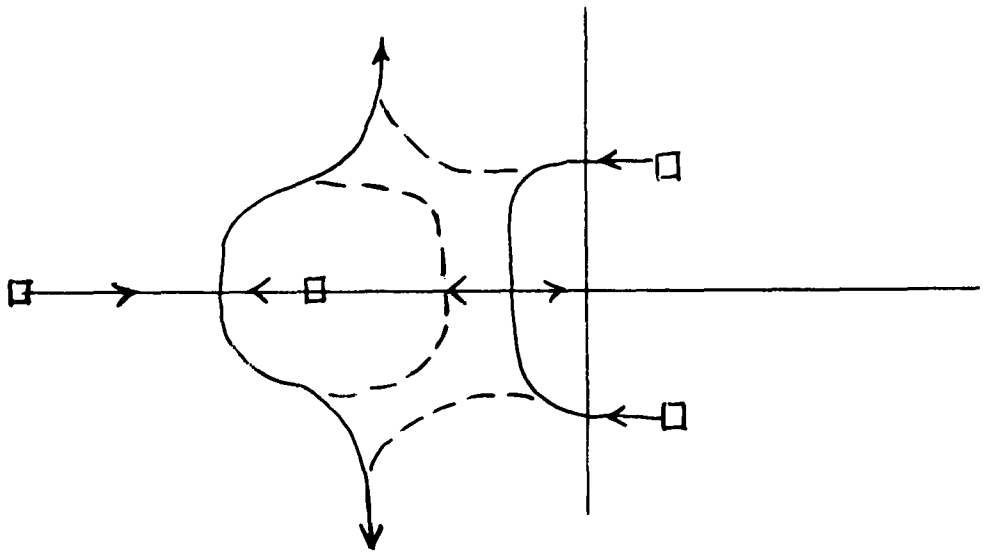

The dotted lines show where the locus was drawn in Figure 12. Which of these lines is correct could be determined by computing the roots for several more values of the tilt angle between 65 and 75 degrees. As, however, this has not yet been done, we will assume in the following discussion that the locus is as shown in Figure 12.

When the aircraft attains some forward velocity the Z-force equation is no longer uncoupled from the X-force and pitching moment equations and there are then four roots rather than three. The fourth root was, of course, present in hovering but it was not necessary to compute it since it is uncoupled from the others and is a very large negative root and thus has little effect on the motion of the aircraft.

As the aircraft gains some velocity this root moves in along the real axis and, as shown by Figure 12, combines with the other real convergent root to form a long period damped oscillation which becomes more lightly damped as the wing tilts further forward. Between 70 and 65 degrees this oscillation again becomes two real roots, one of which becomes unstable. We thus see that a rather radical change takes place in both of the characteristic modes at a tilt angle of about 65 degrees. This is due to the fact that the wing stalls at this point in the conversion.

At this point it is useful to see what happened to the equation to cause the stability characteristics to deteriorate so badly. To do this we consider the roots for a tilt angle of 65 degrees given in Figure 12 and use the root locus plot to determine what changes in the static and maneuver margin would be necessary to obtain satisfactory or at least improved stability characteristics at this tilt angle.

For this tilt angle we have a dynamically stable oscillation and two real roots, one of which decreases to half amplitude in 2.8 seconds while the other doubles amplitude in 2.3 seconds. In order to obtain satisfactory flying qualities, the divergent root should be removed or at least moved much closer to the origin, i.e. the time required to double amplitude should be increased. As the damping is only marginal, it should be increased.

In Figure 14 we see the effect of changing the static margin. The gains shown on this locus are not for changes in the static margin but for $-C_{x\theta}/A$ times the static margin; where A is the coefficient of the λ^4 term in the quartic equation in λ. If (SM) is decreased to zero the two real roots come together. For further decrease in (SM) the roots leave the real axis to form a slightly unstable oscillation with a time to double amplitude of about 17 seconds. For this amount of change in (SM) we see that the short period oscillation is hardly effected at all. Further decrease in the static stability causes the period of both oscillations to decrease. One of the oscillations becomes more unstable while the other becomes more stable. We thus see that making the aircraft statically stable improves its characteristics but that too much static stability is undesirable since it results in a very short-period divergent oscillation. We may also note that no amount of change in the static stability alone will make the stability characteristics completely satisfactory, i.e. make both modes both statically and dynamically stable with a desirable damping ratio.

In Figure 15 is shown the result of changing (MM). As (MM) is increased the real divergence moves closer to the origin; however, as may be seen from the values of the gain shown, large gain changes result in only a small movement while the period of the short-period mode decreases rapidly with increase in the gain. Since the real part of the oscillatory root hardly changes, the damping ratio is decreased. Decreasing (MM), while it improves the damping ratio of the short-period mode, decreases the time to double amplitude of the real divergence and thus is not a desirable change. We thus see that little if any improvement can be obtained by changing (MM).

Figure 16 shows the effect of changing C_{m_α}, which appears in both (SM) and (MM). Decreasing C_{m_α} (increasing $|C_{m_\alpha}|$) decreases the period of the short-period mode and has little effect on the real roots. We see however that increasing C_{m_α} improves the stability characteristics considerably. If it is increased enough to make the aircraft statically stable, then there will be a long-period oscillation with a time to double amplitude of about 10 seconds. This amount of change in C_{m_α} also improves the short period oscillation since the damping ratio is increased considerably. According to this root locus, if the value of C_{m_α} were increased from -.439 to about -.14 the stability characteristics would be considerably improved. It must be realized, however, that changing C_{m_α} in this manner improves the stability only because the wing is stalled at this tilt angle. The derivative $C_{m_{\dot{\alpha}}}$ appears in the static margin multiplied by C_{z_V} which is almost always negative when the wing is not stalled. When the wing is stalled it can be

positive as it is in this case. This makes the effect on the (SM) of changing C_{m_α} just the opposite of what it would be for an unstable wing. For all considerations such as these it should be remembered that the conditions at which the wing will stall can not be predicted accurately in the power-on case. The wing was assumed to obey the power off lift curve shown in Figure 39 but a number of effects are present which may cause the stall to occur at a different effective angle of attack.

As the wing is tilted further forward from 65 degrees, the effective angle of attack becomes still greater and the wing remains stalled. Figure 18 shows how the effective angle of attack varies through the conversion. This chart may be used to quickly find the effective angle of attack at any tilt angle if the forward velocity and the thrust coefficient are known. As may be seen by this chart the angle of attack increases with increase in the velocity and decreases with increase in the thrust coefficient. As a consequence of this fact, the effective angles of attack will be lower for an accelerating aircraft and higher for a decelerating aircraft. The sample conversion shown on this chart is for equilibrium trim conditions, i.e. the trim conditions were computed at each tilt angle as if the airplane were in equilibrium flight at this tilt angle.

In Figure 19 is shown a plot of effective angle of attack versus tilt angle for different amounts of acceleration and deceleration. We see from this that even small amounts of acceleration and deceleration can change the angle of attack considerably. Also note that

the tilt angle at which the maximum angle of attack is attained increases for a decelerating aircraft and decreases for an accelerating aircraft. We also see that for this particular aircraft, an acceleration of about 0.2 g is required in order for the wing to be unstalled over the entire conversion.

The lift coefficients obtained using angles of attack obtained in this way and the power off lift curve slope should not be expected to be too accurate due to the assumptions which have been made. The following three effects have been found experimentally to be present in the slipstream (Ref. 4) and may cause the lift developed to differ somewhat from that predicted on the basis of simplifying assumptions:

1. Slipstream rotation.
2. Delayed stall due to an effective boundary layer control.
3. Variation in induced velocity across disc.

Brenkmann concludes that for prediction of the average lift on the wing the delayed stall effect is the most important and that potential flow solutions may give satisfactory results if this additional lift is taken into account. He also shows that for the wing-propeller combination which he tested, slender-body theory (See Ref. 5) predicts the lift very well if the contribution due to the delayed stall is added to that given by the theory.

As the tilt angle decreases further we see that the period of the short-period mode decreases with essentially no change in the time of half amplitude. This means, however, that the damping ratio of the mode is decreased. The period of this mode thus changes from 4.2 seconds at a tilt angle of 65 degrees to 2.2 seconds at a tilt

angle of 15 degrees. According to the boundaries established by means of an F-94, (Ref. 16) the damping of this mode is still not sufficient, although it is not too far from the acceptable boundary.

With further decrease in the tilt angle the other mode comes back to the real axis, giving for a tilt angle of 65 degrees a pure divergence. With further decrease the time to double amplitude of the divergent mode at first becomes shorter and then longer again. We see that these roots remain on the real axis essentially until the angle of attack becomes small enough for the wing to become unstalled.

We now consider how the roots in this region will be effected by variation in (SM) and (MM) as we did before for a tilt angle of 65 degrees. In this case as a representative angle we will use a tilt angle of 35 degrees.

In Figure 17 we see the results of changing (SM) starting from a tilt angle of 35 degrees. As it is decreased the two real roots move together, the divergent root meeting the imaginary axis when (SM) becomes zero. As (SM) is further decreased the two roots leave the real axis to form a stable oscillation. We note that although the roots to begin with are quite similar to those in the 65 degree tilt angle case, the oscillation here is convergent whereas in the other case it was slightly unstable. For gain sufficient to keep this mode from crossing back over the imaginary axis the short-period mode has moved only a small distance and in the direction of increased damping. We then see that for this tilt angle, giving the aircraft an

adequate amount of static stability makes the period and damping of both modes acceptable.

Changing (MM) for this tilt angle is almost the same as for the 65 degree tilt angle and is thus not shown.

In Figure 20 we see the effect of changing C_{m_α}, the derivative of the pitching moment with respect to angle of attack for constant velocity. We see that decreasing C_{M_α} has almost no effect on the two real roots since the zeros for this root locus are located almost on these poles. The period of the short-period mode is decreased with almost no change in time to half amplitude for a decrease in C_{M_α}. Increasing C_{M_α} is somewhat more interesting. The real divergent root moves toward the imaginary axis and the real convergent root decreases its time to half amplitude. We see however by comparing the gains on the two loci that a C_{M_α} increase sufficient to make the divergent mode stable causes a very large movement of the short-period mode. In fact at about the same gain where the one mode makes the aircraft statically stable, the other mode becomes dynamically unstable. Thus, changing C_{M_α} can improve the dynamic characteristics for this tilt angle somewhat although it will not make them satisfactory.

Finally, going back to Figure 12, we see what happens to the two modes when the tilt angle becomes small enough to unstall the wing. In this case the tilt angle is approximately equal to the effective angle of attack. The angle of attack in normal forward flight is about 7 degrees and this tilt angle is shown in the diagram. The damping of the short period mode decreases considerably without much change in the period and the two real roots form a long period oscillation

similar to the usual phugoid. The aircraft in forward flight then has acceptable, although not ideal, stability characteristics.

Effect of Physical Parameters

In the last section we saw how the quartic roots varied as the tilt angle was changed for a typical tilt-wing VTOL aircraft. It was also shown by means of root locus plots how the stability characteristics at several tilt angles would be changed if the values of the two groups of terms, (SM) and (MM), were changed. We would now like to see how the various derivatives which make up these two groups depend on the aircraft physical parameters.

In our original perturbation equations, there were 18 derivatives. Six of these were found to be either zero or negligibly small. Of the remaining derivatives, five, $C_{M_{\ddot{\theta}}}$, $C_{Z_{\dot{\theta}}}$, $C_{X_{\theta}}$, $C_{X_{\dot{V}}}$, $C_{Z_{\dot{\alpha}}}$, depend essentially on only the mass, moment of inertia, and forward velocity. Two of these derivatives, $C_{Z_{\dot{\theta}}}$, $C_{Z_{\dot{\alpha}}}$, also have small contributions from the tail and other parts of the aircraft, but these are small compared to the inertia contributions. Thus we will be mainly interested in the derivatives of the forces and moment with respect to angle of attack and free stream velocity and the pitch damping derivative $C_{M_{\dot{\theta}}}$. All of these seven derivatives depend rather strongly on the easily alterable physical parameters of the aircraft and are thus of greatest interest.

Consider first the pitch damping. This derivative is mainly due to the tail although, as will be seen, the rotor can also be quite important. The fuselage also contributes some pitch damping but this can not be expressed in analytical form for fuselages of unusual shape

and must therefore be determined experimentally for a particular configuration. Also, the pitch damping of the fuselage is usually quite small compared to that from the other parts of the aircraft.

The contributions to the pitch damping as a function of the rotor angle of attack are shown in Figure 21. We see that the largest contribution here is that of the horizontal stabilizer. This contribution is simply a result of the fact that when the aircraft is pitching at a rate $\dot{\Theta}$, the angle of attack of the tail is increased by an amount $\frac{\ell\dot{\theta}}{V}$, producing a moment which opposes the pitch rate. This moment is thus directly proportional to the distance from the center of gravity to the tail and to the velocity of the fluid at the tail. The contribution of the offset hinges is seen to be independent of the angle of attack and thus of the free stream velocity. It is for this reason that this contribution is particularly important. Although it is small compared to the tail contribution in forward flight, it is almost the only source of damping in hovering. This contribution is directly proportional to the amount of hinge offset. We can see how this moment arises in the following way:

Consider the side view of a two bladed rotor with a mean coning angle β_o and a flapping angle a_1 (See Fig. 7).

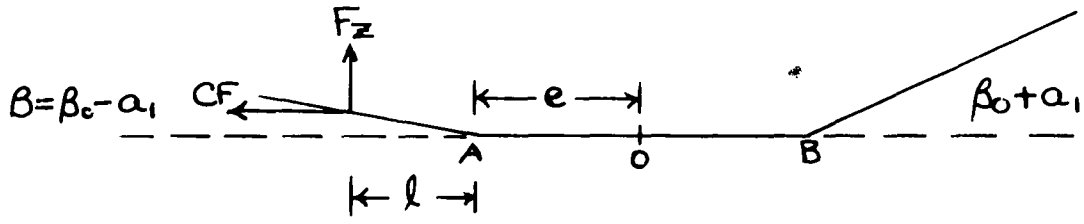

The moments about points A & B due to the lift on the rotor and the centrifugal force must balance since the blades are hinged at these points. Thus,

$$\ell \cos\beta \, F_z - \ell \sin\beta \, CF = 0 \tag{230}$$

and

$$F_z = CF \tan\beta \cong CF\,\beta \tag{231}$$

since β is small. The force F_z produces a moment about point O due to the offset e. The moment due to the two blades is thus,

$$M = -CF\,e\left[(\beta_0 - a_1) - (\beta_0 + a_1)\right] = 2CF\,e\,a_1 \tag{232}$$

Thus, a moment is produced which is proportional to a_1. When the aircraft is rotated at a rate $\dot{\Theta}$ about its center of gravity the rotor can not retain its former position since it is hinged and can only be moved by aerodynamic forces. The rotor thus lags behind producing an effective change in a_1 of magnitude,

$$\Delta a_1 = \frac{\partial a_1}{\partial \dot{\theta}} = \left(-\frac{16}{\gamma\Omega}\right) \tag{233}$$

We thus have,

$$\frac{\partial M}{\partial \dot{\theta}} \propto 2CF\,e\left(-\frac{16}{\gamma\Omega}\right) \tag{234}$$

In the actual case the rotors are moving and these forces must be averaged over the rotation angle Ψ as was done previously. The simple considerations above show, however, the source of the velocity independent moment.

The contribution of the tail fan although non-flapping is also independent of the velocity and is very small due to the smallness of this rotor.

The contribution of the rotor forces are particularly interesting due to the fact that above a certain velocity the H-force actually contributes a "negative damping" force. This phenomenon can be explained in the following way: When the aircraft is pitching at a given rate, the rotor lags behind its position for the non-pitching rotor as mentioned previously. Due to this lage the blades on one side of the rotor are flapping up and on the other side are flapping down. The velocity components due to this flapping causes the angle of attack of the blades to differ on the two sides and hence to change the magnitude and direction of the local lift vector. When the inflow is small, the change in direction is greater than the magnitude change and results in an H-force change which opposes the pitch rate. However, when the inflow becomes sufficiently large, the magnitude change, which is in the opposite direction, is the greatest and the H-force change tends to aid the pitch rate. The pitch damping due to thrust change is then positive. This effect is illustrated in Figure 22.

We see that the pitch damping can be increased by increasing the tail size and the amount of flapping hinge offset, and that there exists a destabilizing contribution to the pitch damping which increases with the inflow ratio.

Consider next the moment resulting from an angle of attack change at constant velocity. The important contributions to this derivative

are shown in Figure 23. We see that the largest contribution here is definitely that due to the change in angle of attack of the tail and it depends on the distance between the aircraft center of gravity and the tail and on the fluid velocity at the tail. All of the other contributions are small but destabilizing except that of the wing Z-force. This, however, is due to the fact that the wing is stalled. If the wing is not stalled throughout the transition, all contributions to this derivative except the tail are always destabilizing. When the wing is not stalled there is a center of gravity position at which the wing and rotor contribution cancel that of the tail. The center of gravity range is thus decreased due to the destabilizing contributions of the rotor.

We must remember, however, that positive C_{M_α} does not necessarily mean static instability as is usually the case with conventional airplanes. For the VTOL the static stability is determined by the sign of,

$$(SM) = C_{z_\alpha} C_{M_V} - C_{z_V} C_{M_\alpha} \tag{235}$$

and the first term may be of equal or greater importance than the second. The relative magnitude of these two terms as a function of rotor angle of attack is shown in Figure 24. From this plot we see that near hovering both terms are stabilizing. At about 20 degrees the wing stalls and both terms change sign and become destabilizing. The C_{M_V} term is then very small up to about 80 degrees while the C_{M_α} term is destabilizing in this region. At about 83 degrees both terms again become stabilizing. Thus, we see that

the derivative C_{M_V} is quite important near hovering and in forward flight.

The important contributions to C_{M_V} are shown in Figure 25. The major contribution in hovering is the wing force in the X-direction. This derivative is mainly due to the change in the lift of the wing in the slipstream since the wing is in a nearly vertical position. It owes its magnitude to the fact that there is considerable vertical separation between the wing center of pressure and the center of gravity of the aircraft, which is not present in a conventional airplane. When the angle of attack is high enough, however, the wing stalls and this contribution becomes small and of opposite sign. The two rotor terms we see depend on the relative position of the rotor and the aircraft center of gravity. The overall effect of the rotor is to give a small positive contribution to C_{M_V} which increases in magnitude as the wing is tilted down.

Positive C_{M_V} usually increases the static stability since C_{Z_α} is always negative for a non-stalled wing and (SM) is negative for static stability. The following shows how the signs of the derivatives effect (SM),

$$(SM) = C_{Z_\alpha} C_{M_V} - C_{Z_V} C_{M_\alpha}$$

$$(-) = \underbrace{(-)\ (+) \quad - \quad (-)}\ (-)$$

Usual sign for unstalled wing.

May change sign for stalled wing.

Always negative if tail is sufficiently large.

We see from this that if wing stall causes C_{Z_V} to change sign, this will give a destabilizing contribution. If both C_{Z_α} and C_{M_V} change the contribution will still be stabilizing while if either changes sign while the other does not, the contribution will be destabilizing.

In Figure 26 we see the contributions to C_{Z_α}, the change in force in the Z-direction with angle of attack at constant velocity. In a conventional aircraft, if the tail lift is neglected, this derivative is just the slope of the wing lift curve. Here we see that while the effect of the wing is still important, the rotor also gives a large contribution. Although the stalled wing gives a large positive contribution, the negative contributions of the rotor and the tail are almost sufficient to keep this derivative negative throughout conversion. The tail contribution is simply due to the change in tail lift with angle of attack and hence is proportional to the dynamic pressure at the tail. The triangular shape of the rotor contribution can be explained as follows: If the angle of attack is slightly changed, this effects the inflow to the rotor, λ, and hence the thrust. Thus, near hovering there is little contribution to C_{Z_α} since the rotor is nearly parallel to the flow and the inflow is hardly effected by a small angle of attack change. In forward flight, on the other hand, the thrust vector is almost parallel to the flow and the thrust force is in the X-direction and does not effect C_{Z_α}. Since both these effects vary approximately linearly with tilt angle, the rotor will have a maximum Z-force change with angle of attack at a tilt angle of about 45 degrees.

The other derivative which appears in (SM) is C_{Z_V}, the change in Z-force with velocity at constant angle of attack. This derivative has a contribution from the rotor and from the wing. These are shown in Figure 27. As mentioned before, this derivative is usually negative for an unstalled wing. However, we see that the rotor contribution is positive and fairly large and hence could be large enough to make C_{Z_V} positive even for an unstalled wing.

The rotor term arises from the fact that if the velocity increases at constant angle of attack the inflow to the rotor is increased, decreasing the angle of attack of the rotor blades and decreasing the thrust. The thrust decrease becomes greater as the wing is tilted down and the freestream velocity has a greater component perpendicular to the rotor disc. Near the forward flight position the thrust is mostly in the X-direction and the contribution to C_{Z_V} is decreased.

The wing contribution here depends on wing angle of attack and becomes positive or destabilizing when the wing stalls.

Consider now how the derivatives we have discussed effect the maneuver margin. The signs of the various contributions are shown by the following:

$$(MM) = C_{Z_\alpha} C_{M_{\dot\theta}} - C_{Z_{\dot\theta}} C_{M_\alpha}$$

$$(+) = (-)\ \underbrace{(-) - (+)\ (-)}$$

Usual sign for unstalled wing.

May change sign for stalled wing.

Always same sign.

We see from this that the wing stall can make the first term decrease the value of (MM). An increase in the magnitude of all the other terms tends to increase (MM). The importance of (MM) can be seen from the short period approximation given earlier,

$$\lambda = \frac{M_{\dot{\theta}}}{2I} \pm i \sqrt{\frac{(MM)}{mVI_y}} \qquad (236)$$

where (MM) in this expression is not made non-dimensional. From this we see that increasing (MM), decreases the period of the short period mode as was also shown by the root locus plots in the previous section.

We will consider now the two X-force derivatives. These derivatives do not appear in either (SM) or (MM) and do not effect the stability characteristics as much as those derivatives already discussed.

The change in the force in the X-direction with an increase in angle of attack is normally negative, i.e. if the angle of attack is increased, a force is produced which tends to oppose the motion of the aircraft. The contributions to this derivative are shown in Figure 28. The tail contribution, as would be expected, is small, negative and increases in proportion to the velocity. The rotor contribution is positive and is given approximately by $13 \cos i_w \frac{\partial \lambda}{\partial \alpha}$. Thus, an increase in angle of attack causes an increased inflow which increases the thrust, producing a positive force in the X-direction. The effect of the thrust increase becomes greater as the wing is tilted forward. The various terms in the wing contribution are shown

in the upper part of this Figure. We see that the biggest term is that involving a change in the angle of attack, i.e. $\left(1 - \frac{\partial \Phi}{\partial \alpha}\Big|_V\right)$, rather than a change in the magnitude of the resultant velocity. The fact that the wing is stalled decreases the value of this contribution but the term involving the lift coefficient is larger at small tilt angles, and the stalled wing has only a small effect on the contribution. The sum of the various contributions is negative as in a normal aircraft and its magnitude increases as the tilt angle decreases.

The X-force change with velocity is also normally negative since a velocity increase will usually produce a force tending to oppose the motion of the aircraft. The rotor contribution to the derivative is always negative and approximately proportional to $C_{\alpha i_W} \frac{\partial \lambda}{\partial \mu_X}$. $\frac{\partial \lambda}{\partial \mu_X}$ is always negative, i.e. an increase in the freestream velocity produces a decrease in the inflow to the rotor. This causes a decrease in the thrust and hence a force in the negative X-direction. The effect of this thrust decrease increases as the tilt angle is decreased. This is shown in Figure 29.

The various terms in the wing contribution are also shown in this Figure. Again the main effect is the change in angle of attack rather than the change in the magnitude of the resultant velocity. The sharp drop at about 70 degrees is due to wing stall. The sum of the wing and rotor contributions has a dip at about 70 degrees since the negative rotor term is still small at this tilt angle.

CONCLUSIONS

1. Values for the derivatives of the resultant velocity and effective angle of attack with respect to forward velocity and aircraft angle of attack can be obtained from general charts without extensive calculations.

2. Typical tilt wing VTOL has a short period mode whose period becomes smaller as the tilt angle is decreased. The time to half amplitude of this mode is approximately equal to a constant times the pitching moment of inertia divided by the pitch damping. The other mode is a long period oscillation which becomes a pure convergence and a pure divergence when the wing stalls.

3. For unaccelerated level flight the wing stalls over part of the transition. The amount of stall is decreased by acceleration or climb and increases by deceleration or descent.

4. The aircraft very quickly becomes statically unstable when the wing stalls.

RECOMMENDATIONS FOR FURTHER STUDY

In order to gain a better understanding of VTOL dynamics, it is necessary that more experimental work be done. Detailed analytical analysis are not particularly useful if it cannot be determined whether or not they accurately represent the physical situation. Two types of experimental work are needed. First, it would be desirable to have accurate measurements of the forces on the wing due to the slipstream in order to determine what parameters of a rotor wing

combination effect the lift characteristics. Also, dynamic stability information is needed to determine whether or not present theoretical treatments give an accurate description of VTOL dynamic characteristics.

A theoretical treatment of the dynamics of a complete transition with time-varying stability derivatives would also be valuable since this type of analysis might differ considerably from the steady state analysis if the acceleration is sufficiently high.

REFERENCES

1. Koning, C.; "Influence of the Propeller on Other Parts of the Airplane Structure," Aerodynamic Theory, Edited by W. F. Durand Vol. IV, Berlin (1935).

2. Rethorst, Scott; "Lift on a Wing in a Propeller Slipstream as Related to Low Speed Flight," IAS National Seminar Meeting June 18-21, 1956, Preprint No. 643.

3. Stuper, J.; "Infuss des Schraubenstrahls auf Flugel und Leitwerk," Luftfahrtforschung, Vol. 15, No. 9 (1938). Also NACA TM 874 (1938).

4. Brenckmann, M.; "Experimental Investigation of the Aerodynamics of a Wing in a Slipstream," Institute of Aerophysics, University of Toronto Tech. Note No. 11, April 1957.

5. Graham, E. W.; Lagerstrom, P. A.; Licher, R. M.; Beane, B. J.; "A Preliminary Investigation of the Effects of Propeller Slipstream on Wing Lift," Douglas Report SM - 14991, November 1953.

6. Rethorst, S.; Royce, W.; Wu, T. Yao-tsu; "Lift Characteristics of Wings Extending Through Propeller Slipstreams," Vehicle Research Corp., Report No. 1 September 1958.

7. Brotherhood, P.; "An Investigation in Flight of the Induced Velocity Distribution under a Helicopter Rotor when Hovering," British ARC R&M No. 2521 June 1947.

8. Smelt, R.; and Davies, H.; "Estimation of Increase in Lift Due to Slipstream," ARC R&M No. 1788, February 1937.

9. "Dynamics of the Airframe," AE-61-4II Bureau of Aeronautics Flight Control System manuals.

10. Nikolsky, A. A.; "Helicopter Analysis" John Wiley & Sons, Inc., 1951.

11. Gessow, A.; and Myers, G. C.; "Aerodynamics of the Helicopter," The Macmillan Co., New York, 1952.

12. Seckel, Edward; and Curtiss, Howard C. Jr.; "Aerodynamic Forces and Stability Derivatives," May 1957, Unpublished.

13. Castles, Walter Jr.; and DeLeeuw, Jacob Henri; "The Normal Component of the Induced Velocity in the Vicinity of a Lifting Rotor and Some Examples of Its Application," NACA Report 1184, 1954.

14. Curtiss, H. C.; "Calculation of Vertol Trim Conditions" (unpublished).

15. A'Harrah, R. C.; Kwiatkowski, S. F.; "A New Look at V/STOL Flying Qualities," IAS Paper No. 61-62, Presented at IAS 29th Annual Meeting, New York, January 23-25, 1961.

16. Chalk, C. R.; "Additional Flight Evaluations of Various Longitudinal Handling Qualities in a Variable-Stability Jet Fighter," WADC Technical Report 57-719 Part I, also Cornell Aeronautical Laboratory Report TB-1141-F-1 March 1958.

17. Newell, F.; and Cambell, G.; "Flight Evaluation of Variable Short-period and Phugoid Characteristics in a B-26" WADC Technical Report 54-594; also Cornell Aeronautical Laboratory Report TB-757-F-11 December 1954.

18. Freck, Peter; "A Preliminary Investigation of the Longitudinal Dynamics of a Tilt-Wing Propeller Driven VTOL Aircraft," Princeton University Department of Aeronautical Engineering Report 456, May 1959.

19. Cromwell, C. H.; and Payne, H. E.; "A Stability Analysis of Tilt-Wing Aircraft," Princeton University Department of Aeronautical Engineering Report No. 477, May 1960.

20. Putman, W. F.; "Results of Experiments on a Tilt-Wing VTOL Aircraft Using the Princeton University Forward Flight Facility," Princeton University Department of Aeronautical Engineering Report No 542, May 1961.

21. Snedeker, R. S.; "Experimental Determination of Spanwise Lift Effects on a wing of Infinite Aspect Ratio Spanning a Circular Jet," Princeton University Department of Aeronautical Engineering Report No. 525, February 1961.

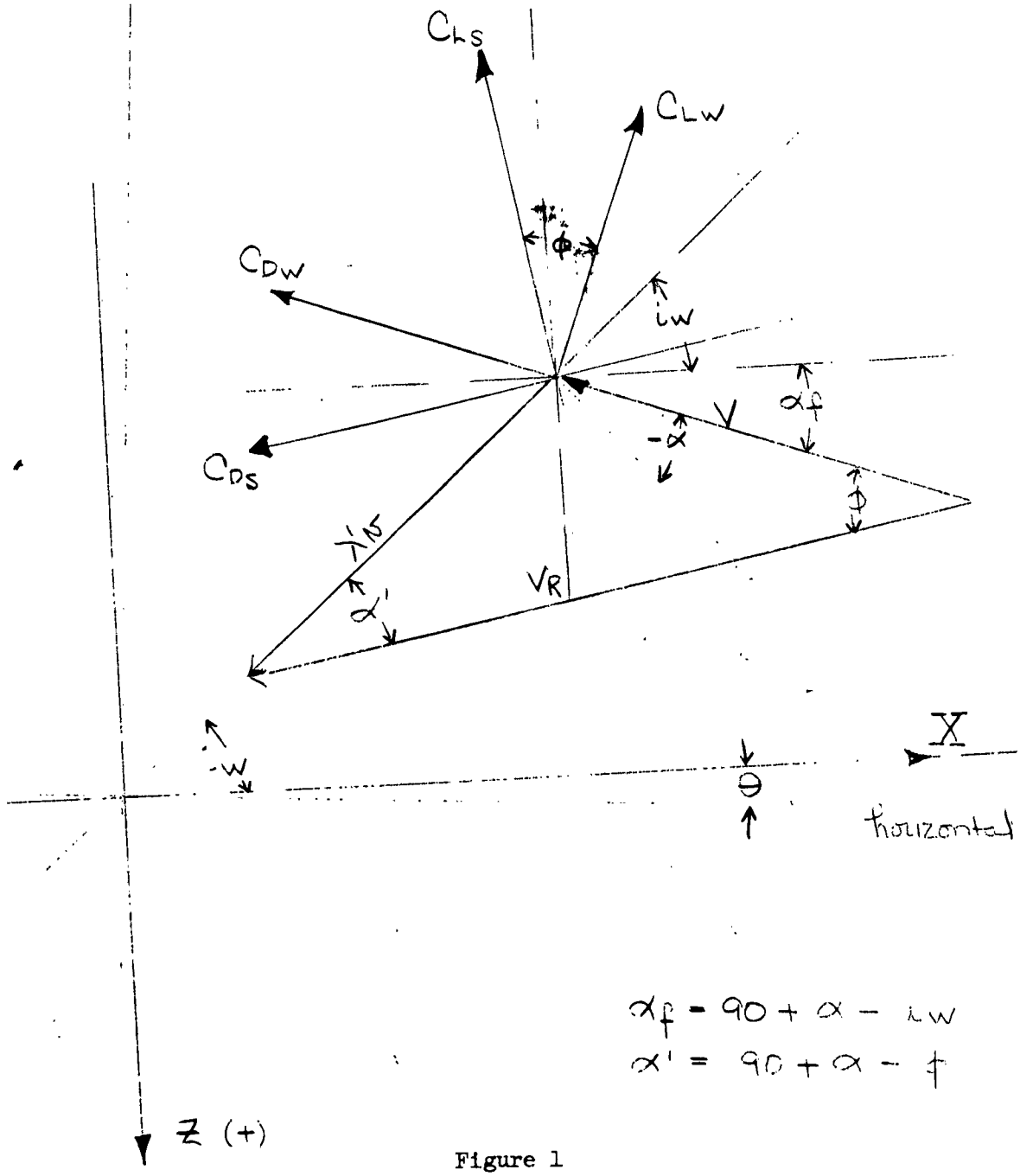

$$\alpha_f = 90 + \alpha - i_W$$

$$\alpha' = 90 + \alpha - \phi$$

Figure 1

Figure 2

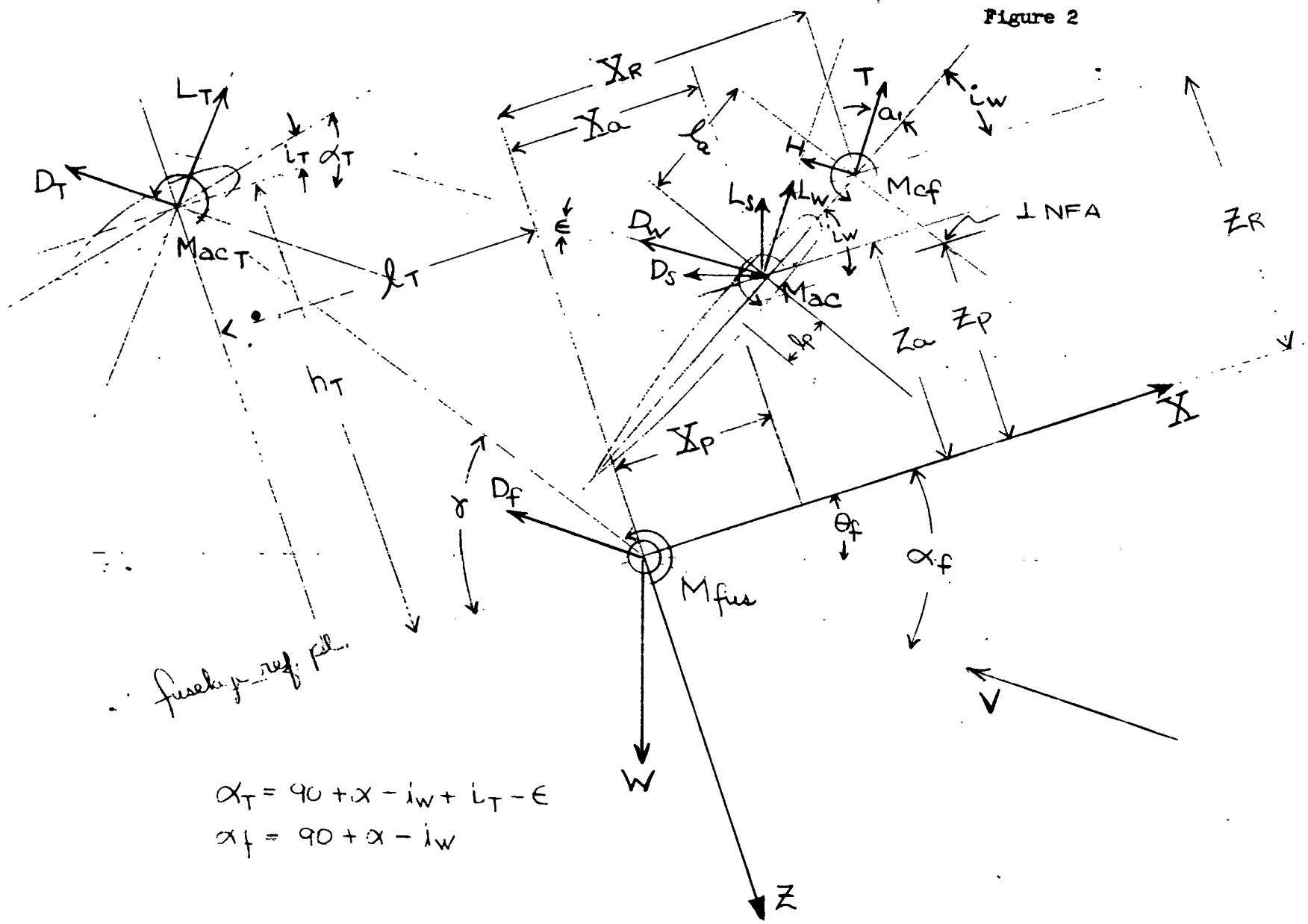

$$\alpha_T = 90 + \alpha - i_w + i_T - \epsilon$$

$$\alpha_f = 90 + \alpha - i_w$$

Figure 3

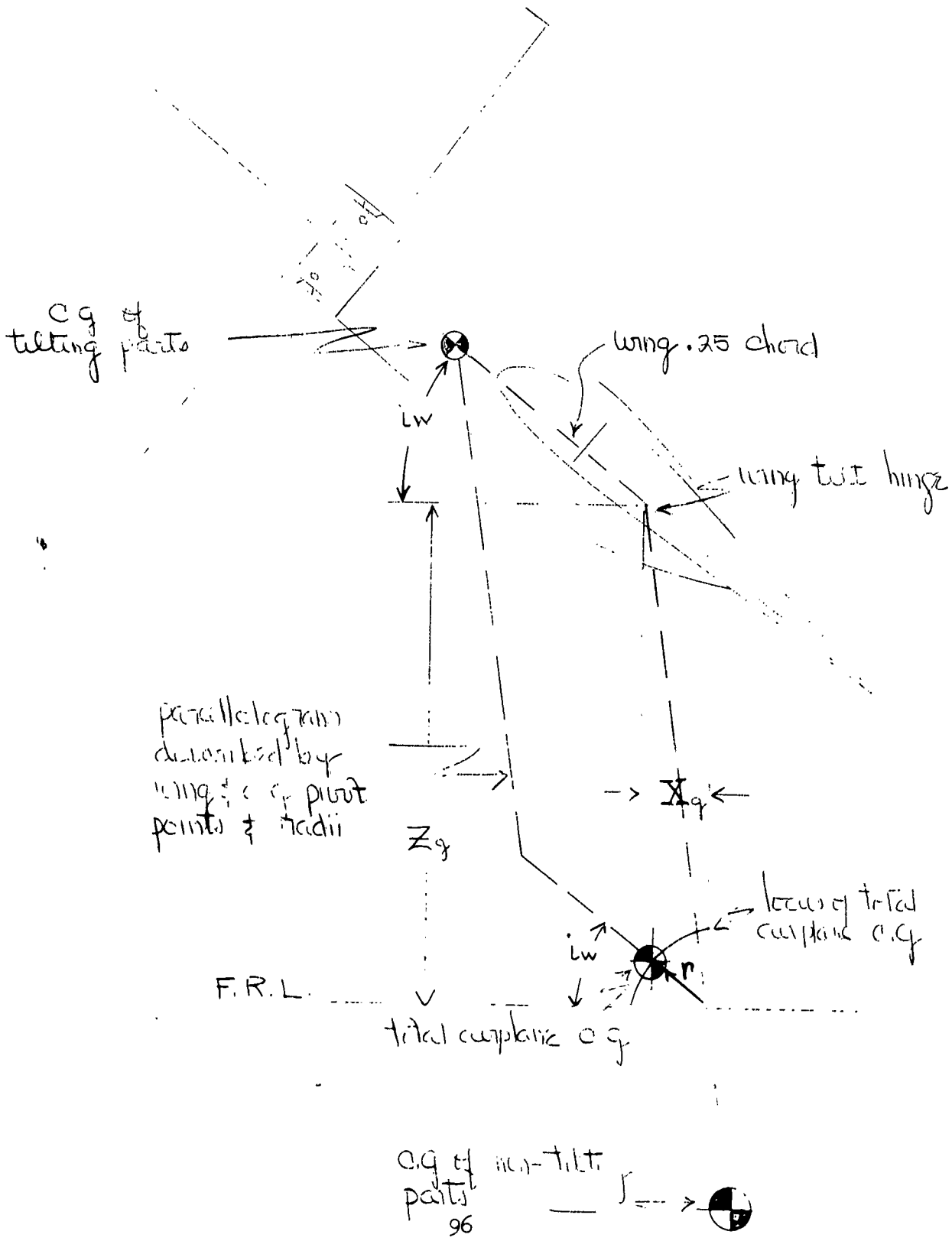
cg of tilting parts
wing .25 chord
l_w
wing tilt hinge
parallelogram described by wing & c.p. pivot points & radii
X_g
Z_g
locus of tilted cockpit c.g.
i_w
r
F.R.L.
tilted cockpit c.g.
c.g. of non-tilt parts

Figure 4

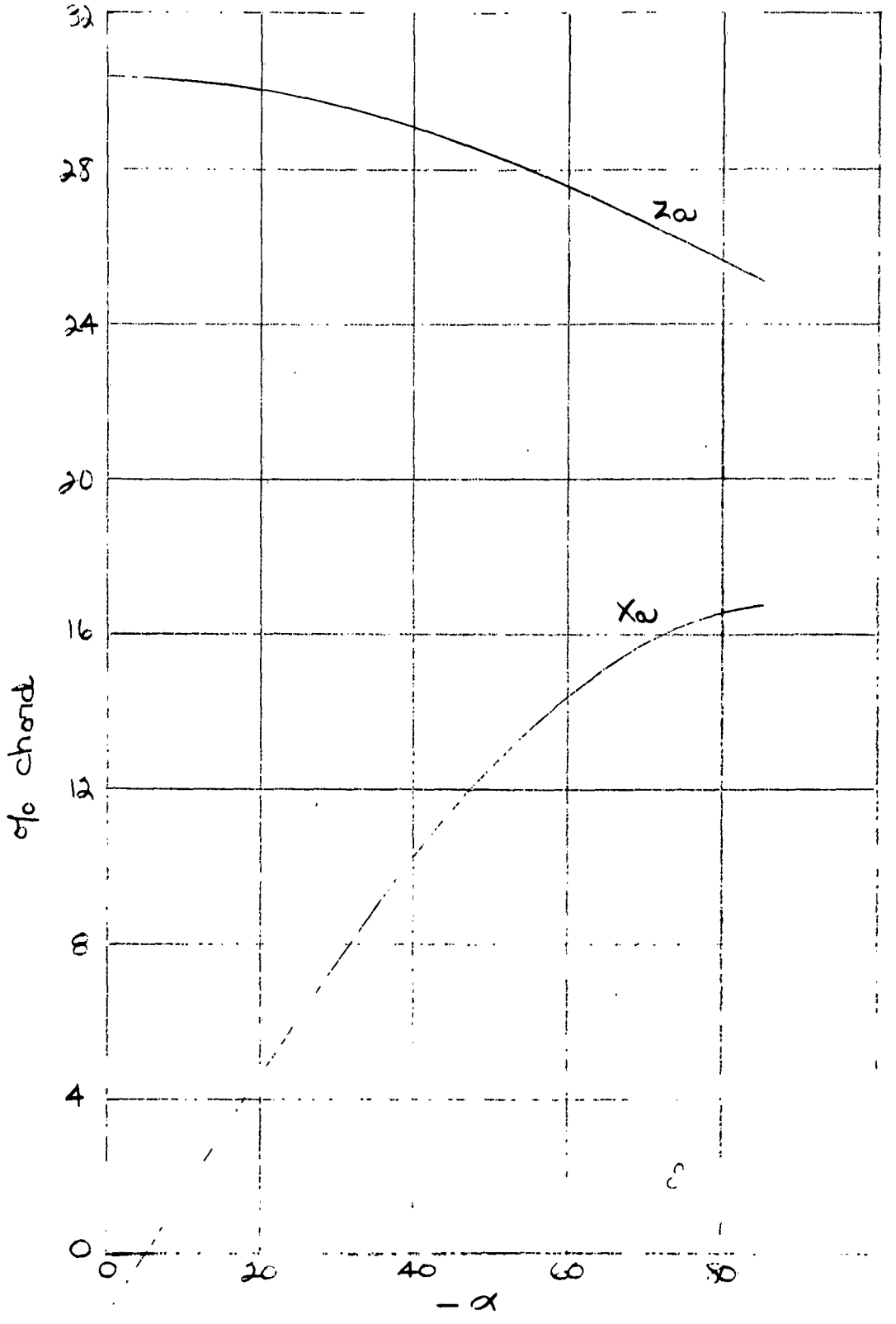

Figure 5-a

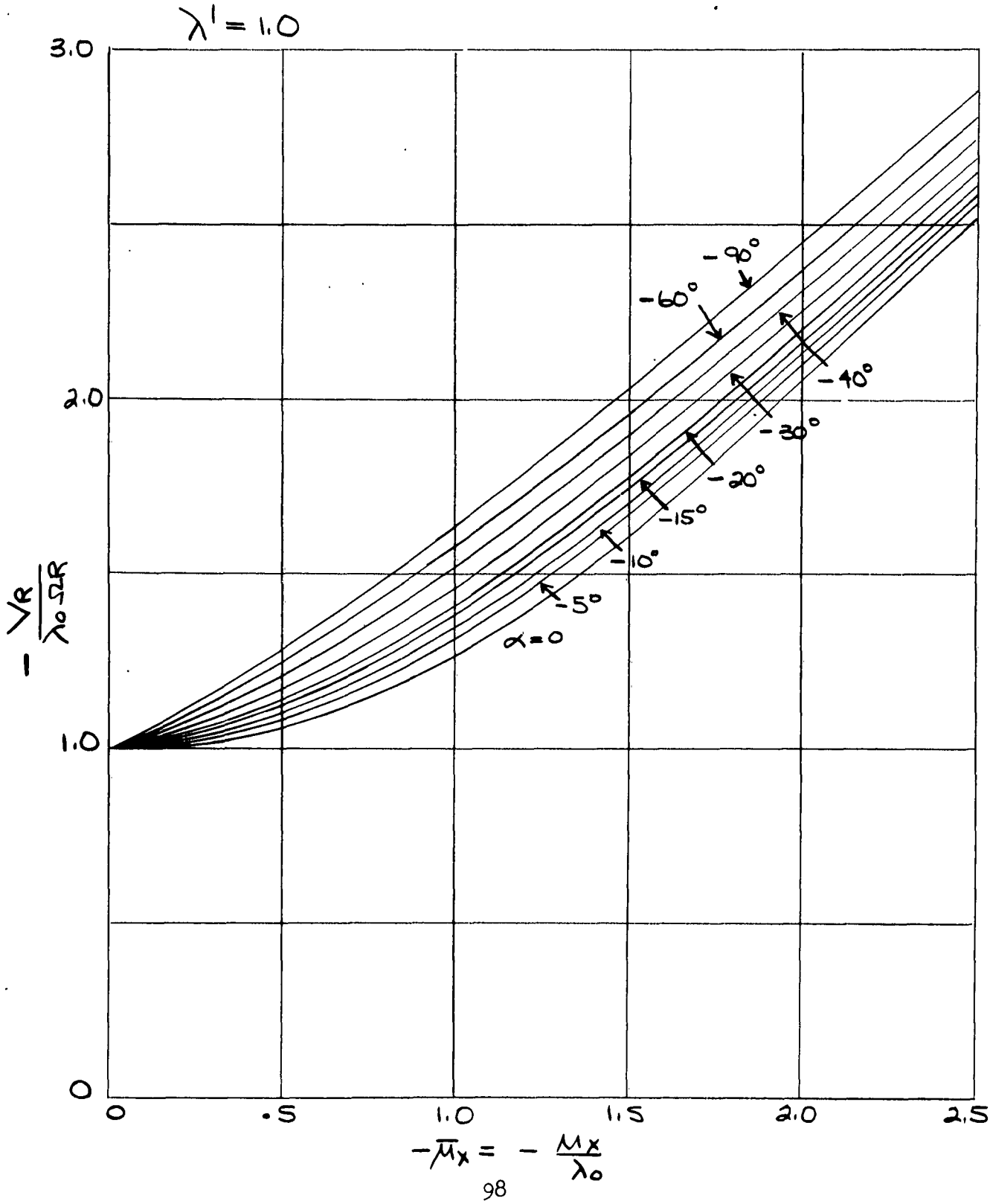
λ' = 1.0
3.0
2.0
1.0
0
0
.5
1.0
1.5
2.0
2.5
$\frac{V_R}{\lambda_0 \Omega R}$
$-\bar{\mu}_x = -\frac{\mu_x}{\lambda_0}$
-90°
-60°
-40°
-30°
-20°
-15°
-10°
-5°
α = 0

Figure 5-b

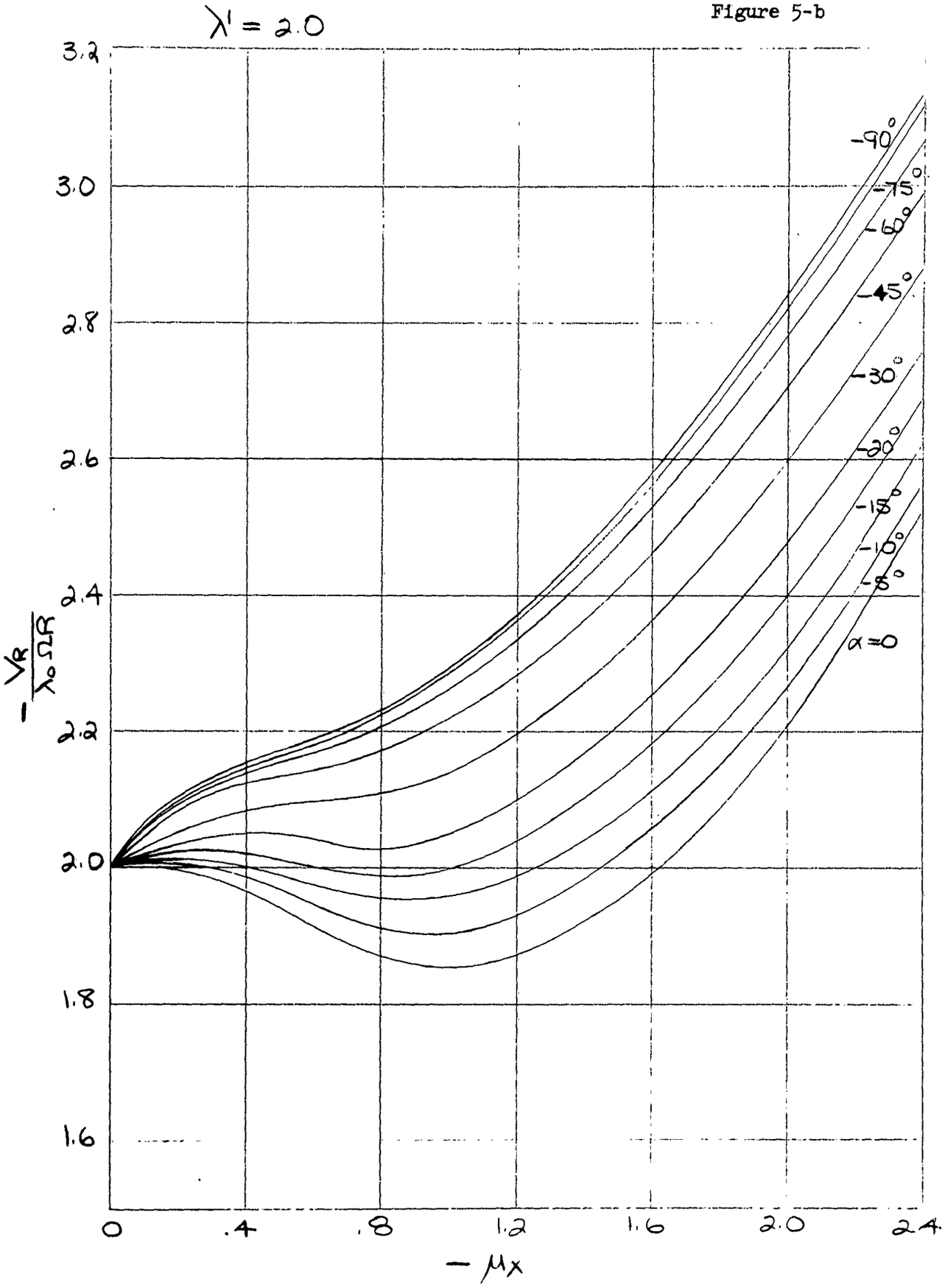
λ' = 2.0
3.2
3.0
2.8
2.6
2.4
2.2
2.0
1.8
1.6
$-\frac{V_R}{\lambda_0 \Omega R}$
0
.4
.8
1.2
1.6
2.0
2.4
$-\mu_x$
-90°
-75°
-60°
-45°
-30°
-20°
-15°
-10°
-5°
α=0

Figure 5-c

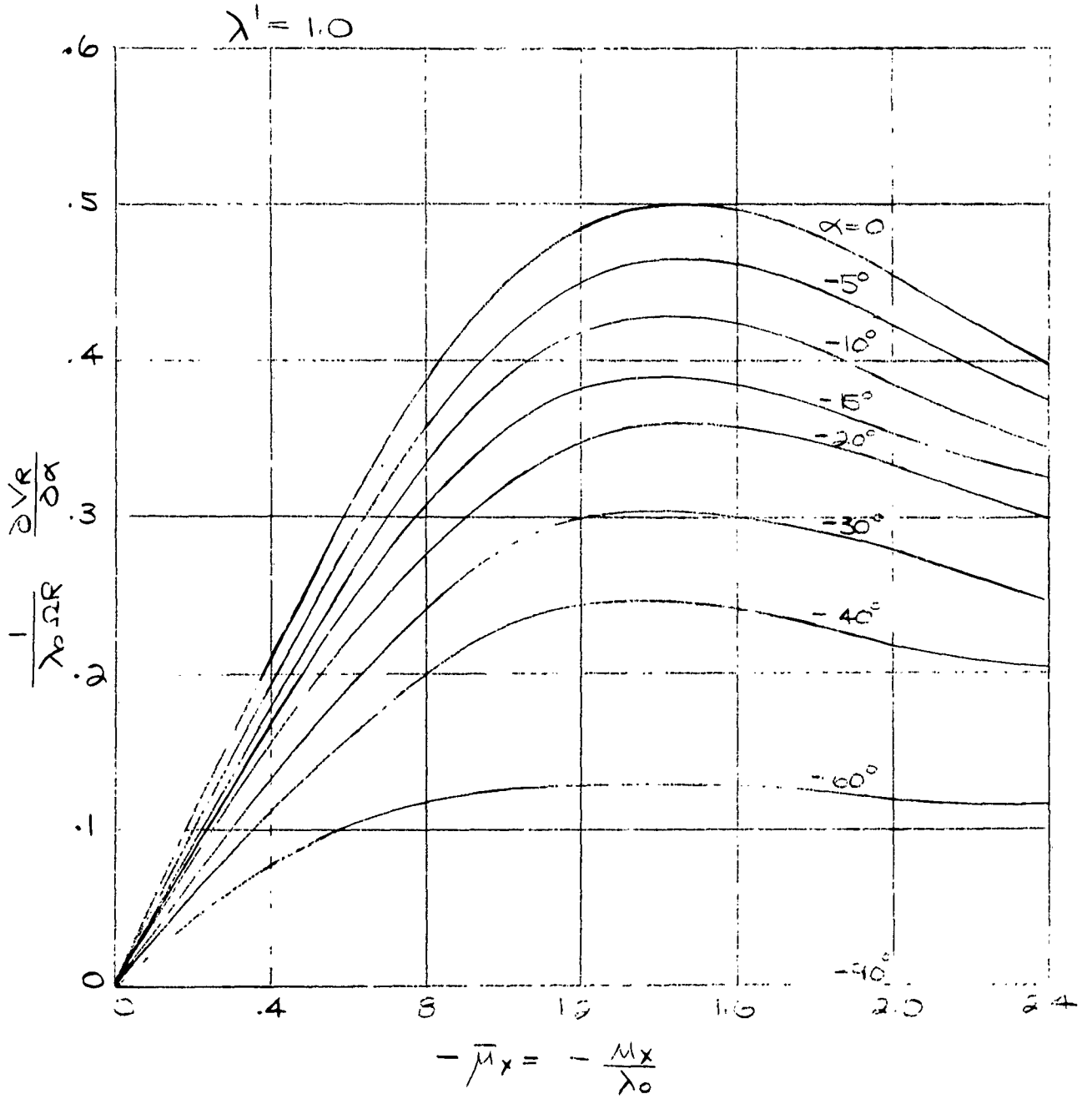
λ' = 1.0
.6
.5
.4
.3
.2
.1
0
∂V_R/∂α
1/λ_c ΩR
α = 0
-5°
-10°
-15°
-20°
-30°
-40°
-60°
-90°
0
.4
.8
1.2
1.6
2.0
2.4
−μ̄_x = −M_x/λ_0

Figure 5-d

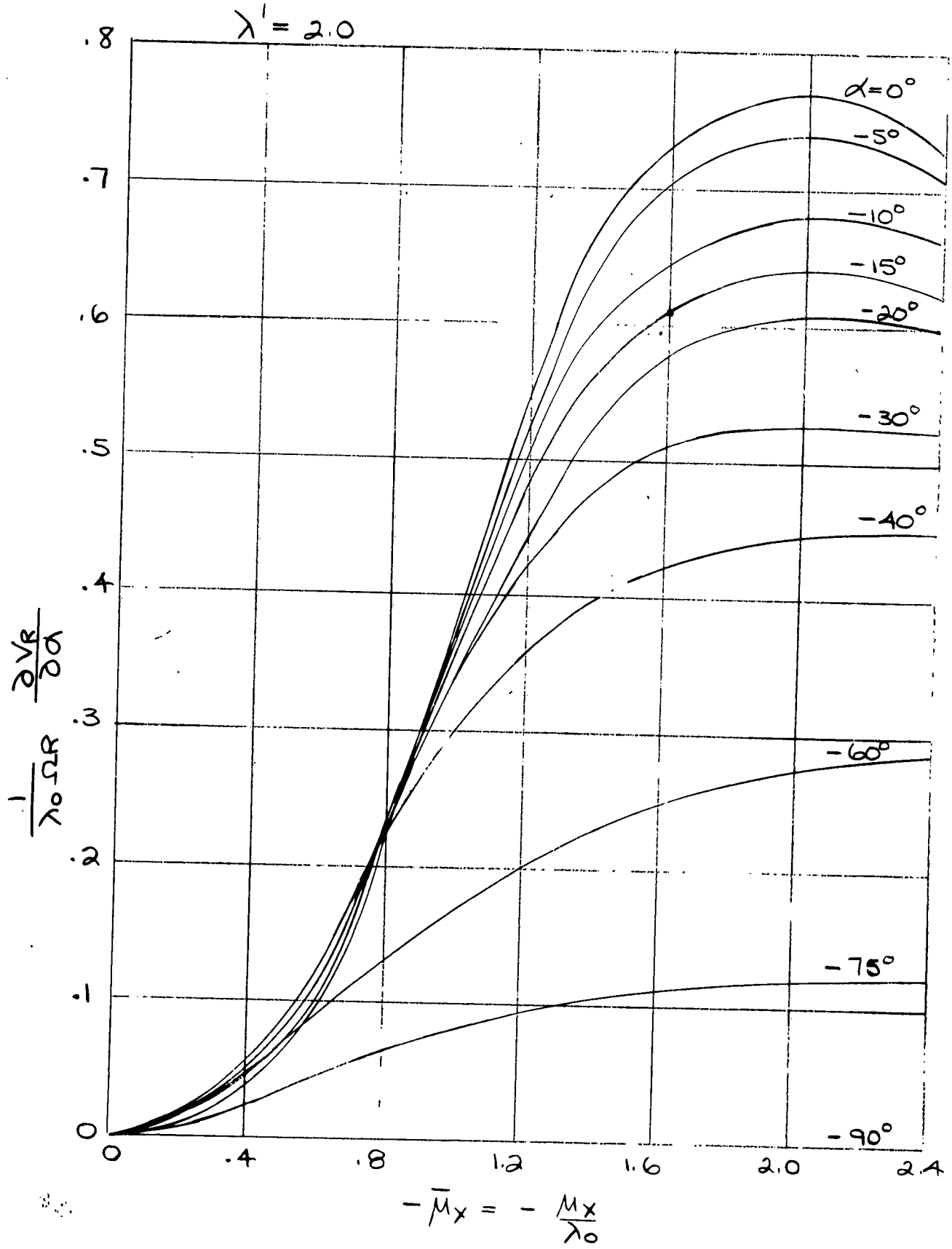
λ' = 2.0
α=0°
-5°
-10°
-15°
-20°
-30°
-40°
-60°
-75°
-90°
.8
.7
.6
.5
.4
.3
.2
.1
0
0
.4
.8
1.2
1.6
2.0
2.4
$\frac{1}{\lambda_0 \Omega R} \frac{\partial V_R}{\partial \sigma}$
$-\bar{\mu}_x = -\frac{\mu_x}{\lambda_0}$

Figure 5-e

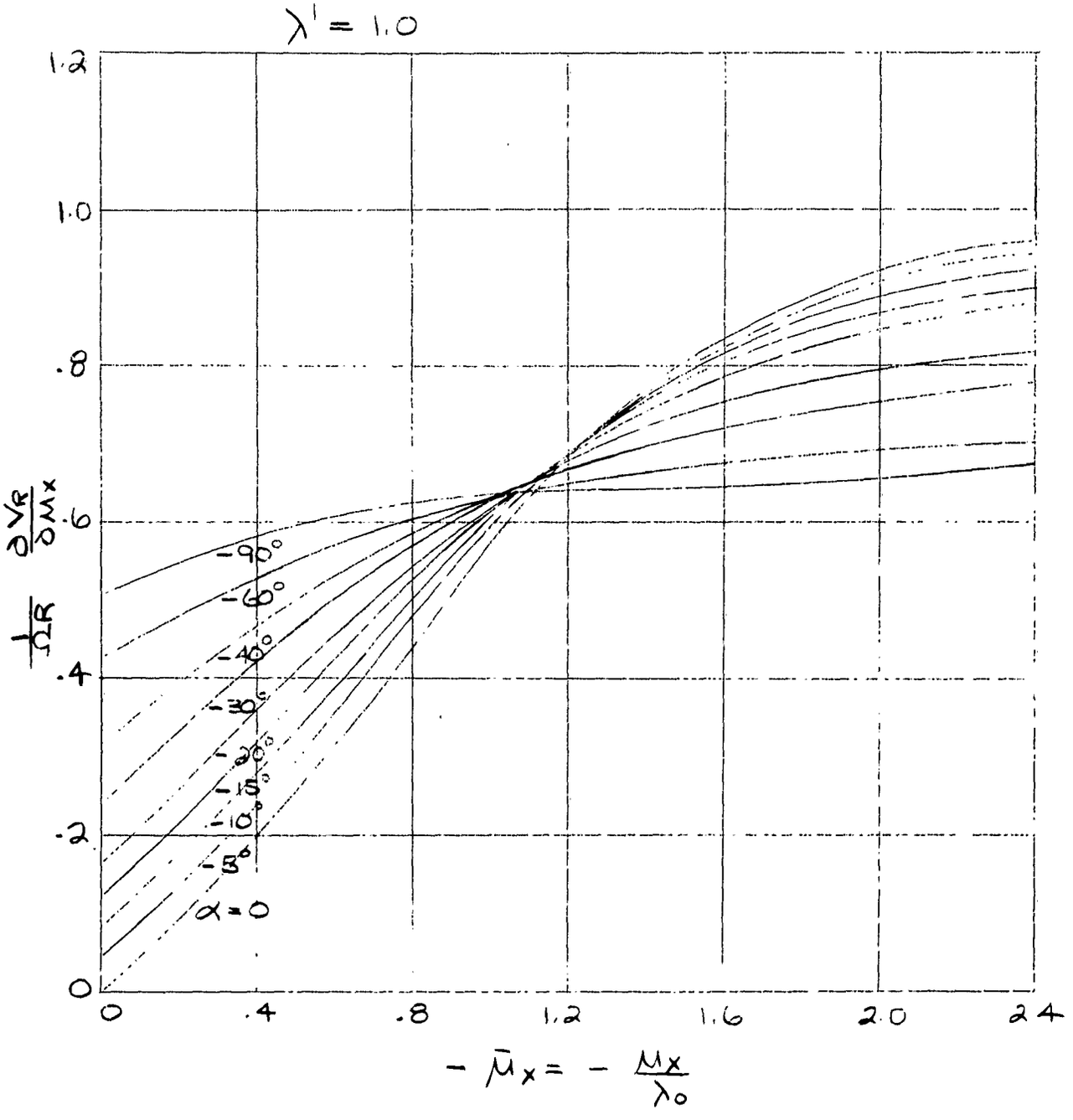
λ' = 1.0
1.2
1.0
.8
.6
.4
.2
0
0
.4
.8
1.2
1.6
2.0
2.4
∂V_R/∂M_x
1/ΩR
-90°
-60°
-40°
-30°
-20°
-15°
-10°
-5°
α = 0
- μ̄_x = - M_x/λ_0

Figure 5-f

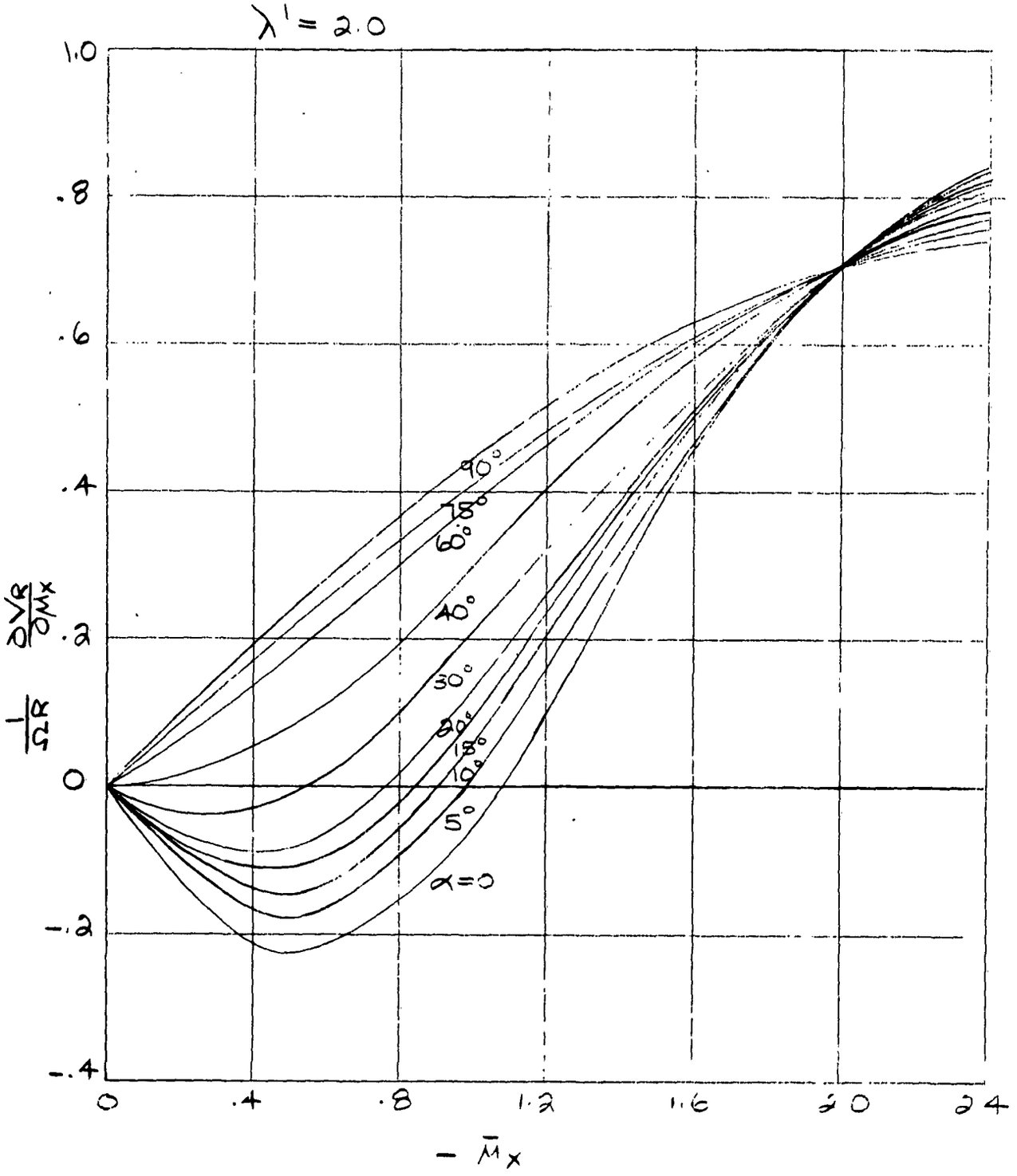
λ' = 2.0
1.0
.8
.6
.4
.2
0
-.2
-.4
0
.4
.8
1.2
1.6
2.0
2.4
$\frac{\partial V_R}{\partial M_x}$
$\frac{1}{\Omega_R}$
$-\bar{M}_x$
90°
78°
60°
40°
30°
18°
10°
5°
α=0

Figure 5-g

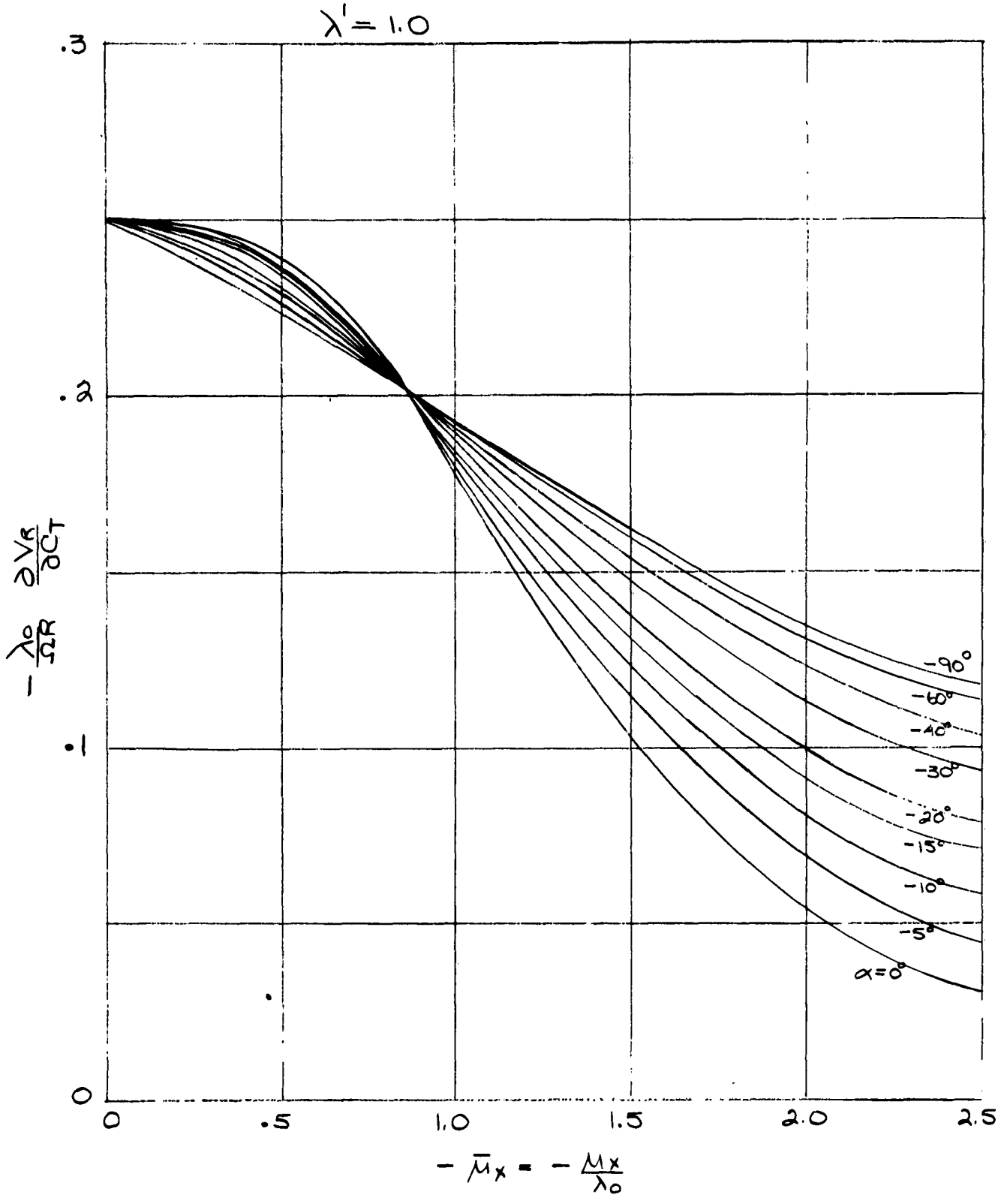
λ' = 1.0
.3
.2
.1
0
0
.5
1.0
1.5
2.0
2.5
$-\frac{\lambda_0}{\Omega R}\frac{\partial V_R}{\partial C_T}$
$-\bar{\mu}_x = -\frac{\mu_x}{\lambda_0}$
-90°
-60°
-40°
-30°
-20°
-15°
-10°
-5°
α=0°

Figure 5-h

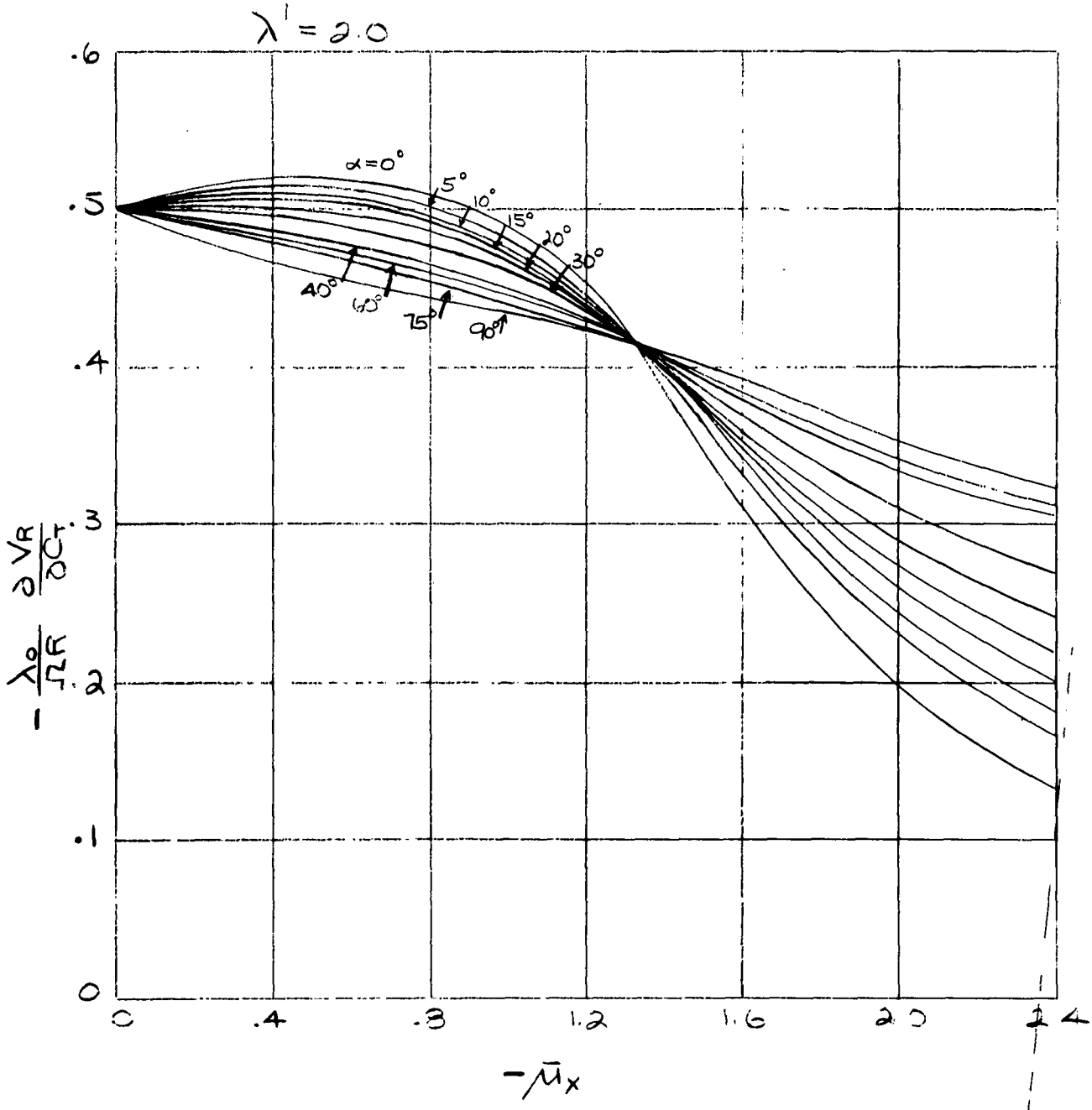
λ' = 2.0
α=0°
5°
10°
15°
20°
30°
40°
60°
75°
90°
.6
.5
.4
.3
.2
.1
0
0
.4
.8
1.2
1.6
2.0
2.4
$-\frac{\lambda^0}{\Omega R}\frac{\partial V_R}{\partial C_T}$
$-\bar{\mu}_x$

Figure 6-a

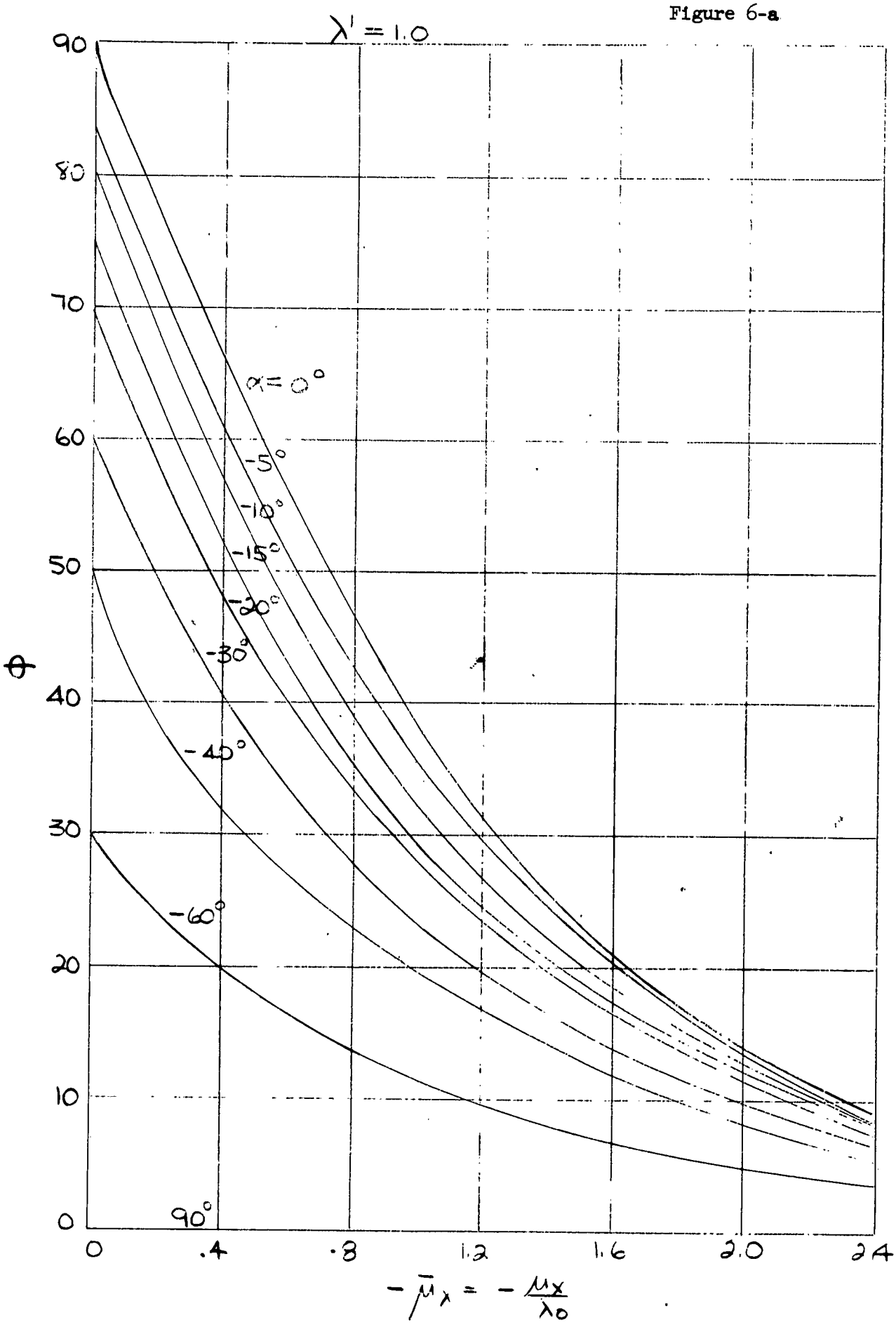
λ' = 1.0
90
80
70
60
50
40
30
20
10
0
θ
α = 0°
-5°
-10°
-15°
-20°
-30°
-45°
-60°
90°
0
.4
.8
1.2
1.6
2.0
2.4
$-\bar{\mu}_\lambda = -\frac{\mu_x}{\lambda_0}$

Figure 6-b

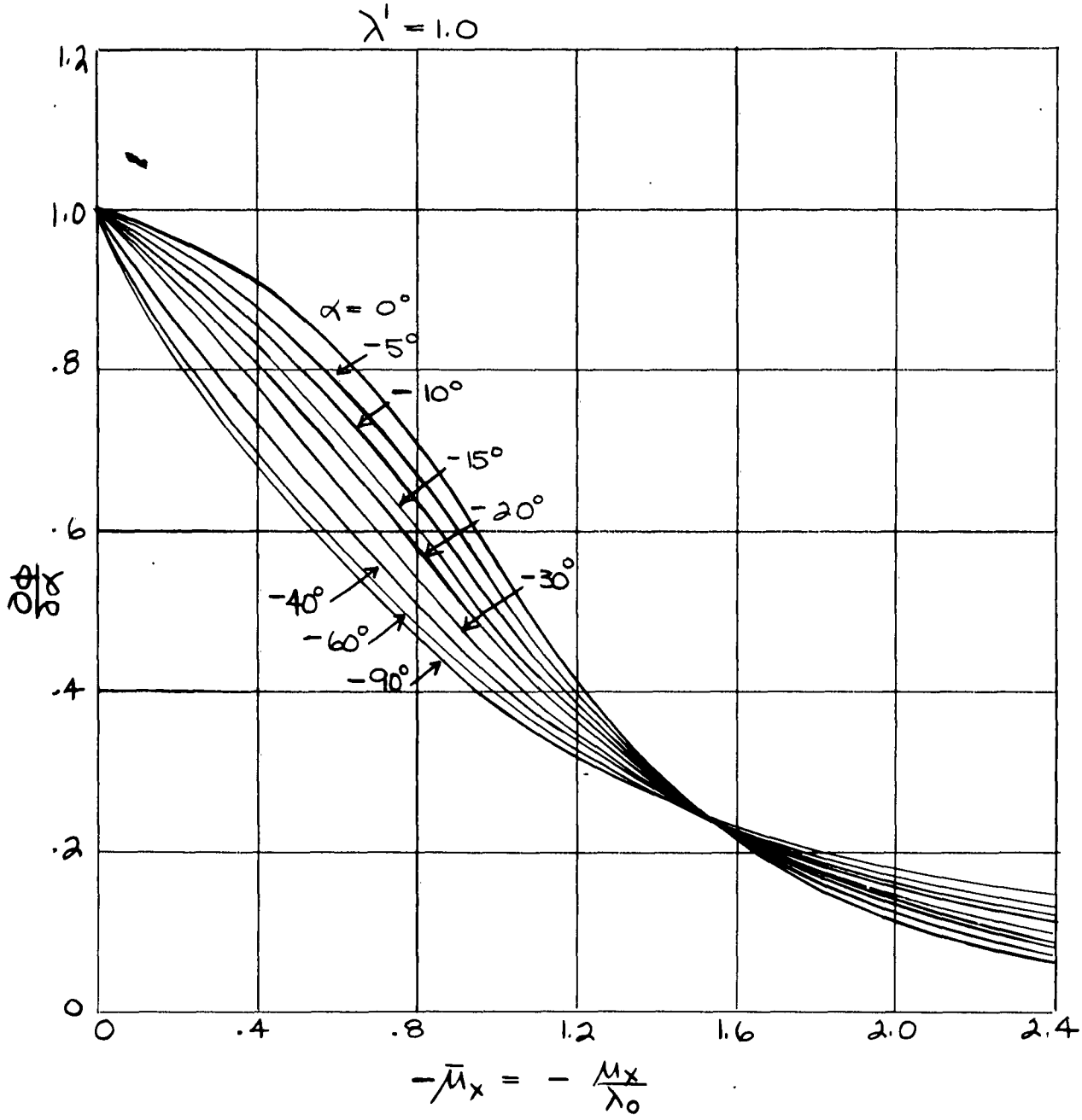
λ' = 1.0
1.2
1.0
.8
.6
.4
.2
0
θ/δ
α = 0°
-5°
-10°
-15°
-20°
-30°
-40°
-60°
-90°
0
.4
.8
1.2
1.6
2.0
2.4
$-\bar{\mu}_x = -\frac{\mu_x}{\lambda_0}$

Figure 6-c

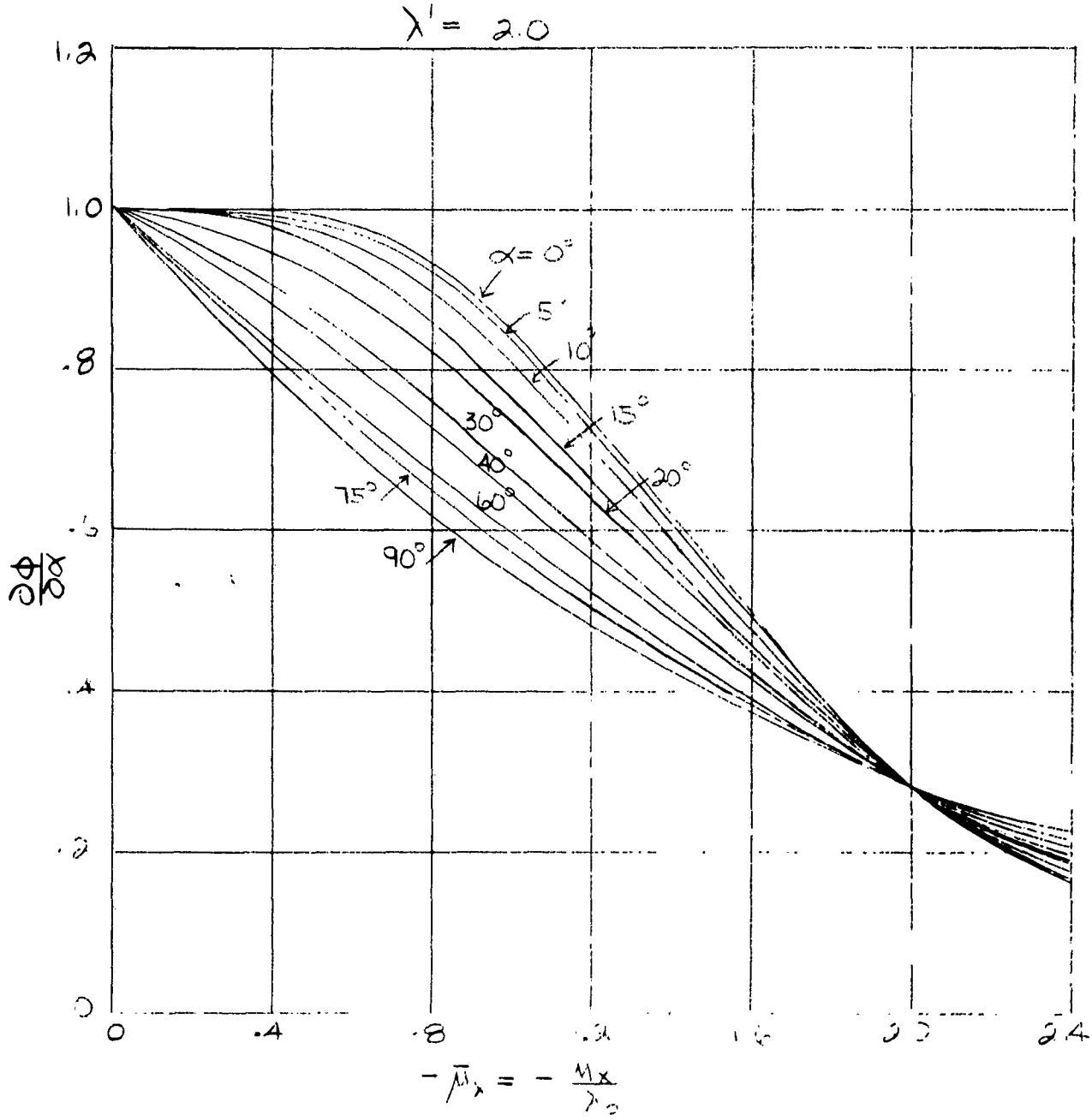
λ' = 2.0
1.2
1.0
.8
.6
.4
.2
0
∂φ/∂x
α = 0°
5°
10°
15°
20°
30°
40°
60°
75°
90°
0
.4
.8
2.4
$-\bar{\mu}_\lambda = -\frac{\mu_x}{\lambda_0}$

Figure 6-d

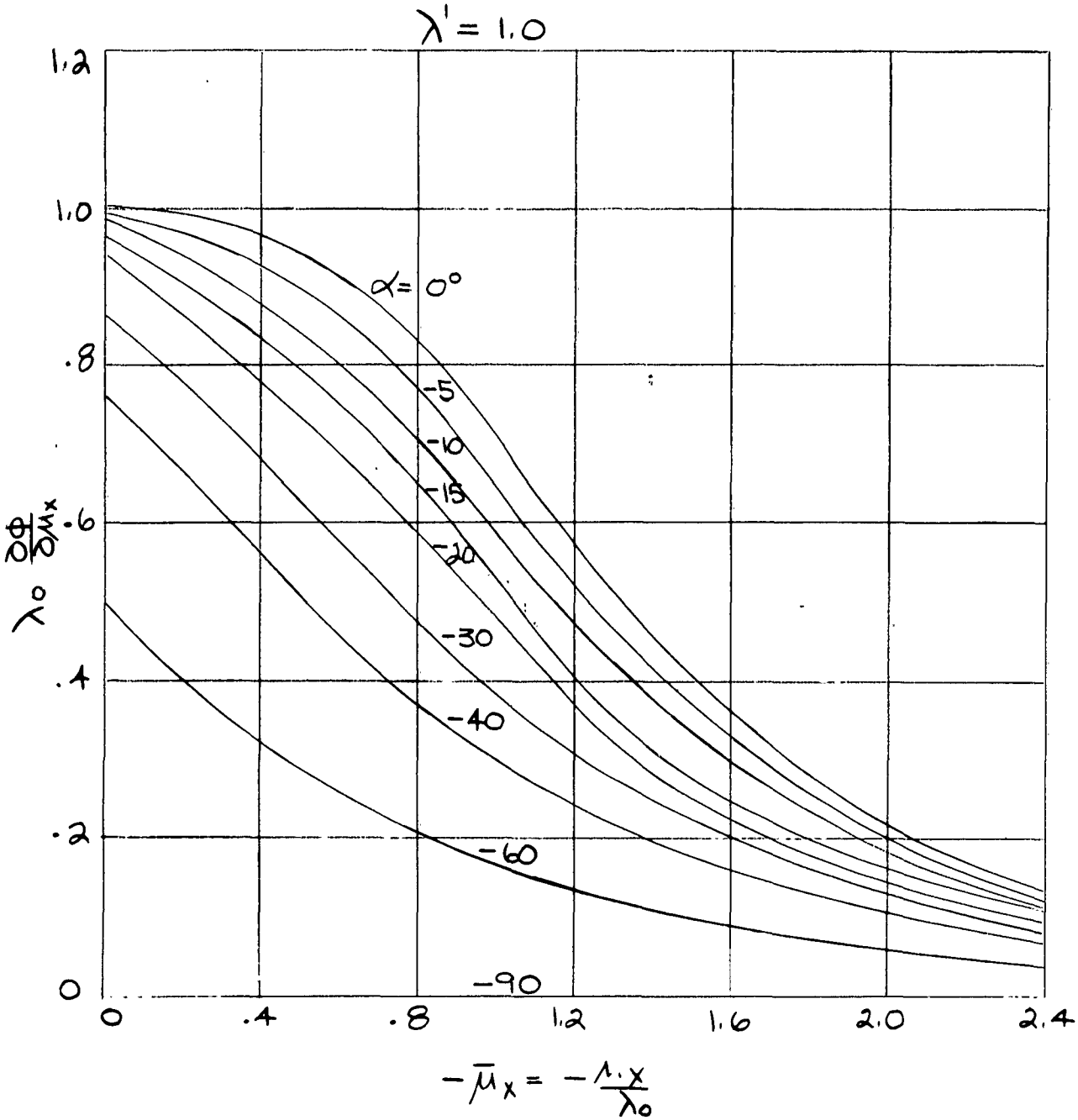
λ' = 1.0
1.2
1.0
.8
.6
.4
.2
0
λ° ∂φ/∂μx
α = 0°
-5
-10
-15
-20
-30
-40
-60
-90
0
.4
.8
1.2
1.6
2.0
2.4
−μ̄x = −λ'x/λ0

Figure 6-e

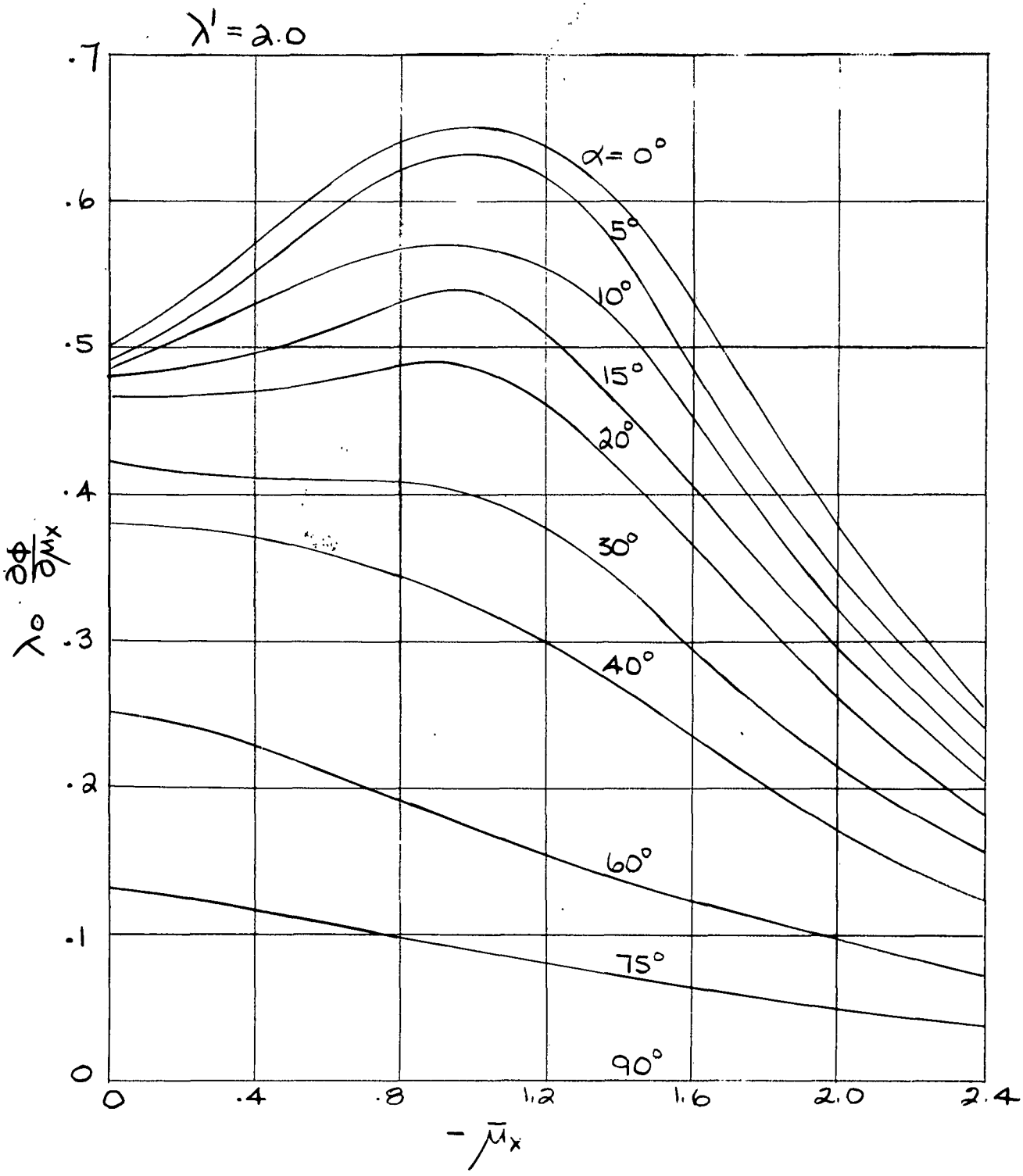
λ' = 2.0
.7
.6
.5
.4
.3
.2
.1
0
α = 0°
5°
10°
15°
20°
30°
40°
60°
75°
90°
0
.4
.8
1.2
1.6
2.0
2.4
$\lambda^0 \partial\theta/\partial\bar{\mu}_x$
$-\bar{\mu}_x$

Figure 6-f

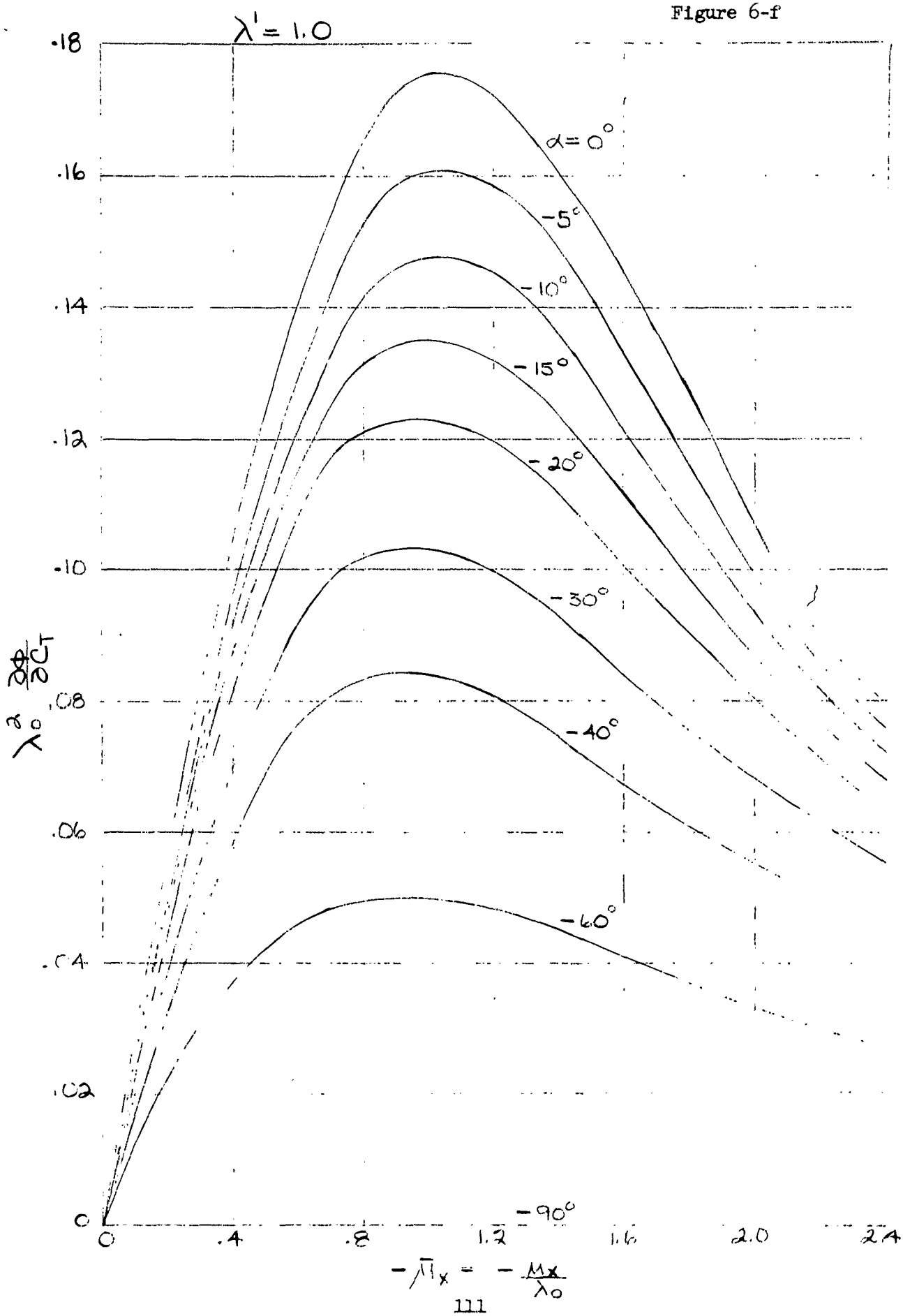
λ' = 1.0
.18
.16
.14
.12
.10
.08
.06
.04
.02
0
α = 0°
-5°
-10°
-15°
-20°
-30°
-40°
-60°
-90°
$\lambda_0^2 \frac{\partial \phi}{\partial C_T}$
0
.4
.8
1.2
1.6
2.0
2.4
$-\bar{\Pi}_x = -\frac{M_x}{\lambda_0}$

Figure 6-g

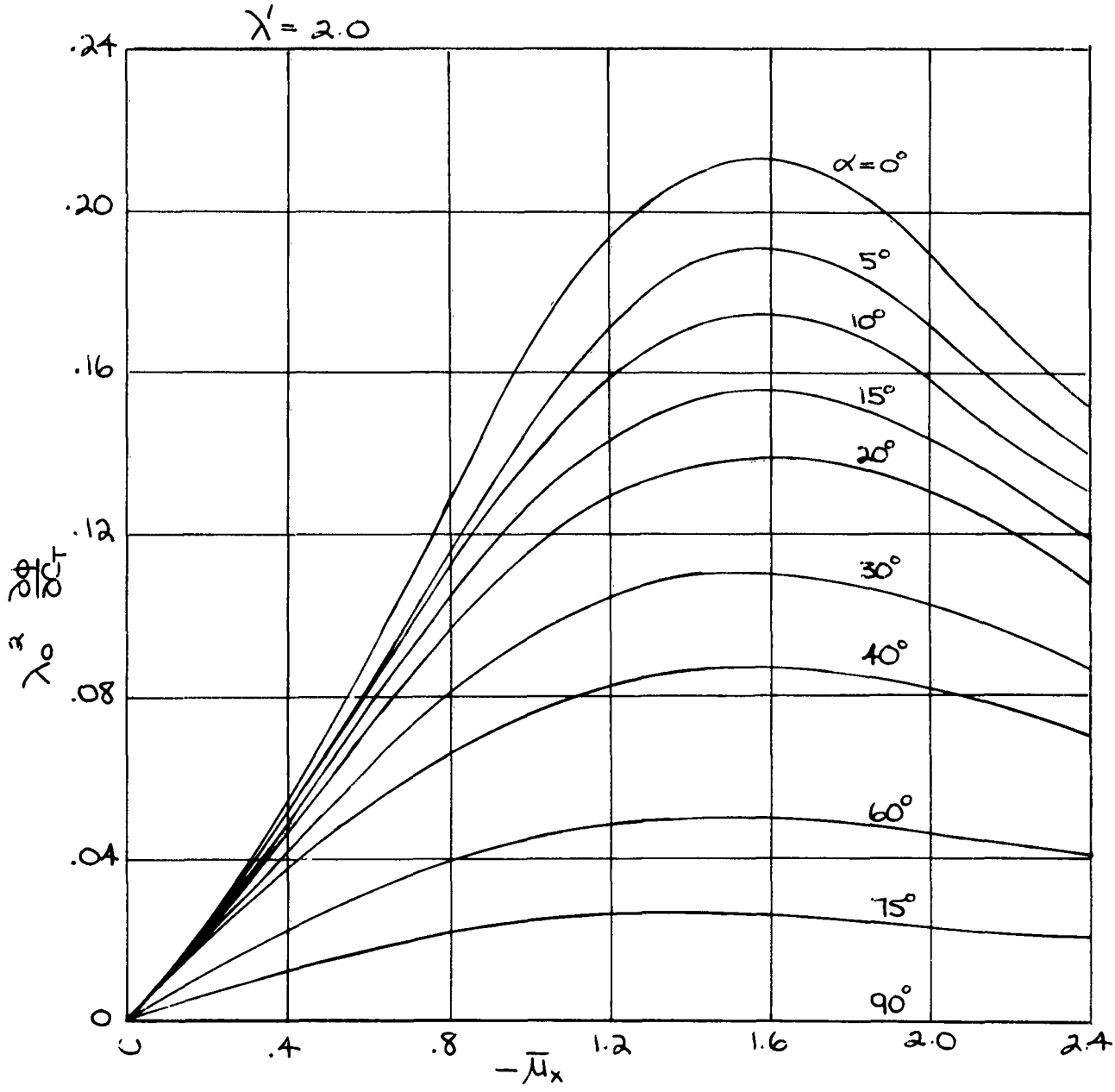
λ' = 2.0
.24
.20
.16
.12
.08
.04
0
$\frac{\partial C_T}{\partial \alpha}$
λ^2
α = 0°
5°
10°
15°
20°
30°
40°
60°
75°
90°
0
.4
.8
1.2
1.6
2.0
2.4
$-\bar{\mu}_x$

Figure 7

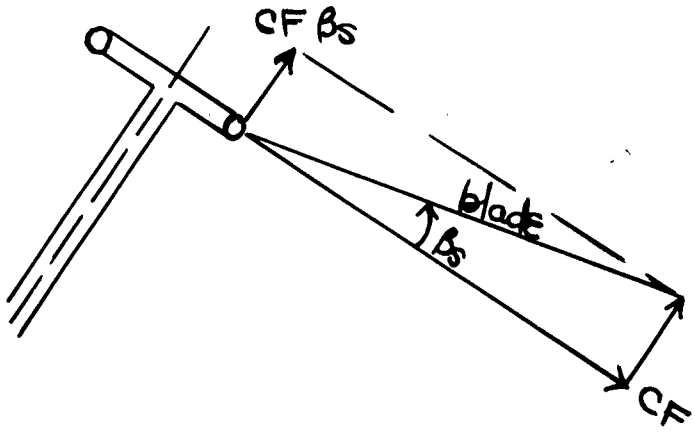

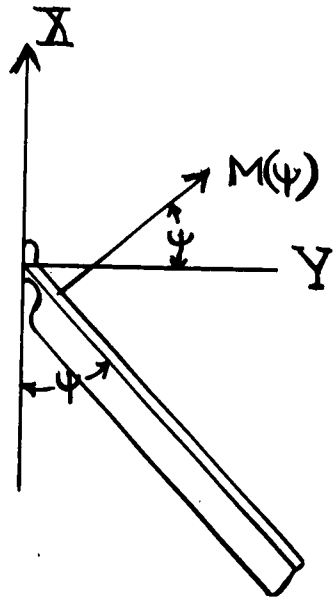

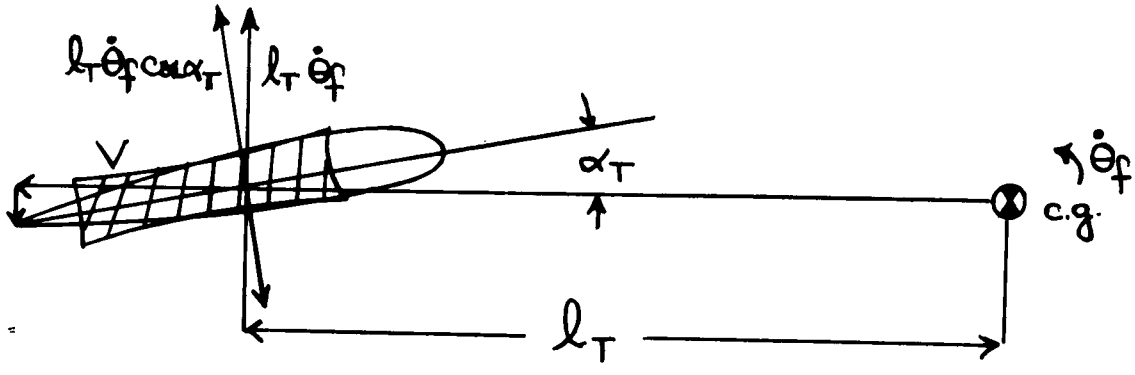

velocity at tail due to pitching

Figure 9

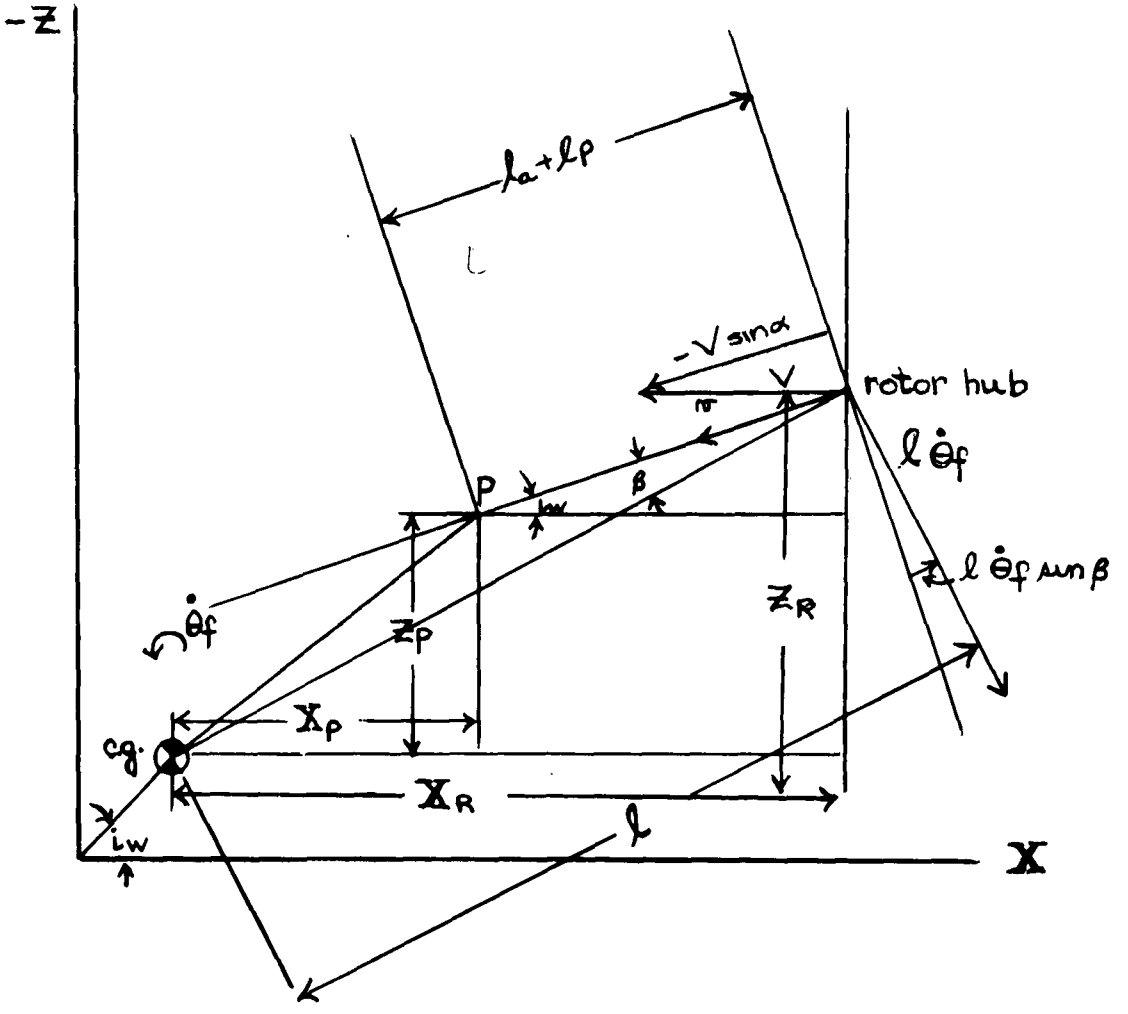
-Z
$l_a + l_p$
$-V \sin\alpha$
V
rotor hub
$l\dot{\theta}_f$
P
i_w
β
$l\dot{\theta}_f \sin\beta$
$\dot{\theta}_f$
Z_P
Z_R
X_P
c.g.
X_R
l
i_w
X

Figure 8

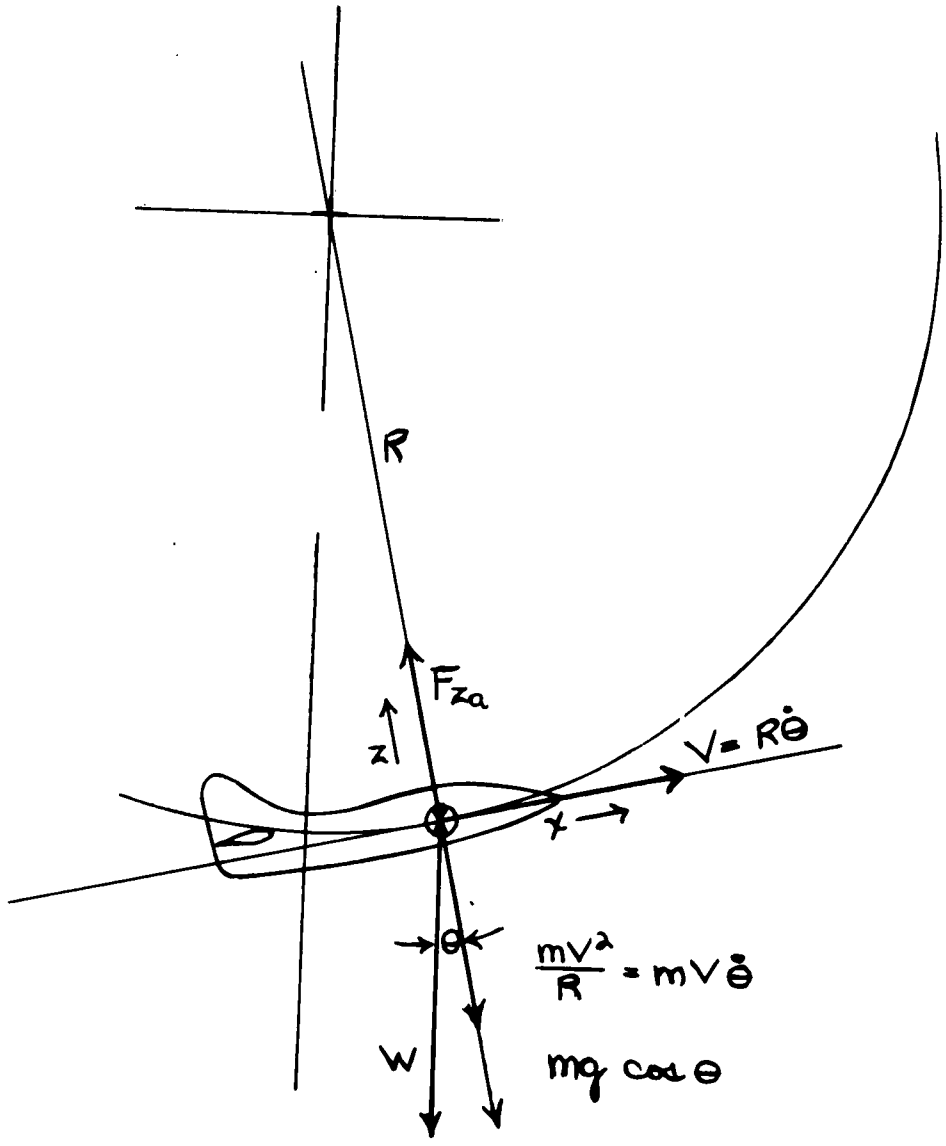

Figure 10

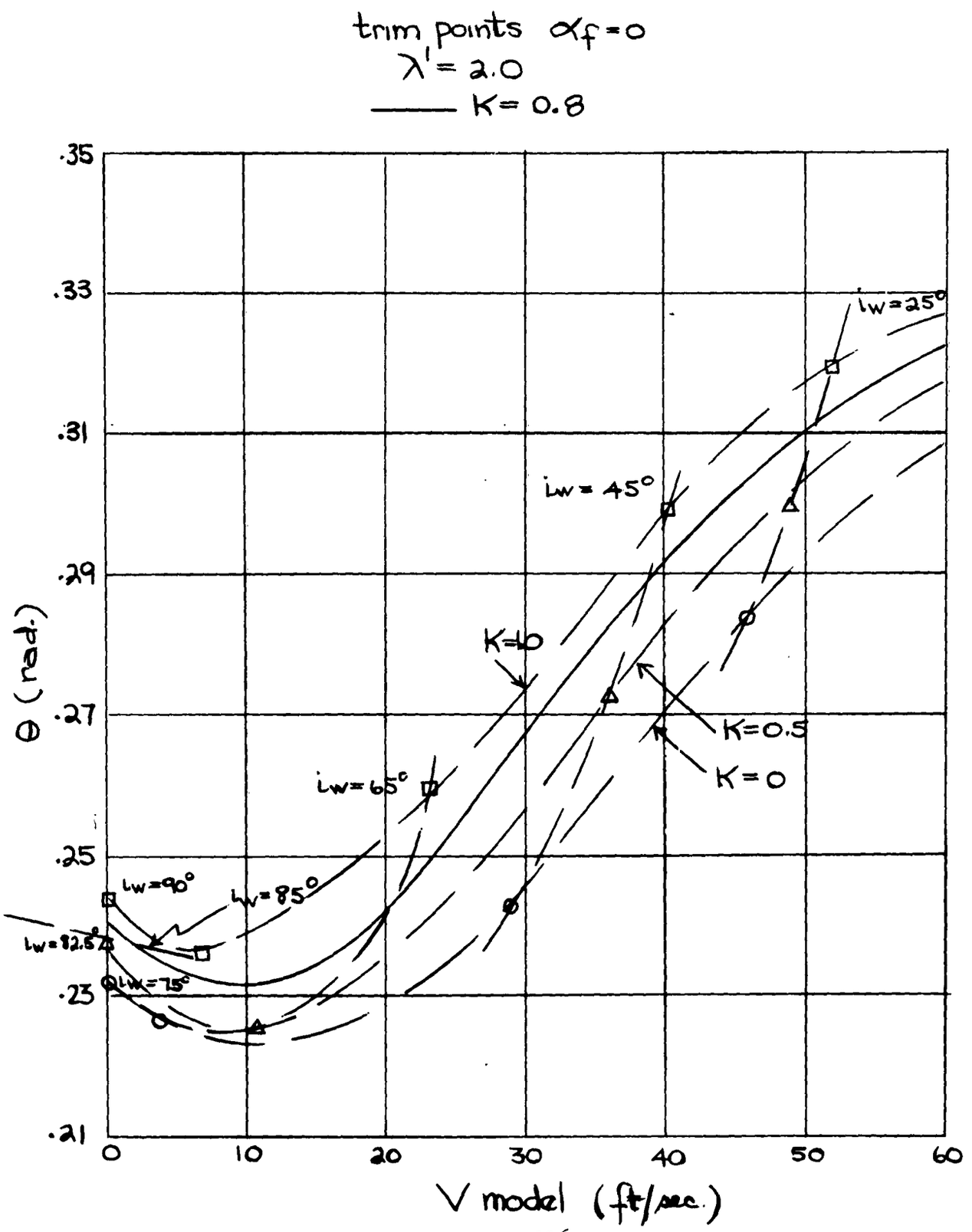
trim points $\alpha_f = 0$
$\lambda' = 2.0$
—— K = 0.8
.35
.33
.31
.29
.27
.25
.23
.21
Θ (rad.)
0
10
20
30
40
50
60
V model (ft/sec.)
iw = 25°
iw = 45°
iw = 65°
iw = 85°
iw = 90°
iw = 82.5°
iw = 75°
K = 1.0
K = 0.5
K = 0

trim points $\alpha_f = 0$

$\lambda = 1.5$

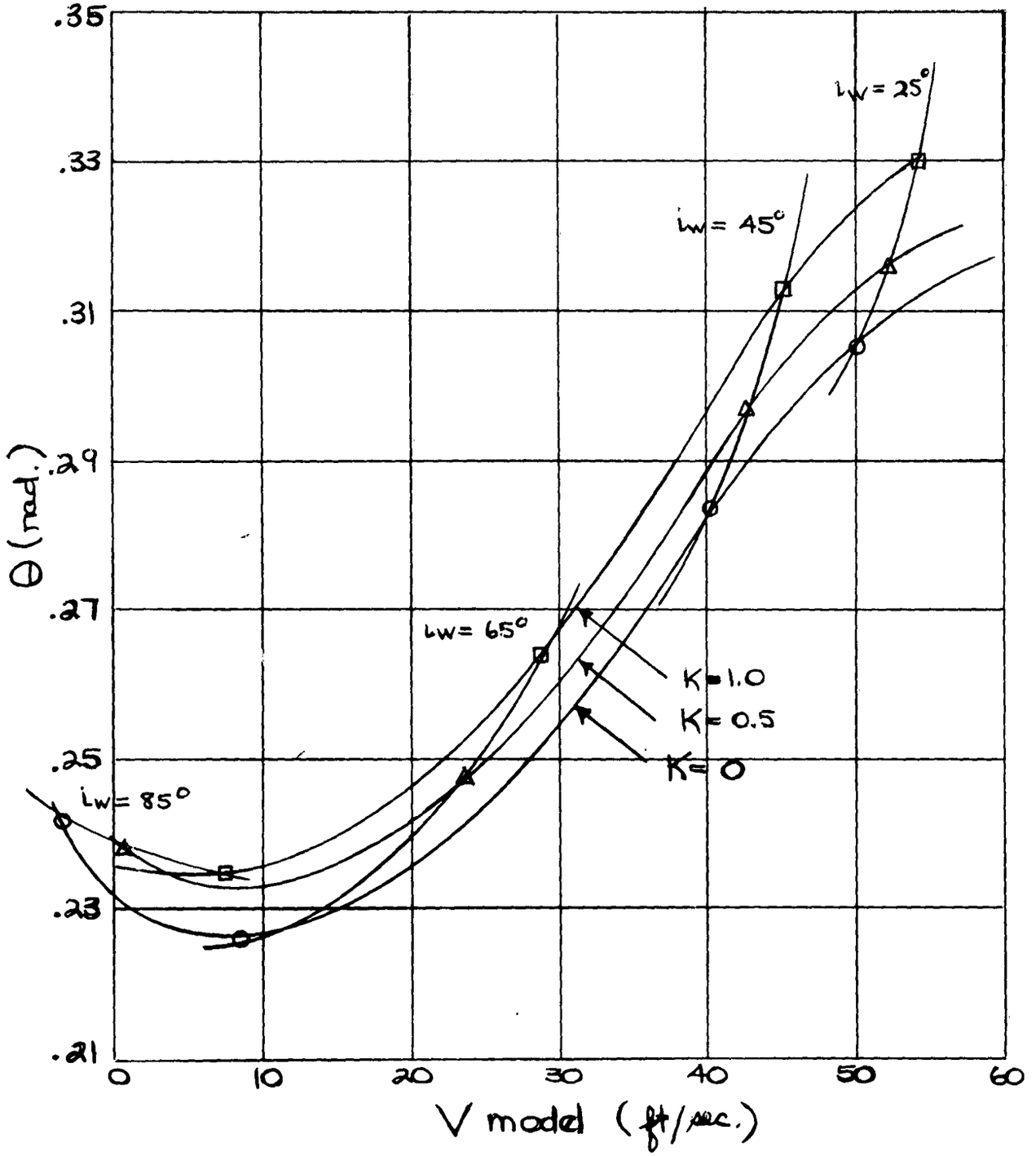

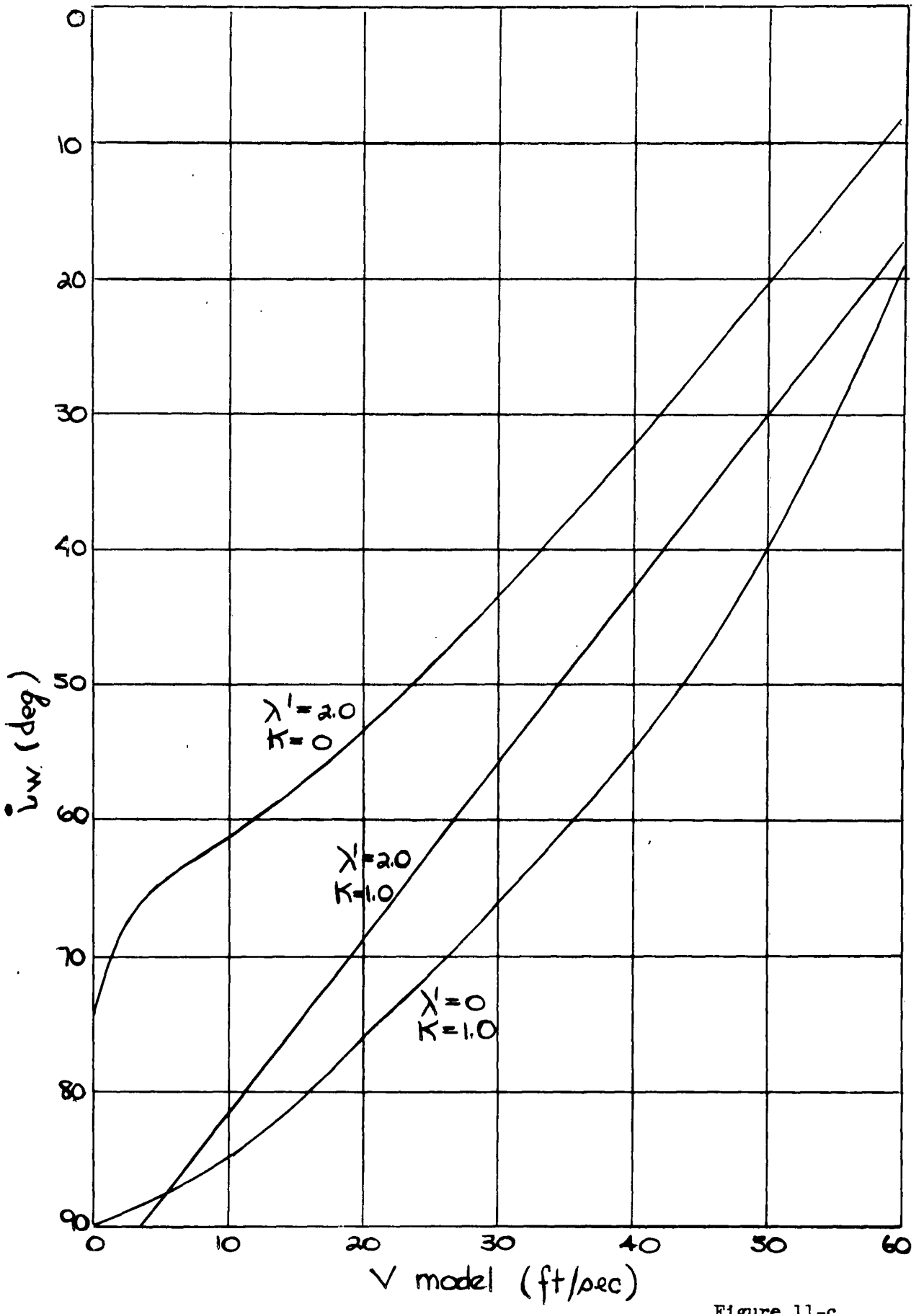
0
10
20
30
40
50
60
70
80
90
i_w (deg)
$\lambda' = 2.0$
$K = 0$
$\lambda' = 2.0$
$K = 1.0$
$\lambda' = 0$
$K = 1.0$
0
10
20
30
40
50
60
V model (ft/sec)

Figure 11-c

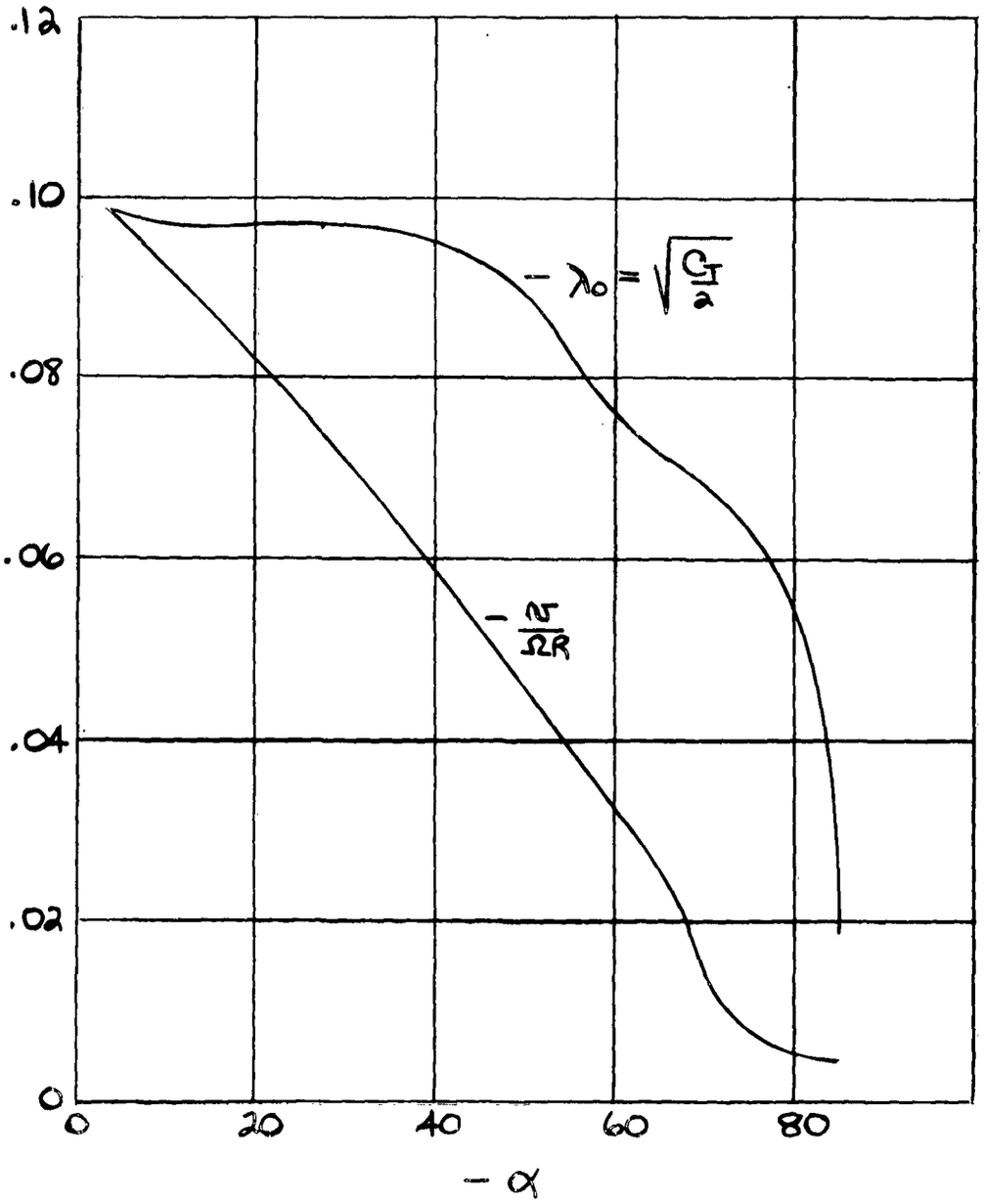
.12
.10
.08
.06
.04
.02
0
0
20
40
60
80
$-\lambda_0 = \sqrt{\frac{C_T}{2}}$
$-\frac{v}{\Omega R}$
$-\alpha$

Figure 11-d

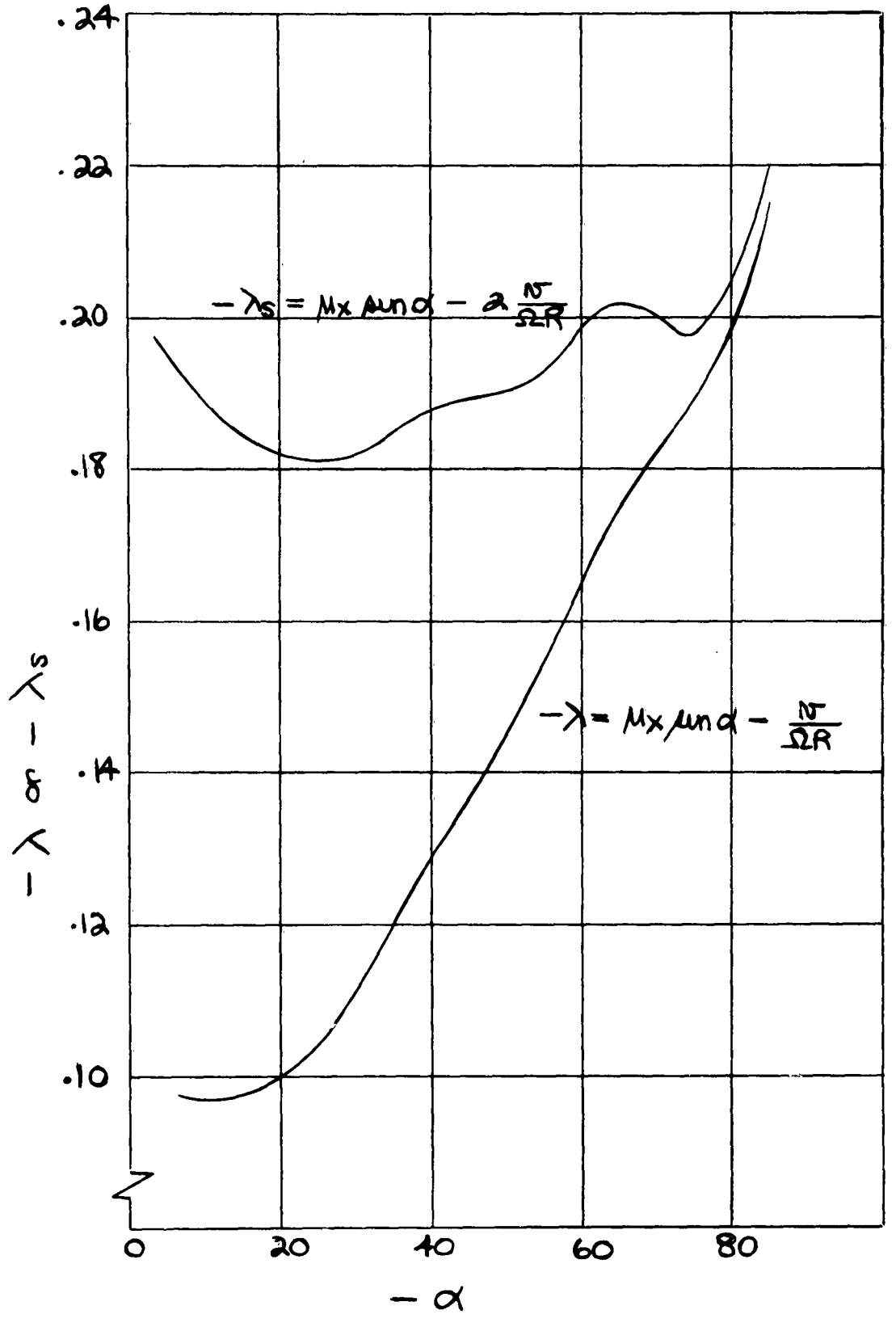
.24
.22
.20
.18
.16
.14
.12
.10
$-\lambda_s = M_x \sin\alpha - 2\frac{N}{\Omega R}$
$-\lambda = M_x \sin\alpha - \frac{N}{\Omega R}$
$-\lambda_1 - \delta - \lambda_s$
0
20
40
60
80
$-\alpha$

Figure 11-e

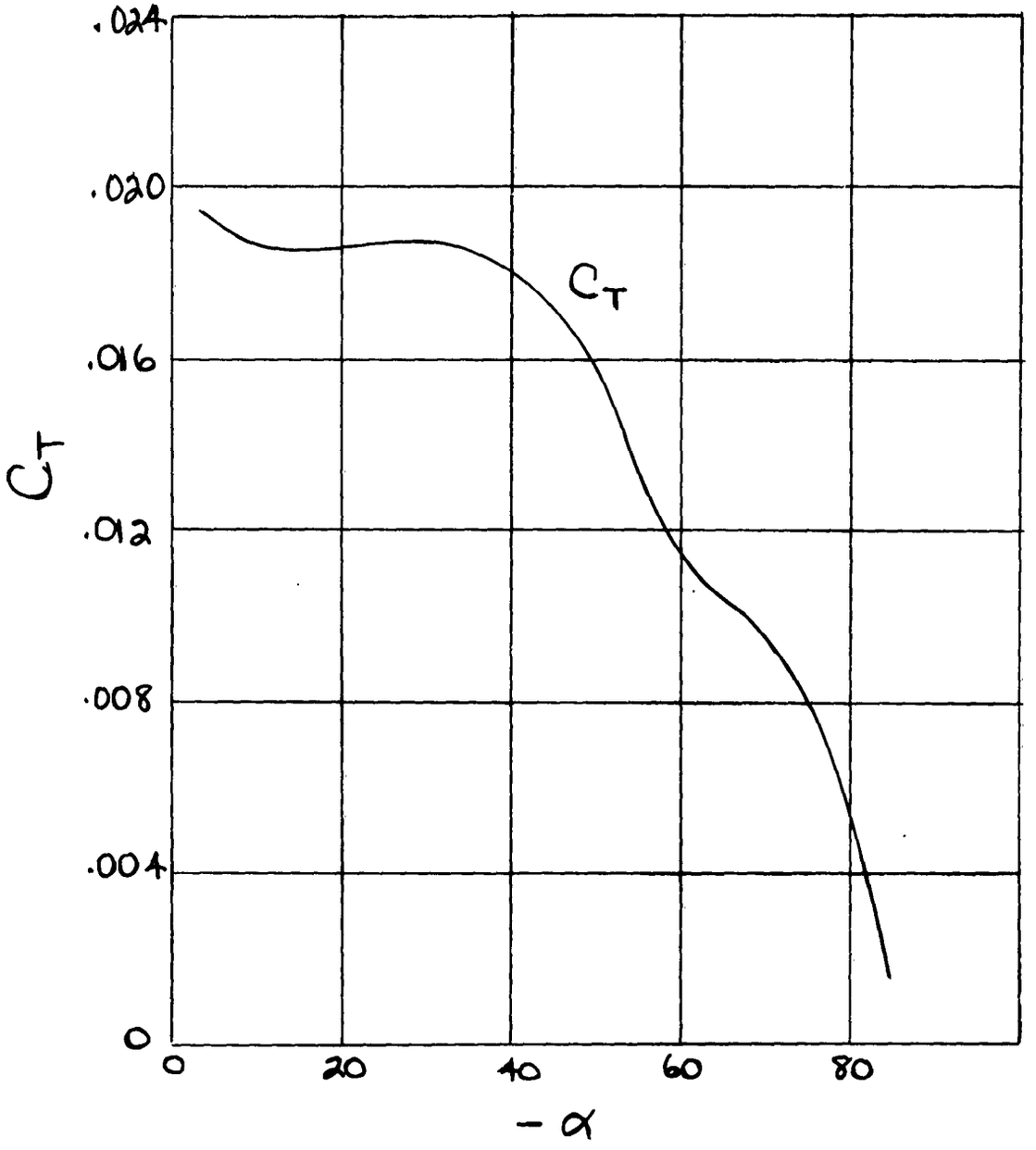

Figure 11-f

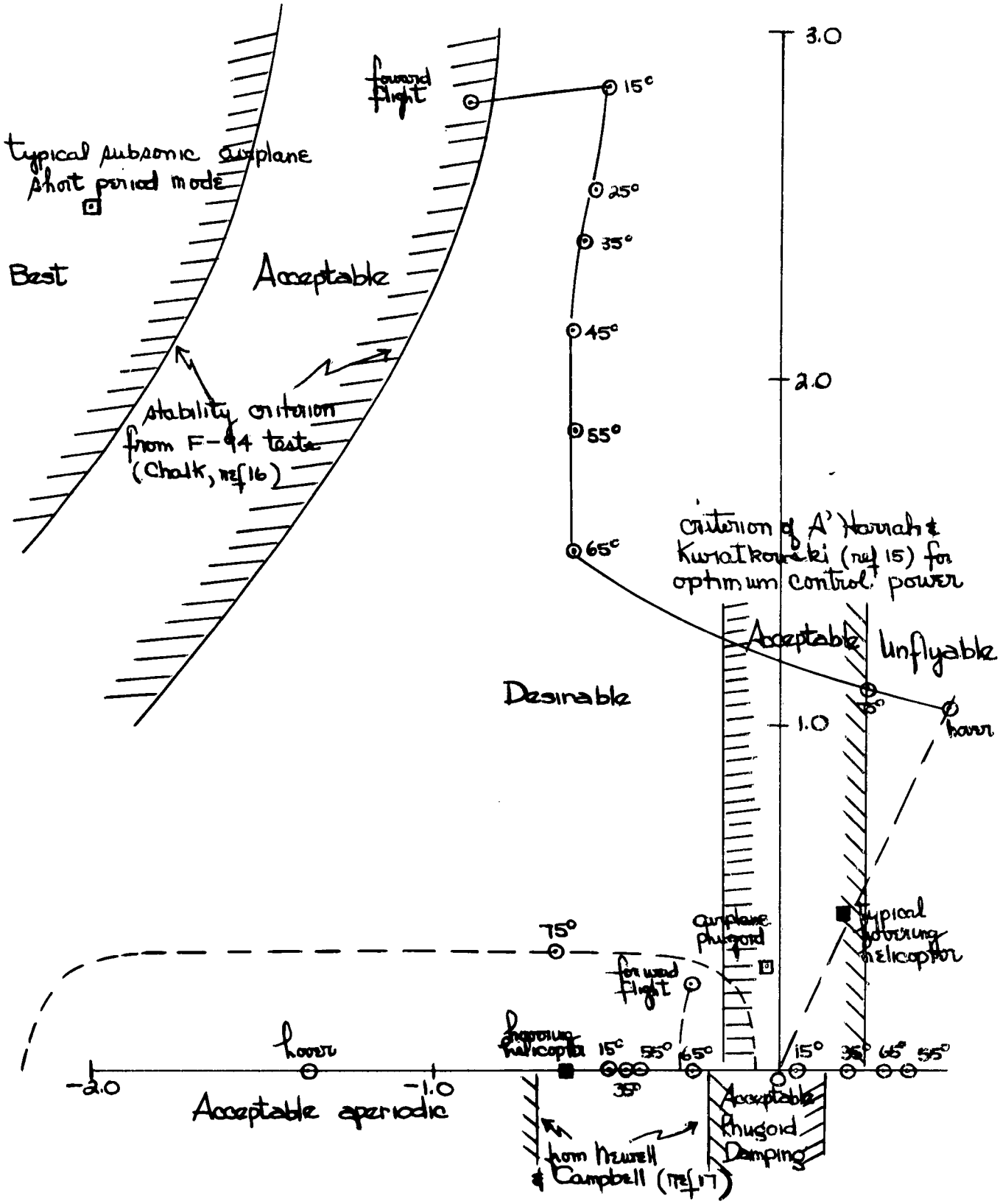
typical subsonic airplane short period mode
Best
Acceptable
Desirable
stability criterion from F-94 tests (Chalk, ref 16)
forward flight
15°
25°
35°
45°
55°
65°
3.0
2.0
1.0
criterion of A' Harrah & Kuriatkowski (ref 15) for optimum control power
Acceptable
Unflyable
hover
75°
forward flight
airplane phugoid
typical hovering helicopter
hover
hovering helicopter
15°
35°
65°
15°
35°
65°
55°
-2.0
-1.0
35°
Acceptable aperiodic
Acceptable phugoid Damping
from Newell & Campbell (ref 17)

Figure 12

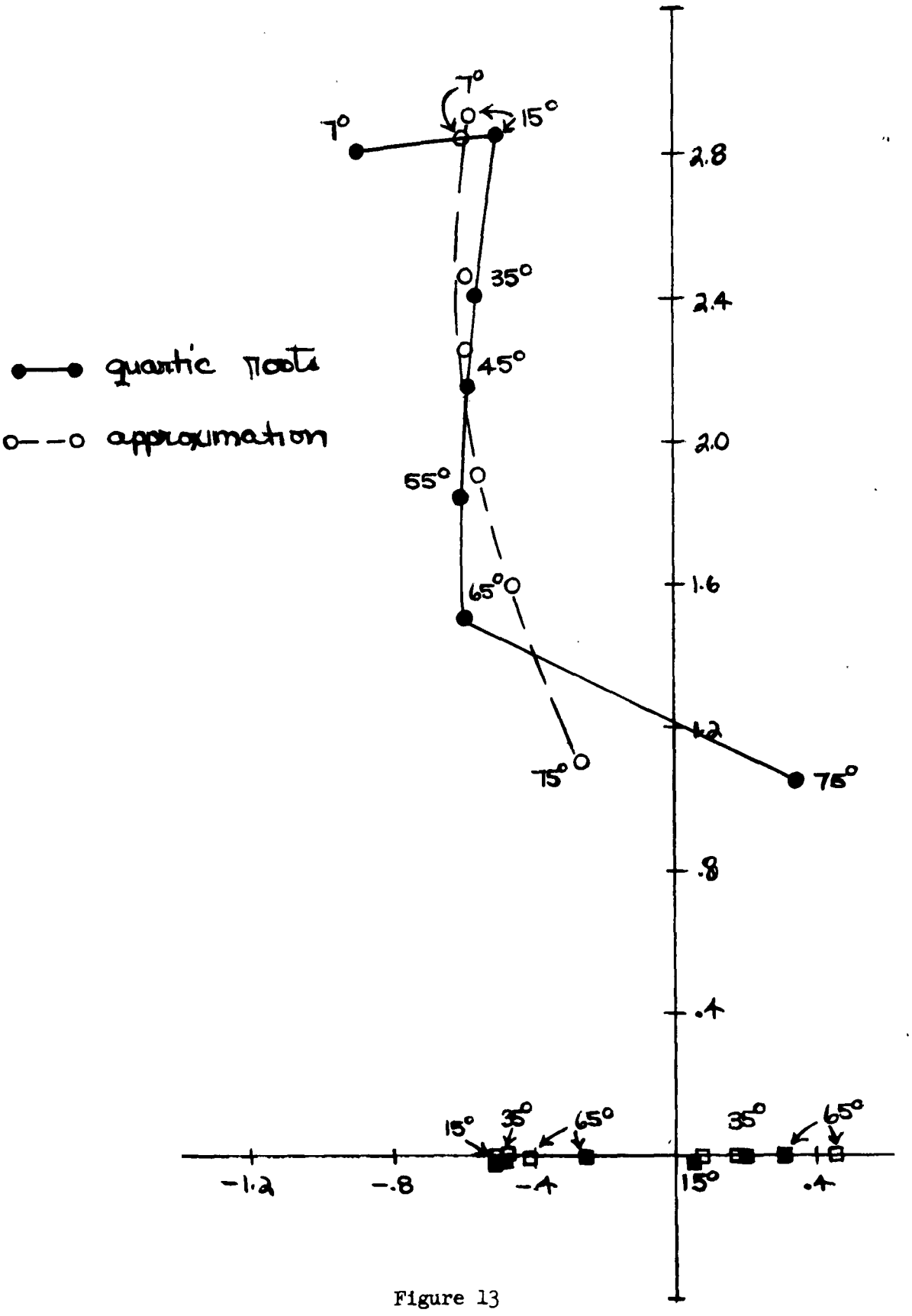
quartic roots
approximation
7°
7°
15°
35°
45°
55°
65°
75°
75°
2.8
2.4
2.0
1.6
1.2
.8
.4
15°
35°
65°
35°
65°
-1.2
-.8
-.4
15°
.4

Figure 13

Figure 14

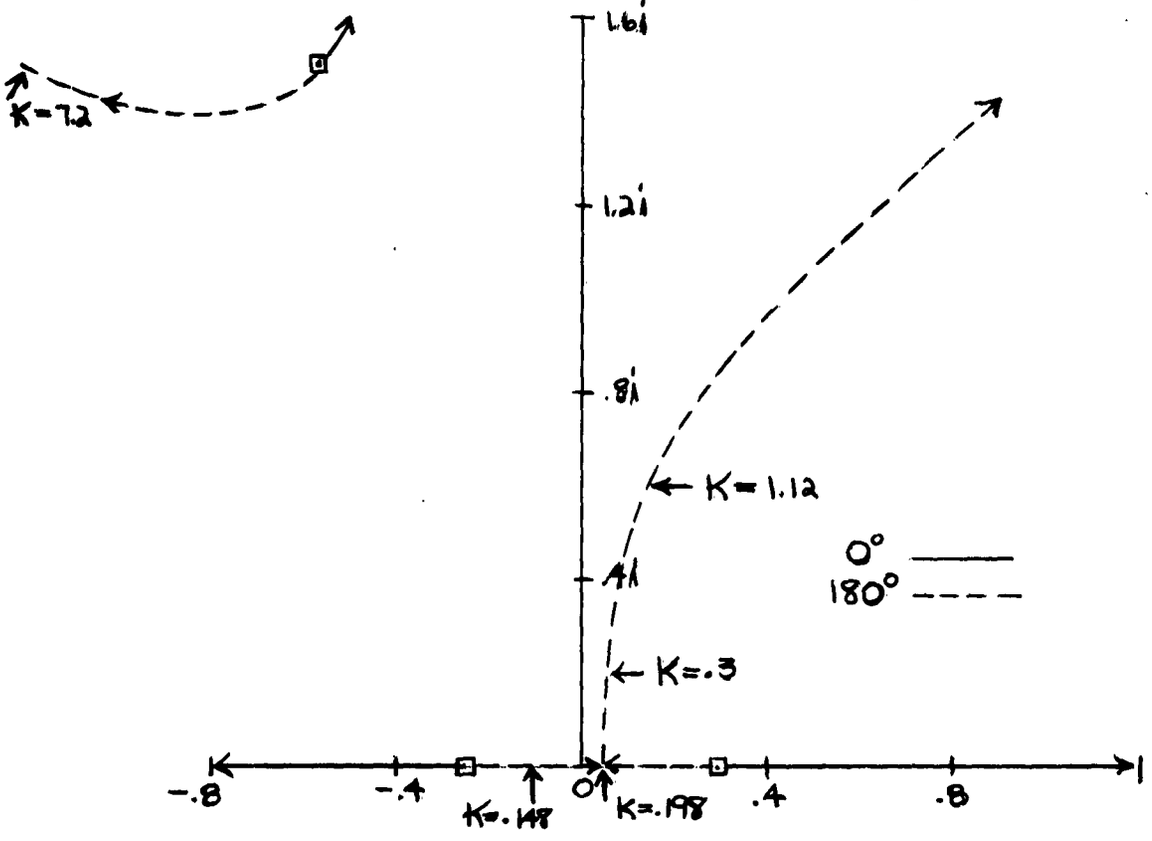

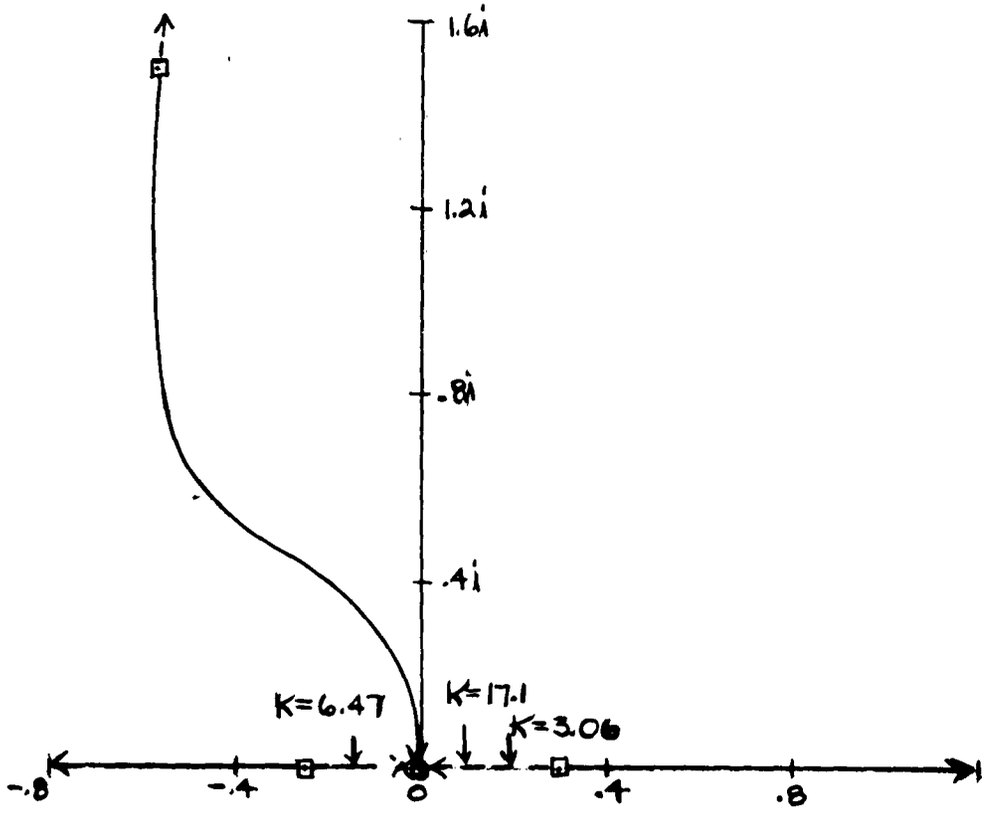

Figure 15

Figure 16

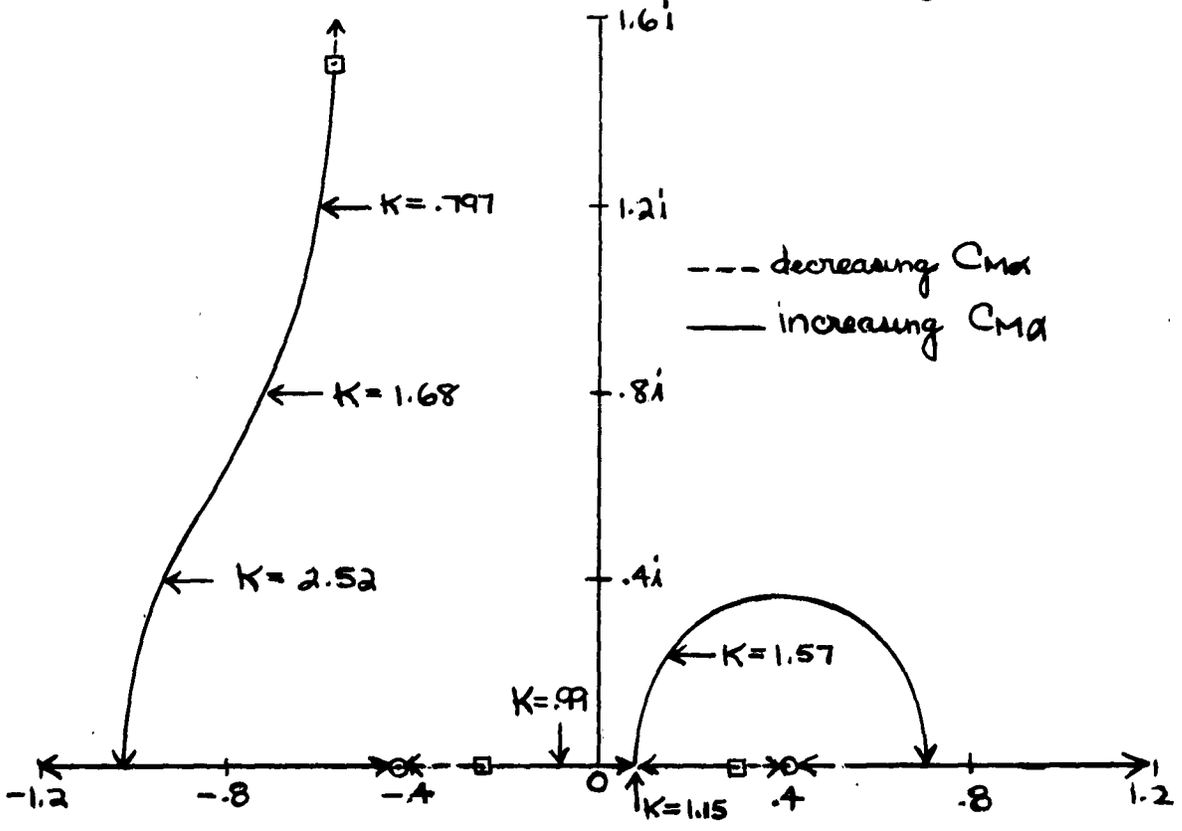

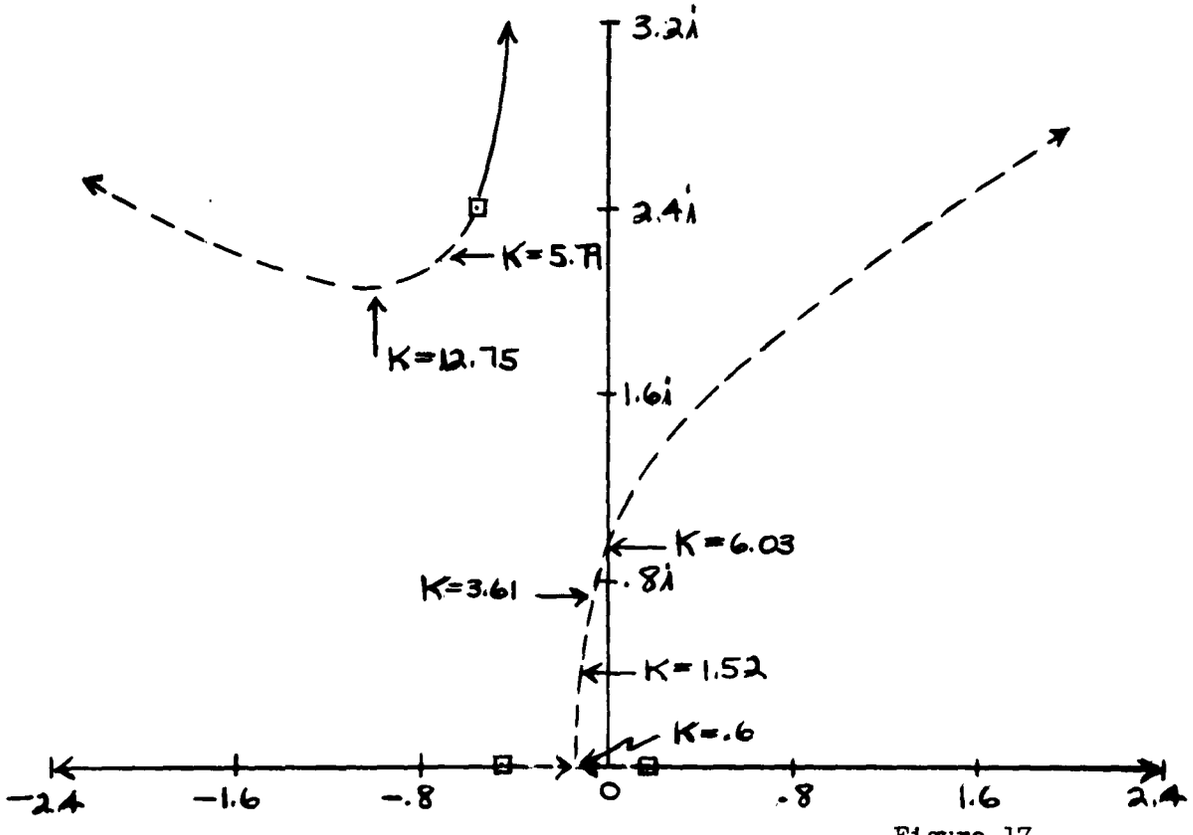

Figure 17

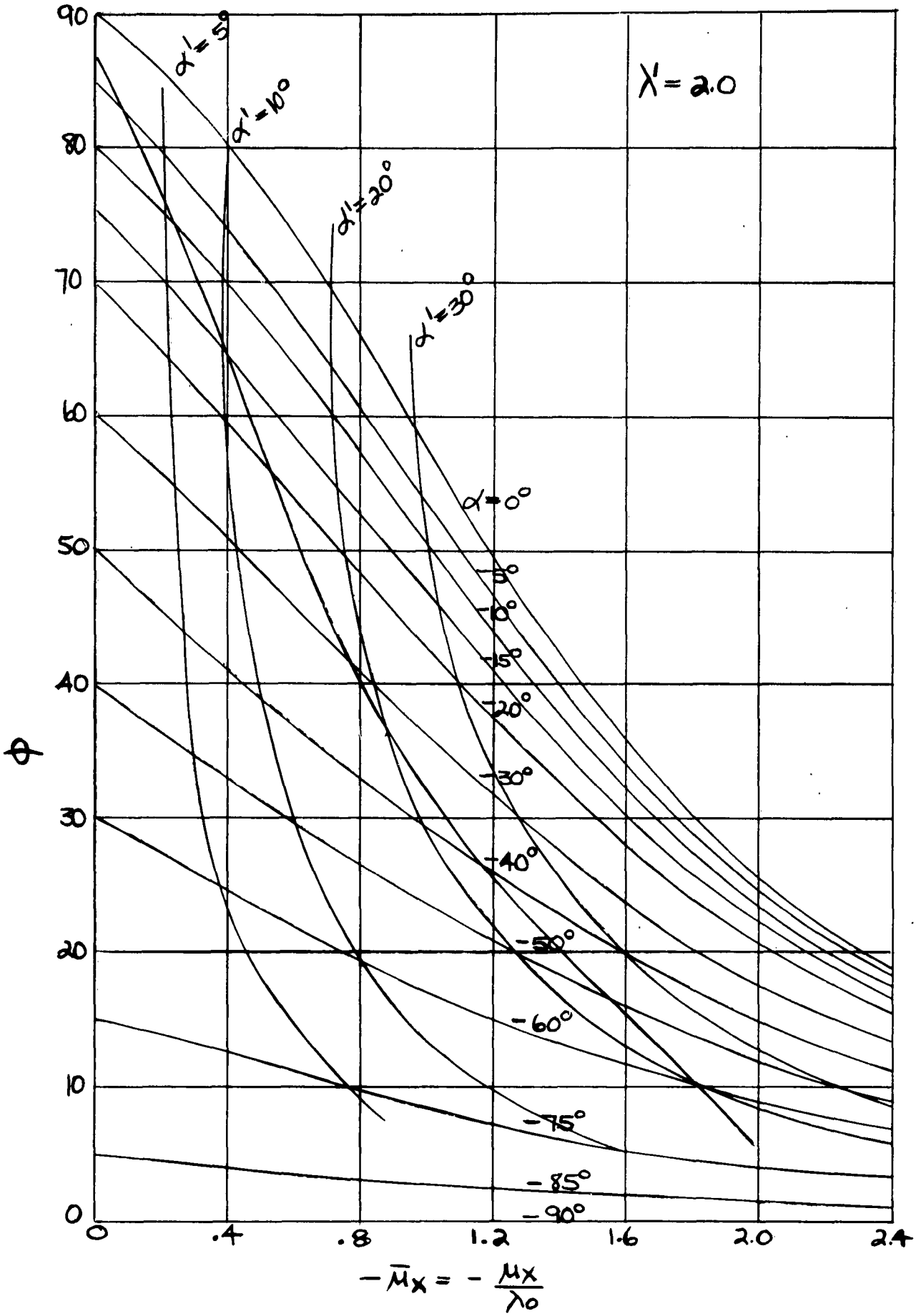
λ' = 2.0
α'=5°
α'=10°
α'=20°
α'=30°
α=0°
-5°
-10°
-15°
-20°
-30°
-40°
-50°
-60°
-75°
-85°
-90°
90
80
70
60
50
40
30
20
10
0
θ
0
.4
.8
1.2
1.6
2.0
2.4
$-\bar{\mu}_x = -\frac{\mu_x}{\lambda_0}$

Figure 18

Figure 19

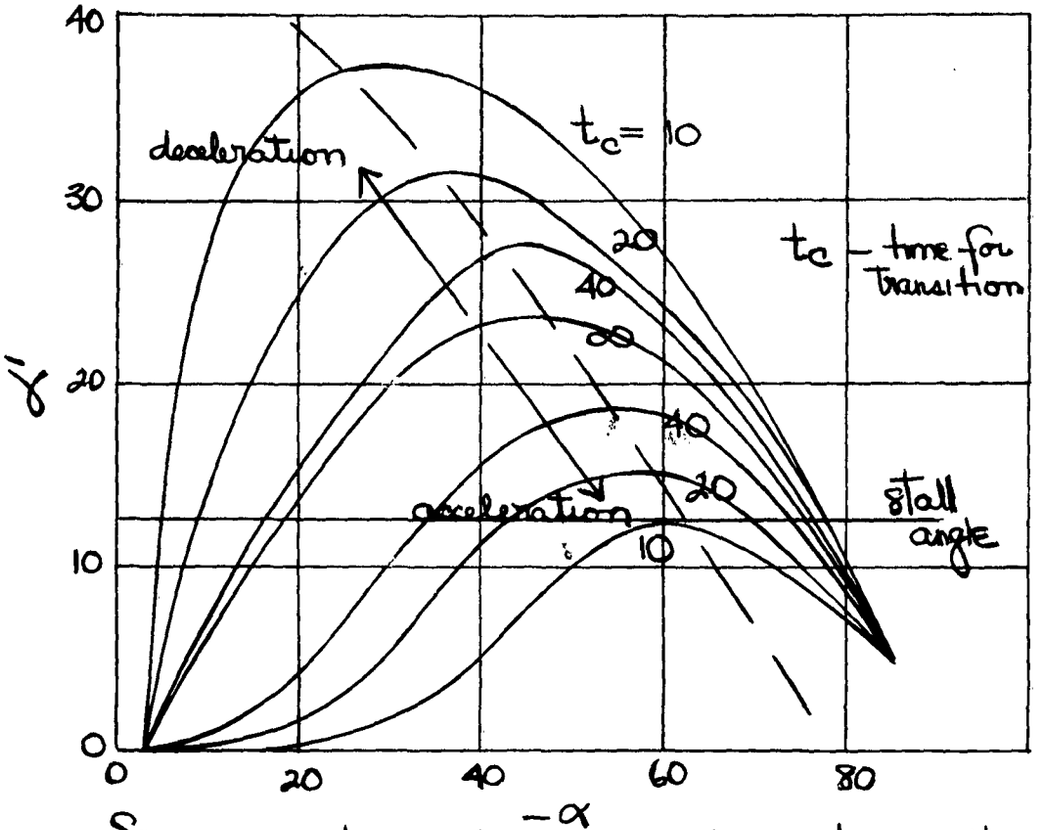

Effective angle of attack vs. rotor angle of attack for various accelerations and decelerations

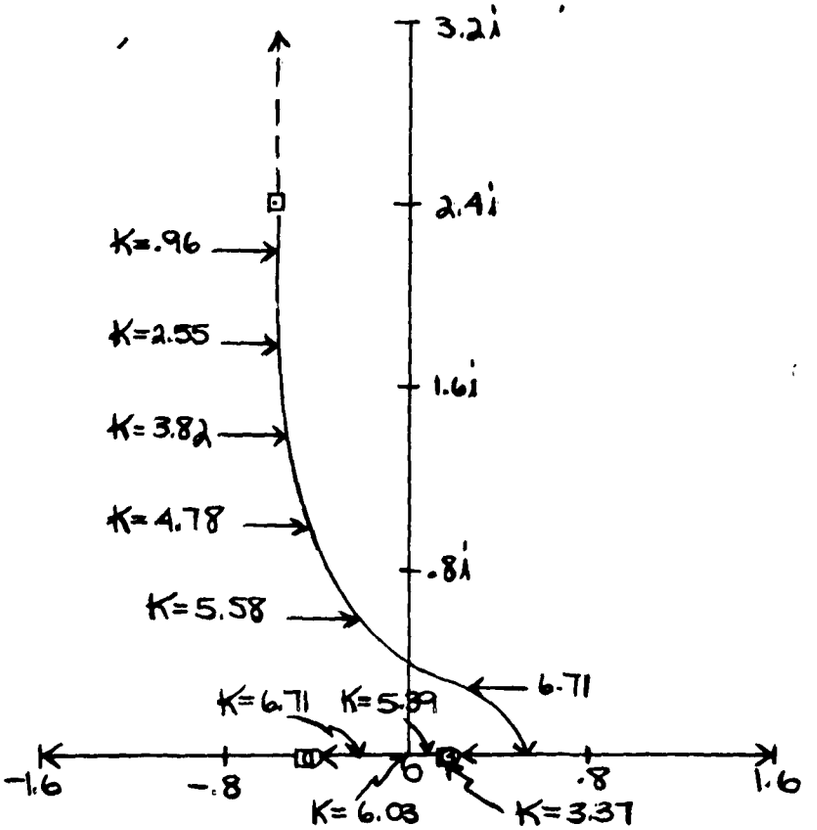

Figure 20

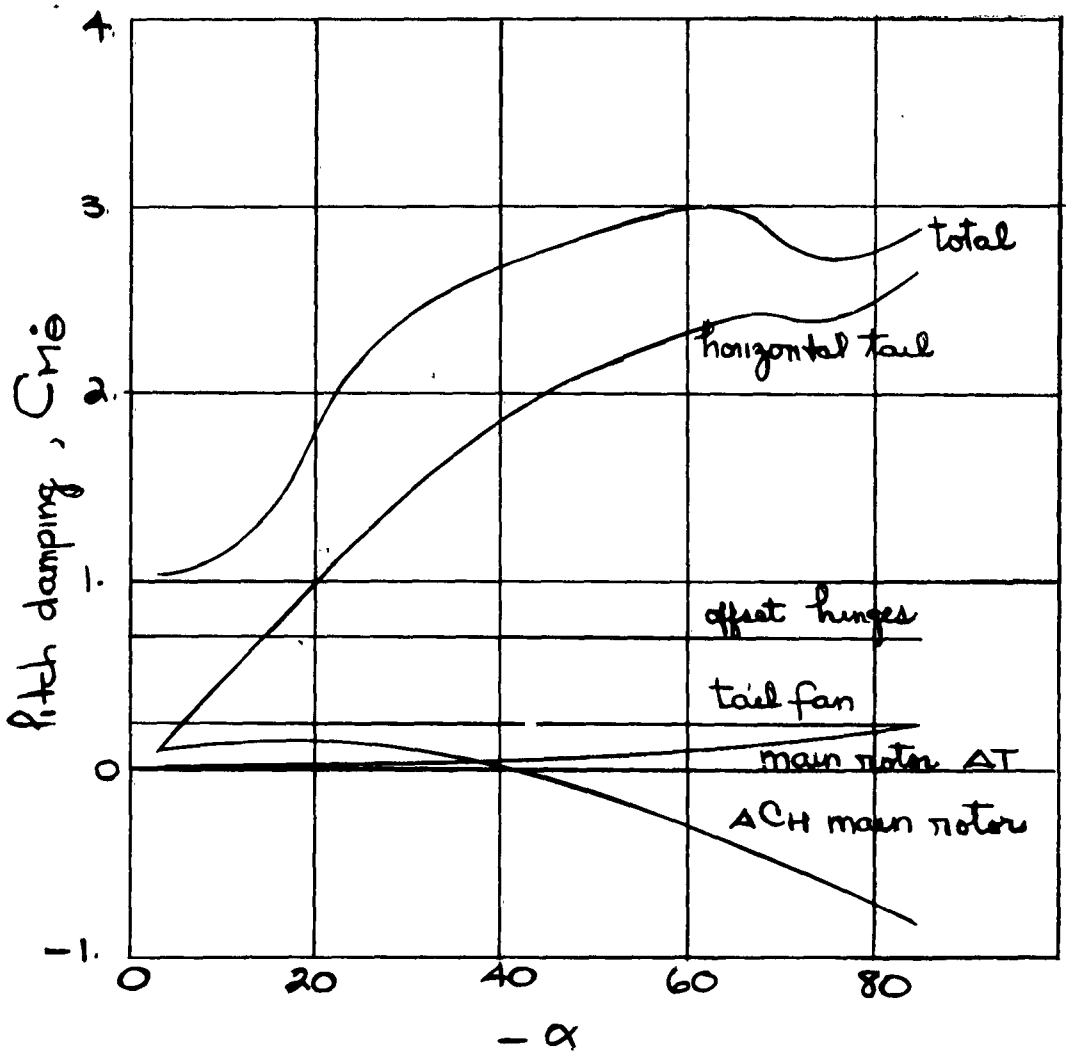
4
3
2
1
0
-1
0
20
40
60
80
$-\alpha$
Pitch damping, $C_{m_\dot{\theta}}$
total
horizontal tail
offset hinges
tail fan
main rotor ΔT
ΔC_H main rotor

Figure 21

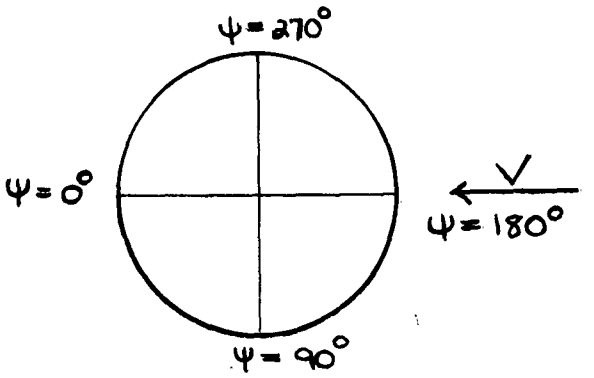

A. Rotor – Top view

L_b – local blade lift
Δv – change in inflow due to pitching
ΔH – local H-force change due to pitching

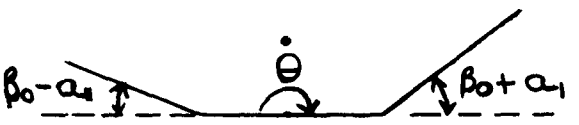

B. Rotor – side view

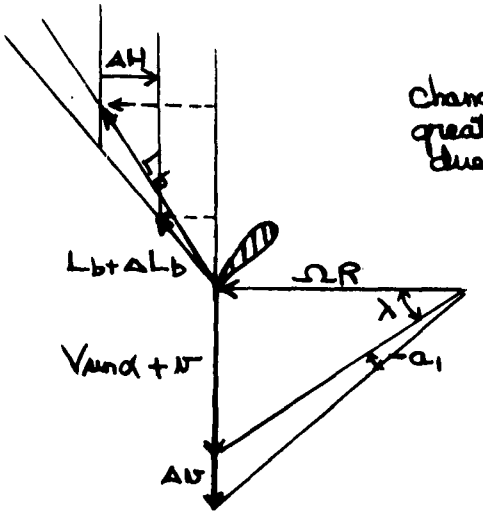

C. λ large, ψ = 90°

Change due to magnitude greater than change due to rotation

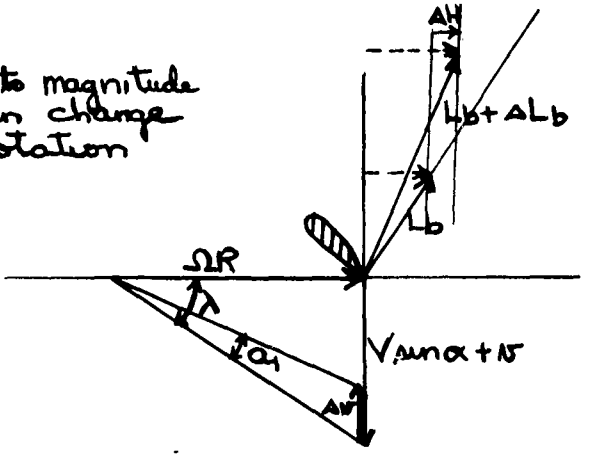

D. λ large, ψ = 270°

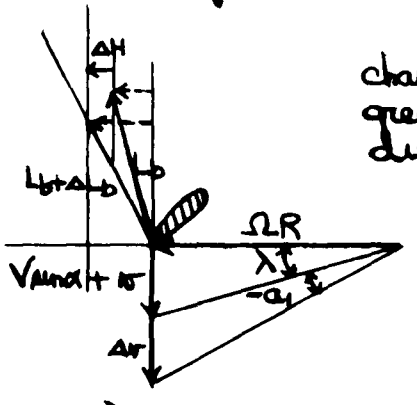

E. λ small, ψ = 90°

Change due to rotation greater than change due to magnitude

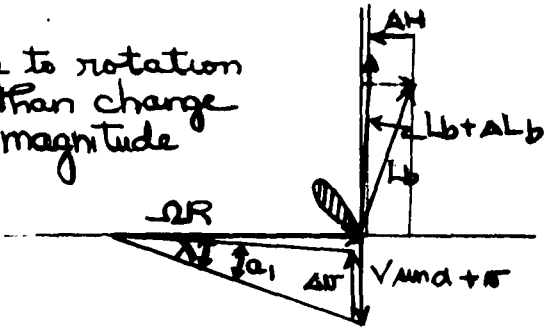

F. λ small, ψ = 270°

Figure 22

Figure 23

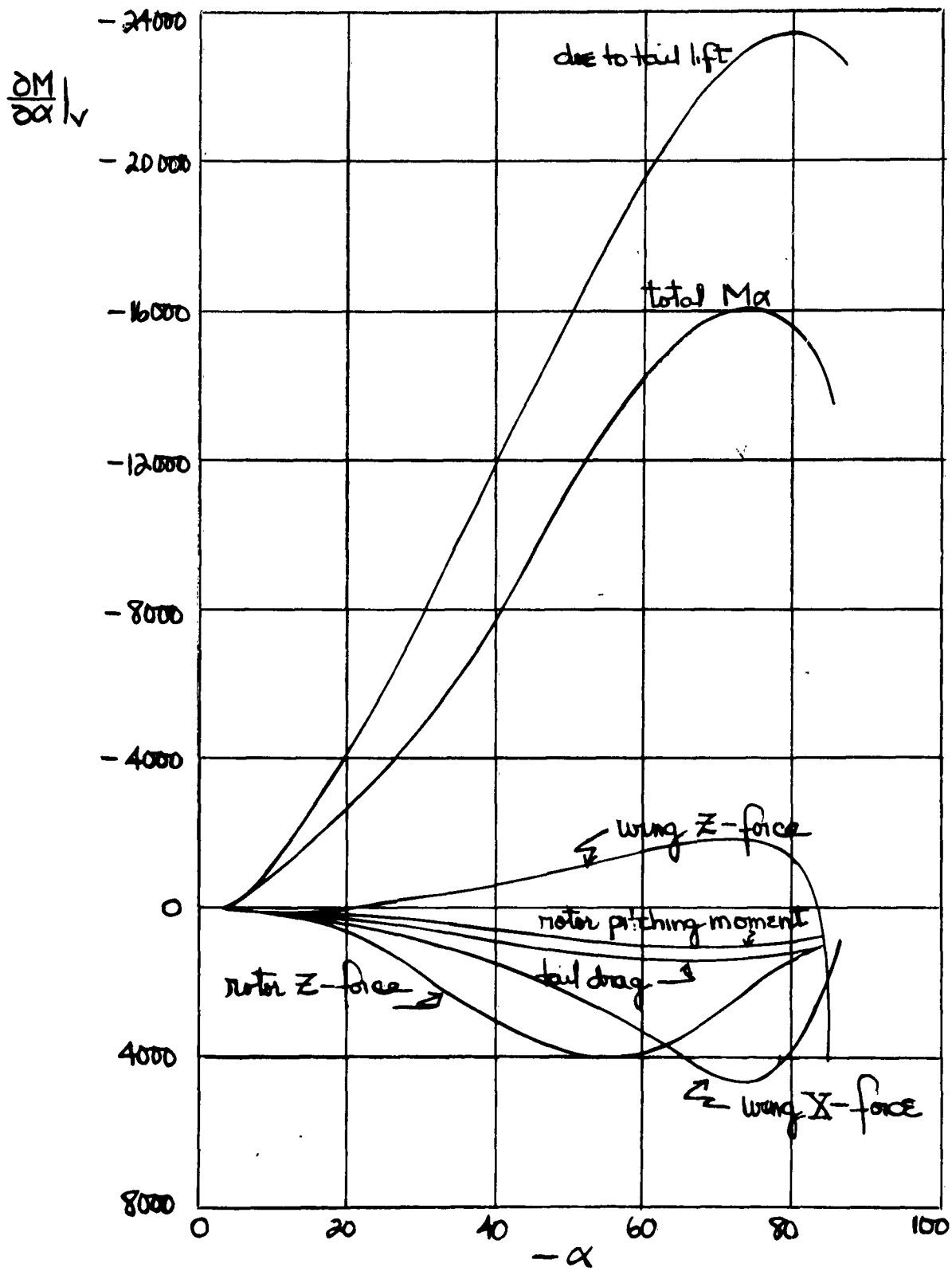
$\frac{\partial M}{\partial \alpha}\Big|_V$
-24000
-20000
-16000
-12000
-8000
-4000
0
4000
8000
0
20
40
60
80
100
$-\alpha$
due to tail lift
total M_α
wing Z-force
motor pitching moment
tail drag
motor Z-force
wing X-force

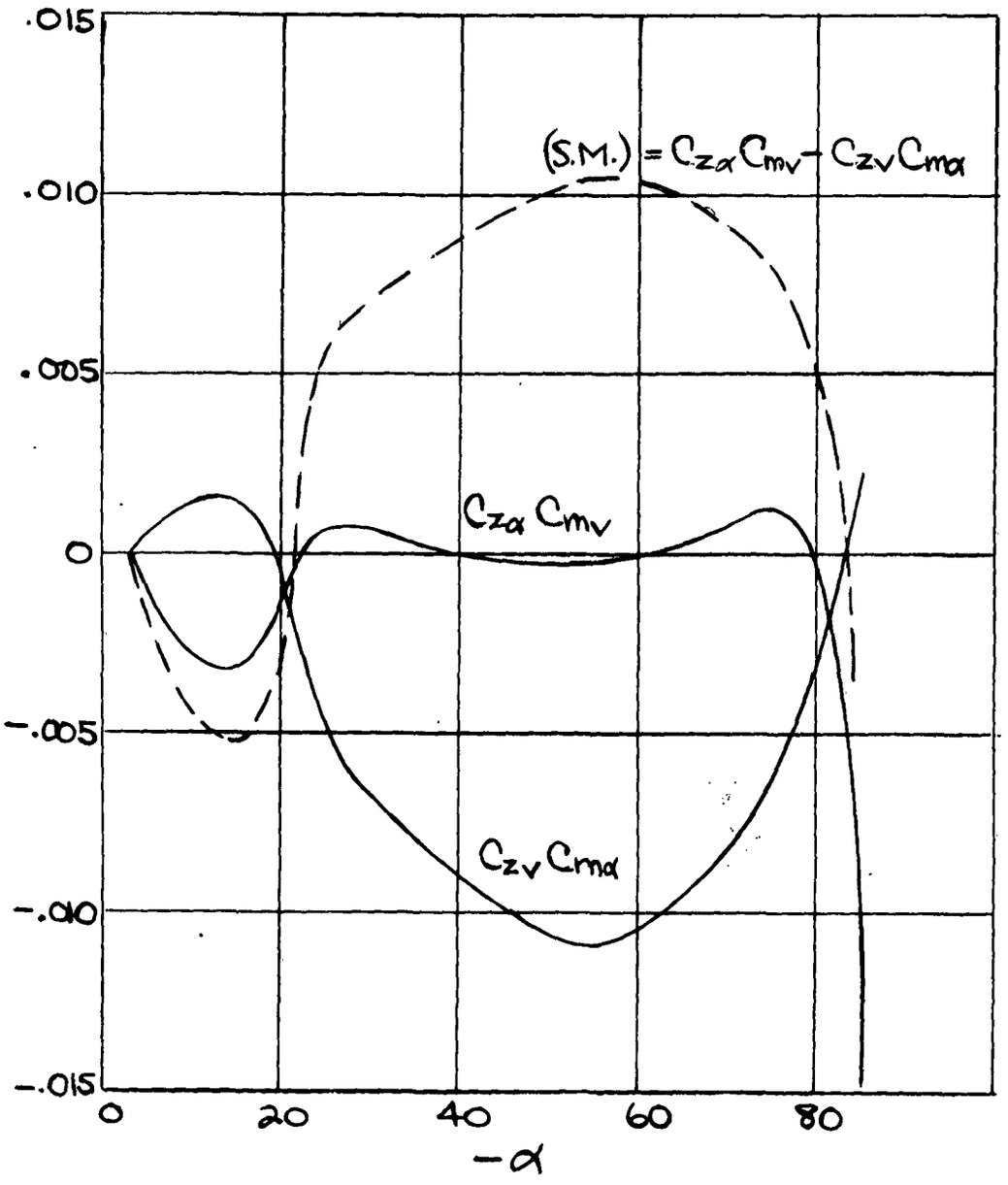
.015
.010
.005
0
-.005
-.010
-.015
0
20
40
60
80
-α
(S.M.) = Cza Cmv - Czv Cmα
Cza Cmv
Czv Cmα

Figure 24

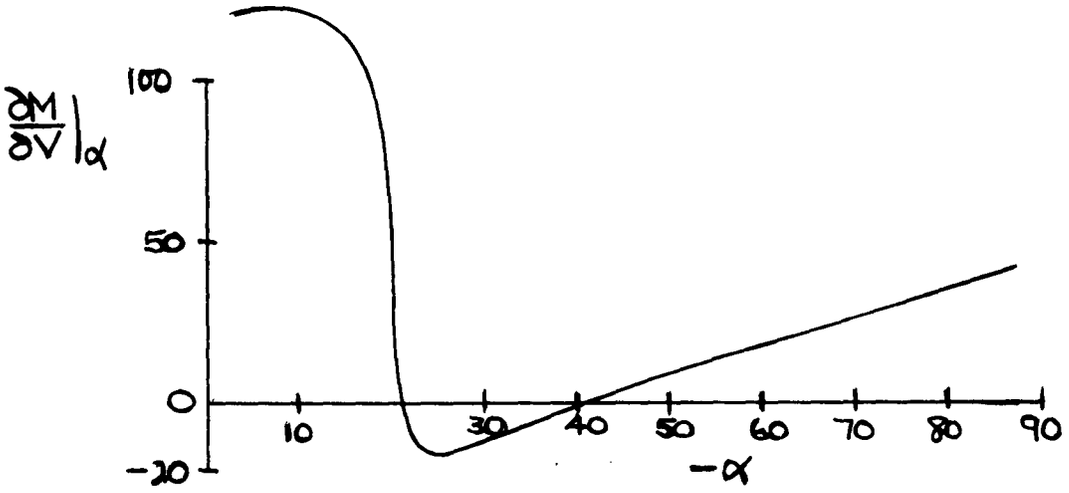
$\frac{\partial M}{\partial V}|_\alpha$
100
50
0
-20
10
30
40
50
60
70
80
90
$-\alpha$

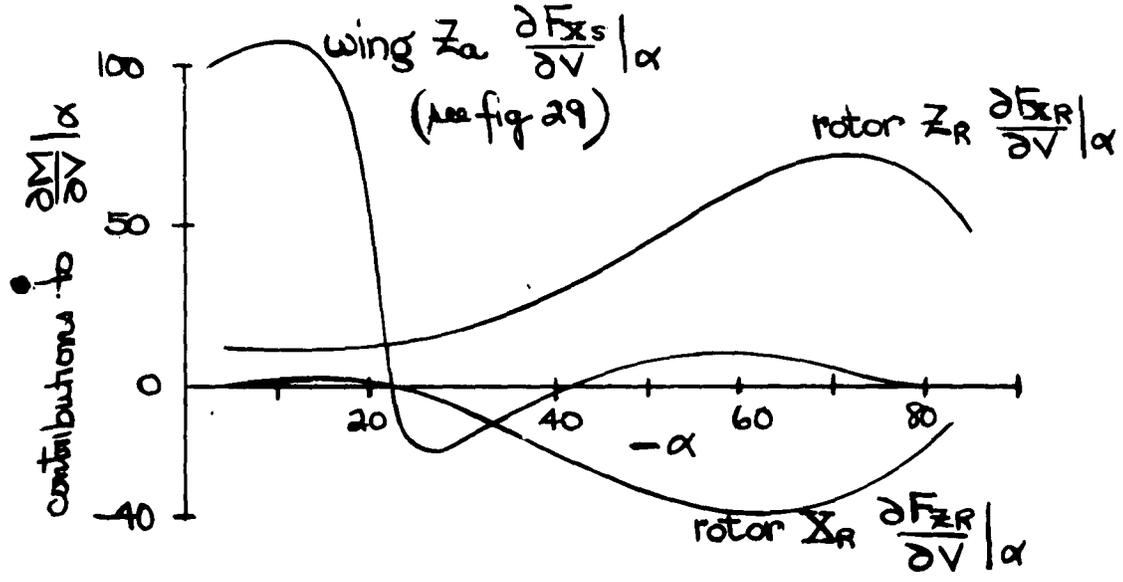
wing Z_a $\frac{\partial F_{xs}}{\partial V}|_\alpha$
(see fig 29)
rotor Z_R $\frac{\partial F_{xR}}{\partial V}|_\alpha$
$\frac{\partial M}{\partial V}|_\alpha$
contributions to
100
50
0
-40
20
40
60
80
$-\alpha$
rotor X_R $\frac{\partial F_{zR}}{\partial V}|_\alpha$

Figure 25

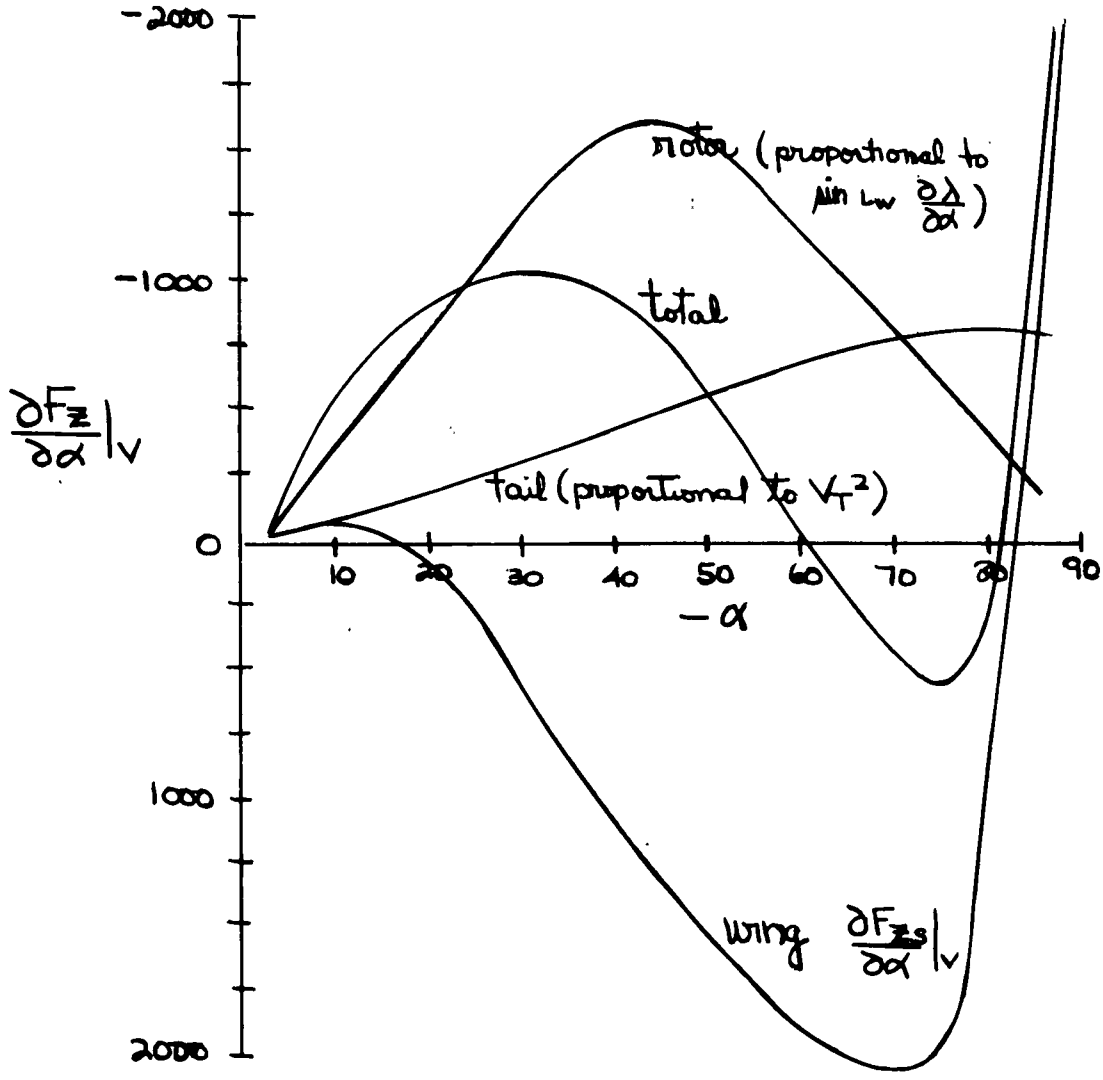
-2000
-1000
1000
2000
0
10
20
30
40
50
60
70
80
90
$-\alpha$
$\frac{\partial F_z}{\partial \alpha}\Big|_V$
rotor (proportional to $\frac{\partial \Delta}{\partial \alpha}$)
total
tail (proportional to V_T^2)
wing $\frac{\partial F_{z_3}}{\partial \alpha}\Big|_V$

Figure 26

$$\frac{\partial C_{Zs}}{\partial V}\Big|_\alpha \cong C_{Ls}\,\frac{\partial \phi}{\partial V}\Big|_\alpha \sin\phi + \frac{\partial C_{Ls}}{\partial \alpha'}\,\frac{\partial \phi}{\partial V}\Big|_\alpha \cos\phi$$

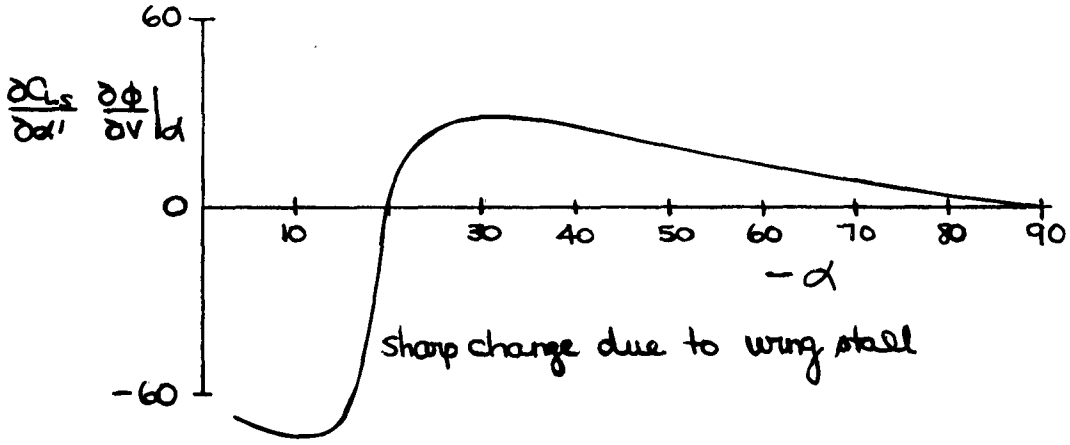

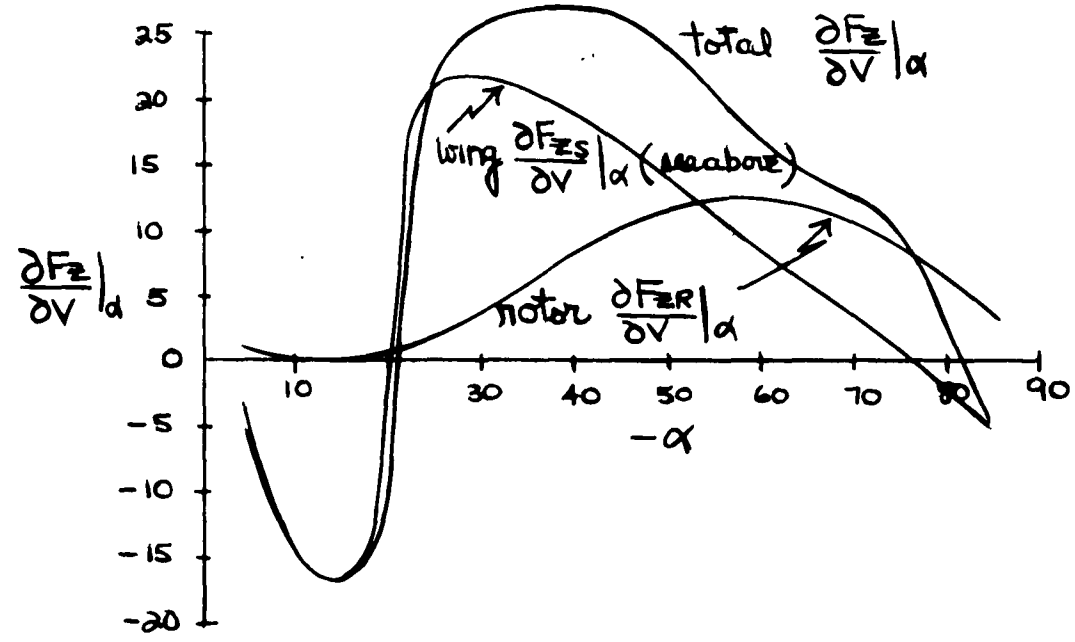

Figure 27

$$\frac{\partial C_{xs}}{\partial \alpha}\Big|_v = -\frac{2}{V_R}\frac{\partial V_R}{\partial \alpha}\Big|_v (C_{Ls}\sin\phi + C_{Ds}\cos\phi)$$
$$-(1-\frac{\partial \phi}{\partial \alpha}\Big|_v)\left[(\frac{\partial C_{Ls}}{\partial \alpha}\Big|_v + C_{Ds})\sin\phi + (\frac{\partial C_{Ds}}{\partial \alpha}+C_{Ls})\cos\phi\right]$$

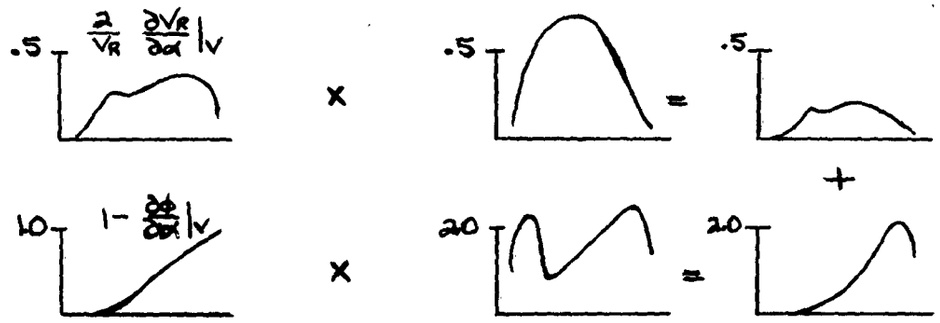

$$= -\frac{\partial C_{xs}}{\partial \alpha}\Big|_v$$

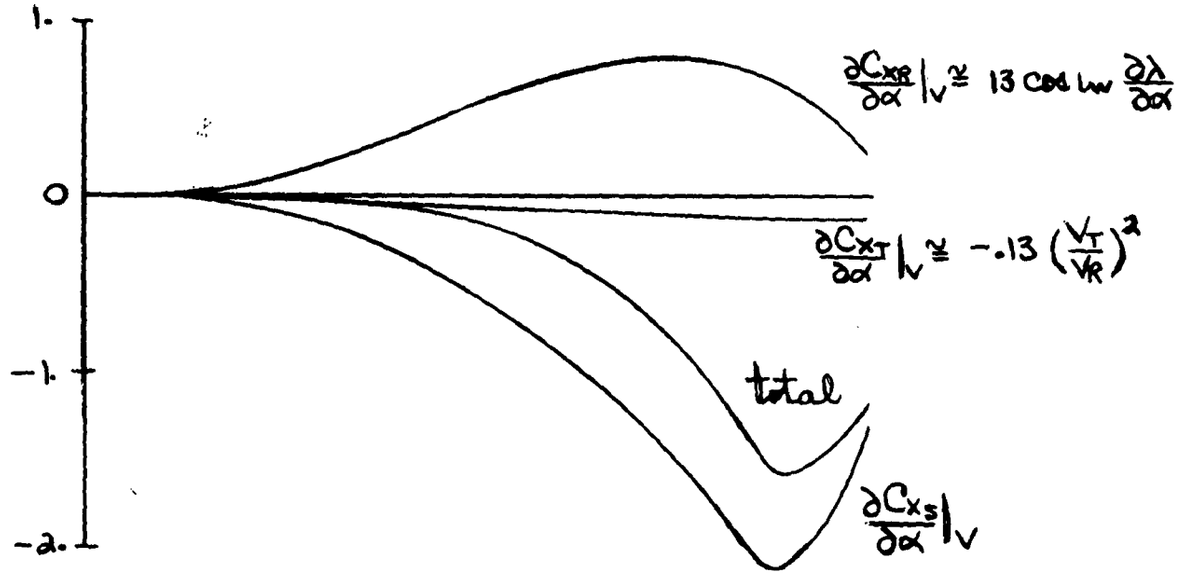

Figure 28

$$\frac{\partial C_{xs}}{\partial V}\Big|_\alpha = -\left(C_{Ls}\sin\phi + C_{Ds}\cos\phi\right)\frac{2}{V_R}\frac{\partial V_R}{\partial V}\Big|_\alpha + \left[\left(\frac{\partial C_{Ls}}{\partial \alpha'} + C_{Ds}\right)\sin\phi + \left(\frac{\partial C_{Ds}}{\partial \alpha'} - C_{Ls}\right)\cos\phi\right]\frac{\partial \phi}{\partial V}\Big|_\alpha$$

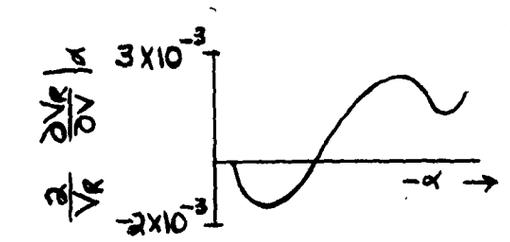

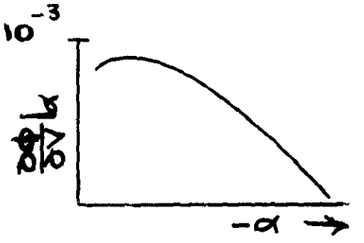

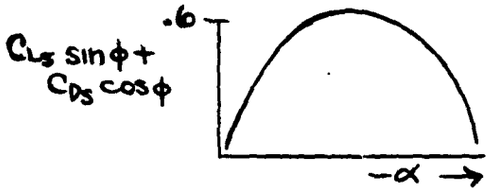

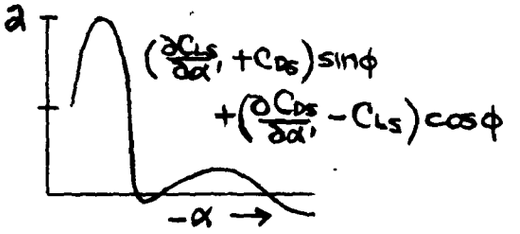

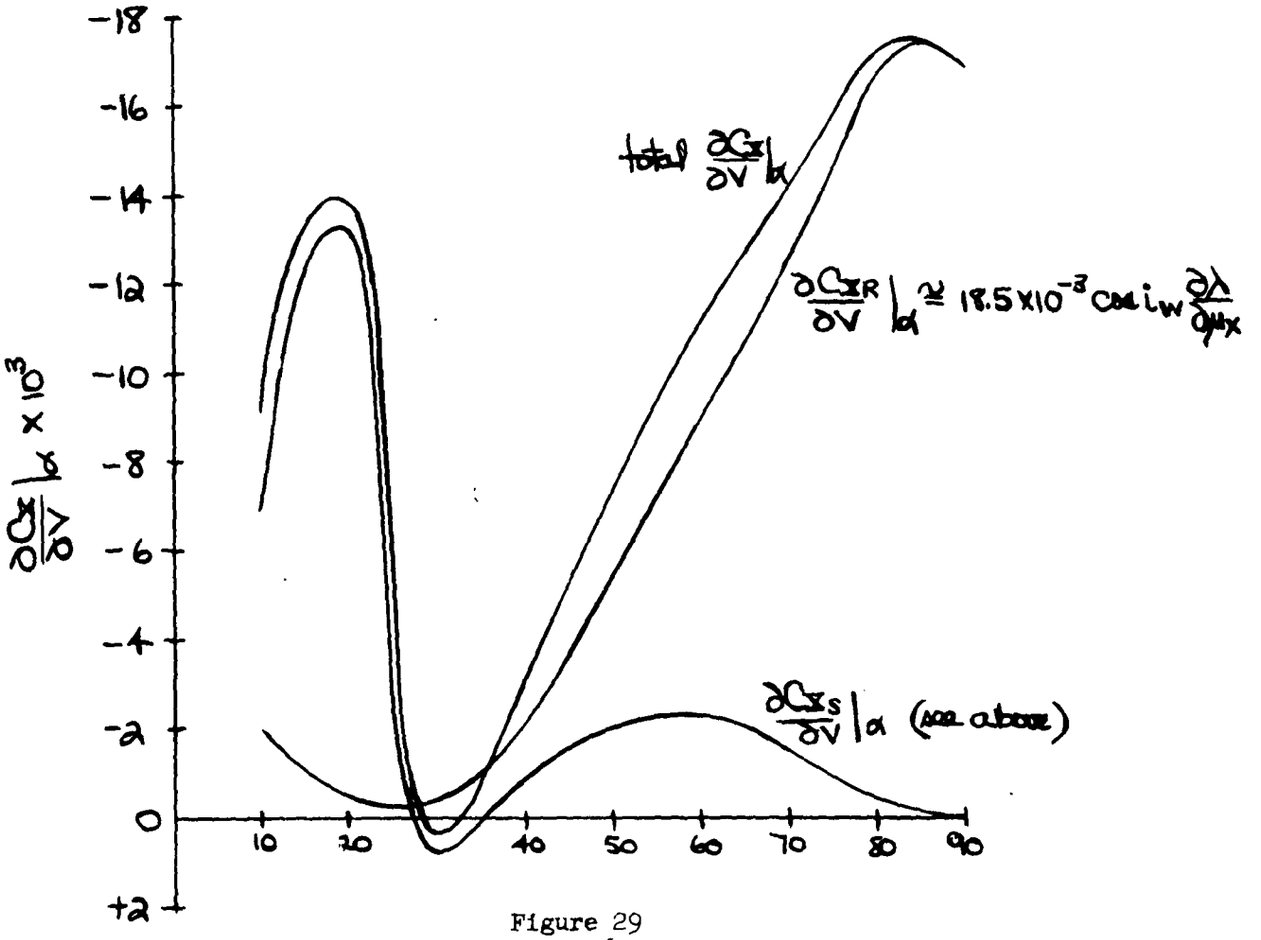

Figure 29

APPENDICES

A. Inflow Ratio and Induced Velocity Derivatives

In this section we will give expressions for the derivatives of λ, the inflow ratio, and v, the induced velocity, with respect to α, μ_x, and C_T. These expressions are also plotted in the form of charts in Figures 30 through 37. The H-force coefficient derivatives which were derived earlier are plotted in Figure 38.

The inflow ratio in the slipstream is determined as follows:

$$\lambda_s = \mu_x \sin\alpha - \lambda\, v/\Omega R$$
$$= \lambda' \lambda + (1-\lambda')\mu_x \sin\alpha \qquad \text{A-1}$$

Thus,

$$\bar{\lambda}_s = \frac{\lambda_s}{\lambda_0} = \lambda' \frac{\lambda}{\lambda_0} + (1-\lambda') \frac{\mu_x}{\lambda_0} \sin\alpha \qquad \text{A-2}$$

This expression is plotted in Figure 30.

The λ derivatives were given in Reference 12. The expressions for these derivatives will be summarized here and are plotted in Figures 33-37.

Using equation (5) and noting that (See Figure 1),

$$V_R^2 = \lambda^2 + \mu_x^2 \cos^2\alpha \qquad \text{A-3}$$

(where V_R here is the resultant velocity at the rotor plane and not at the wing center of pressure), we easily obtain the following expression for λ :

$$\lambda = \mu_x \sin\alpha - \frac{C_T}{2\sqrt{\lambda^2 + \mu_x^2 \cos^2\alpha}} \qquad \text{A-4}$$

Since this equation is of fourth degree in λ it is desirable to plot it in such a manner that λ can be determined if μ_x, α and C_T are known. Dividing the equation by $\lambda_0 = -\sqrt{C_T/2}$ gives,

$$\bar{\lambda} = \bar{\mu}_x \sin\alpha - \frac{1}{\sqrt{\bar{\lambda}^2 + \bar{\mu}_x^2 \cos^2\alpha}} \qquad \text{A-5}$$

where $\bar{\lambda} = \lambda/\lambda_0$, $\bar{\mu}_x = \mu_x/\lambda_0$ & $\lambda_0 = -\sqrt{C_T/2}$

This expression is plotted in Figure 37.

From the definition of λ we obtain,

$$-\frac{\nu}{\lambda_0 \Omega R} = \bar{\lambda} - \bar{\mu}_x \sin\alpha \qquad \text{A-6}$$

This is plotted in Figure 33.

Using the definition of λ the following expressions can easily be obtained for the λ derivatives:

$$\lambda_0 \frac{\partial\lambda}{\partial C_T} = \frac{1/2\left[\bar{\lambda}^2 + \bar{\mu}_x^2 \cos 2\alpha\right]}{\bar{\lambda} + \left(\bar{\lambda}^2 + \bar{\mu}_x^2\right)^{3/2}} \qquad \text{A-7}$$

$$\frac{1}{\mu_x \cos\alpha} \frac{\partial\lambda}{\partial\alpha} = \frac{\left(\bar{\lambda}^2 + \bar{\mu}_x^2 \cos 2\alpha\right)^{3/2} + \bar{\mu}_x \sin\alpha}{\left(\bar{\lambda}^2 + \bar{\mu}_x^2 \cos^2\alpha\right)^{3/2} + \bar{\lambda}} \qquad \text{A-8}$$

$$\frac{\partial\lambda}{\partial\mu_x} = \frac{\sin\alpha\left(\bar{\lambda}^2 + \bar{\mu}_x^2 \cos^2\alpha\right)^{3/2} + \bar{\mu}_x \cos 2\alpha}{\left(\bar{\lambda}^2 + \bar{\mu}_x^2 \cos^2\alpha\right)^{3/2} + \bar{\lambda}} \qquad \text{A-9}$$

Using the charts for these derivatives the induced velocity derivatives can easily be formed from the following expressions:

$$\frac{1}{\Omega R}\frac{\partial v}{\partial \mu_x} = \mu \sin\alpha - \frac{\partial \lambda}{\partial \mu_x} \qquad \text{A-10}$$

$$\frac{1}{\Omega R}\frac{1}{\lambda_0}\frac{\partial v}{\partial \alpha} = \bar{\mu}_x \cos\alpha \left[1 - \left(\frac{1}{\bar{\mu}_x \cos\alpha}\frac{\partial \lambda}{\partial \alpha}\right)\right] \qquad \text{A-11}$$

These are plotted in Figures 31 and 32. The derivative $\frac{\partial v}{\partial C_T}$ differs from $\frac{\partial \lambda}{\partial C_T}$ by only a constant and can thus be found from the chart for $\frac{\partial \lambda}{\partial C_T}$ (Figure 34).

B. Values of physical parameters for Vertol 76 (Full scale; model scale factor: 5.2)

N = 2

l_p = .572 ft.

X_g = .075 ft.

l_a = 2.593 ft.

Z_g = 1.17 ft.

r = 0.3025 ft.

a = 0.238 ft.

M_s = 1.08 slug

ρ = .002374 $\frac{\text{slug}}{\text{ft}^3}$

ΩR = 702 ft/sec

C_w = 4.75 ft.

α = 5.73

σ = 0.218

S_s = 90.4 ft^2 (wing area in slipstream)

S_W = 24.3 ft^2 (wing area outside slipstream)

$\pi AR e$ = 9.88

K_T = 4.29×10^5

$C_{D_{OF}}$ = 1

$C_{M_{ac}}$ = - 0.1

a_w = 4.5

$K_{M_{CF}}$ = 1.6×10^3

R = 4.75 ft.

S_T = 20 ft^2 (area of horizontal tail)

S_F = 20 ft^2 (fuselage equivalent flat plate area)

W = 3160 lbs.

δ = 0.0087

ℓ_T = 12.5 ft.

h_T = 5.4 ft.

C_T = 3 ft. (tail chord)

i_T = 2°

I_{y} = 1872 (average over all i_w values)

$I_{y\ max}$ = 1885

$I_{y\ min}$ = 1858

γ (main rotor) = 3.28

γ (tail rotor) = 2.0

m_{TR} mass of tail rotor blade = .005 slug

Ω (tail rotor) = 406 rad/sec

R_T = 1.0 ft. (radius of tail rotor)

C_{RT} = .25 ft. (tail rotor chord)

m_R mass main rotor blade = 0.455 slug

a_T = 3.7 (tail lift curve slope)

a_{RT} = 5 (tail rotor blade lift curve slope)

C. Determination of Value for K from Experimental Data

A tilt-wing VTOL aircraft will not hover with the rotor exactly vertical since the lift force on the wing due to the slipstream produces a force acting in the negative X-direction. Thus for hovering the wing must be tilted forward by an amount such that the component of the wing lift in the X-direction. Since the wing lift is a function of the arbitrary parameter K, K can be determined if it is known at what wing tilt angle the full scale aircraft or a model of it will hover.

When the aircraft is hovering, the wing drag is parallel to the thrust and the lift is perpendicular to it. Thus we have,

$$T \sin \alpha_o = L \cos \alpha_o + D \sin \alpha_o \qquad \text{C-1}$$

where $\alpha_o = 90 - i_{wo}$ is the hovering rotor angle of attack.

Expressing T, L, and D in terms of coefficients

$$\rho N \pi R^2 (\Omega R)^2 C_T \sin \alpha_o =$$

$$= \frac{1}{2} \rho S V_R^2 C_{LS} \cos \alpha_o + \frac{1}{2} \rho V_R^2 S C_{DS} \sin \alpha_o \qquad \text{C-2}$$

C_{LS} is given by,

$$C_{LS} = C_{LSo} (1 - K) \qquad \text{C-3}$$

Substituting this into the above expression and solving for K we obtain

$$K = 1 - \frac{1}{C_{L_{OS}}} \left[2N \frac{\pi R^2}{S} \frac{(\Omega R)^2}{(V_R)^2} C_T - C_{D_S} \right] \tan(90 - \xi_0) \qquad C\text{-}4$$

Using values from appendix B and D gives,

$$K = 1 - 3.57 \tan(90 - \xi_0) \qquad C\text{-}5$$

The model of the Vertol 76 tested at the Princeton University Forward Flight Facility was found to hover at $\xi_0 = 87^\circ$ or $\alpha_0 = 3^\circ$. Thus,

$$K = 1 - 3.57 (.052) = .814$$

Figure 30

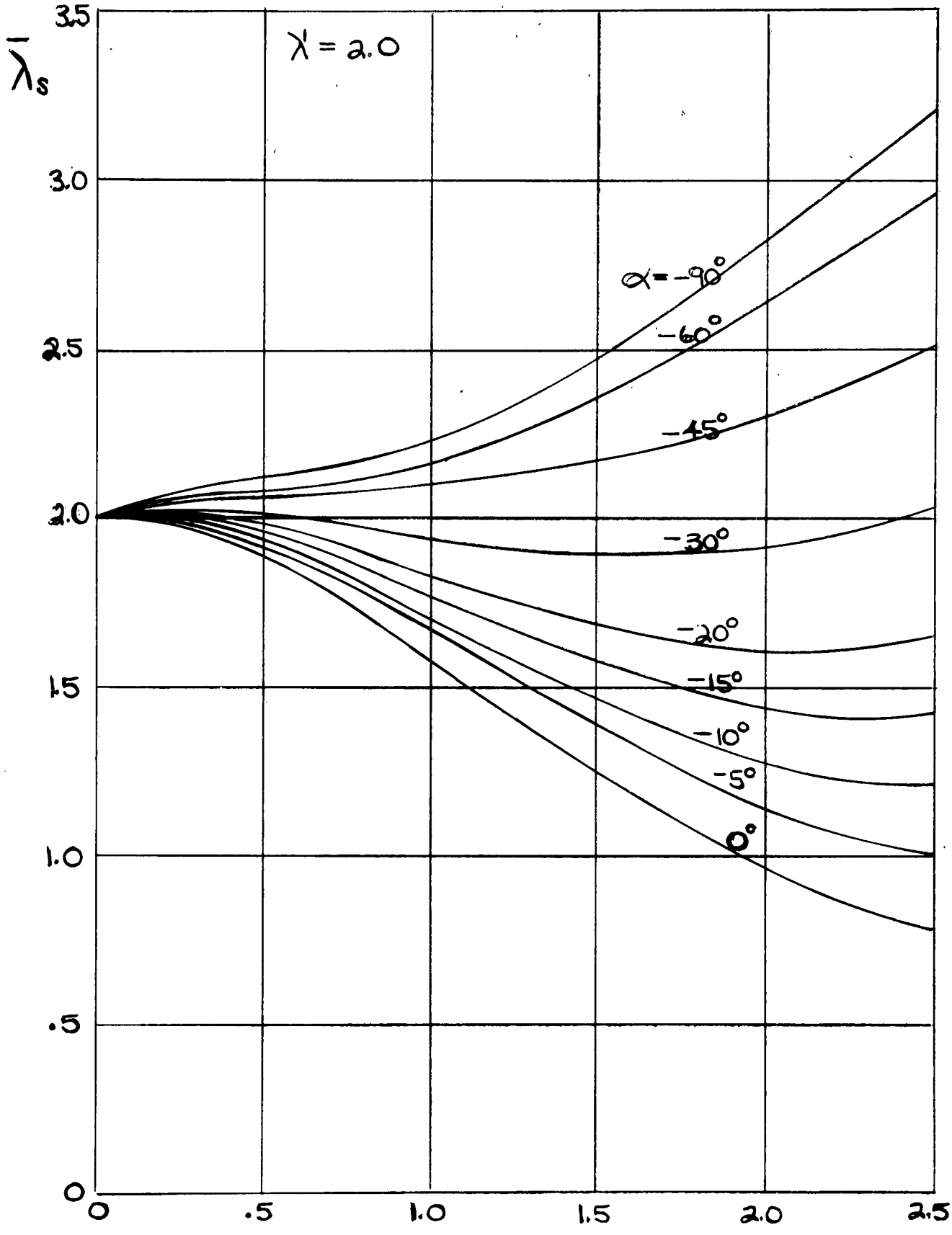
$\bar{\lambda}_s$
$\lambda' = 2.0$
3.5
3.0
2.5
2.0
1.5
1.0
.5
0
$\alpha = -90°$
$-60°$
$-45°$
$-30°$
$-20°$
$-15°$
$-10°$
$-5°$
$0°$
0
.5
1.0
1.5
2.0
2.5
$\bar{\mu}_x = -\frac{\mu x}{\lambda_0}$

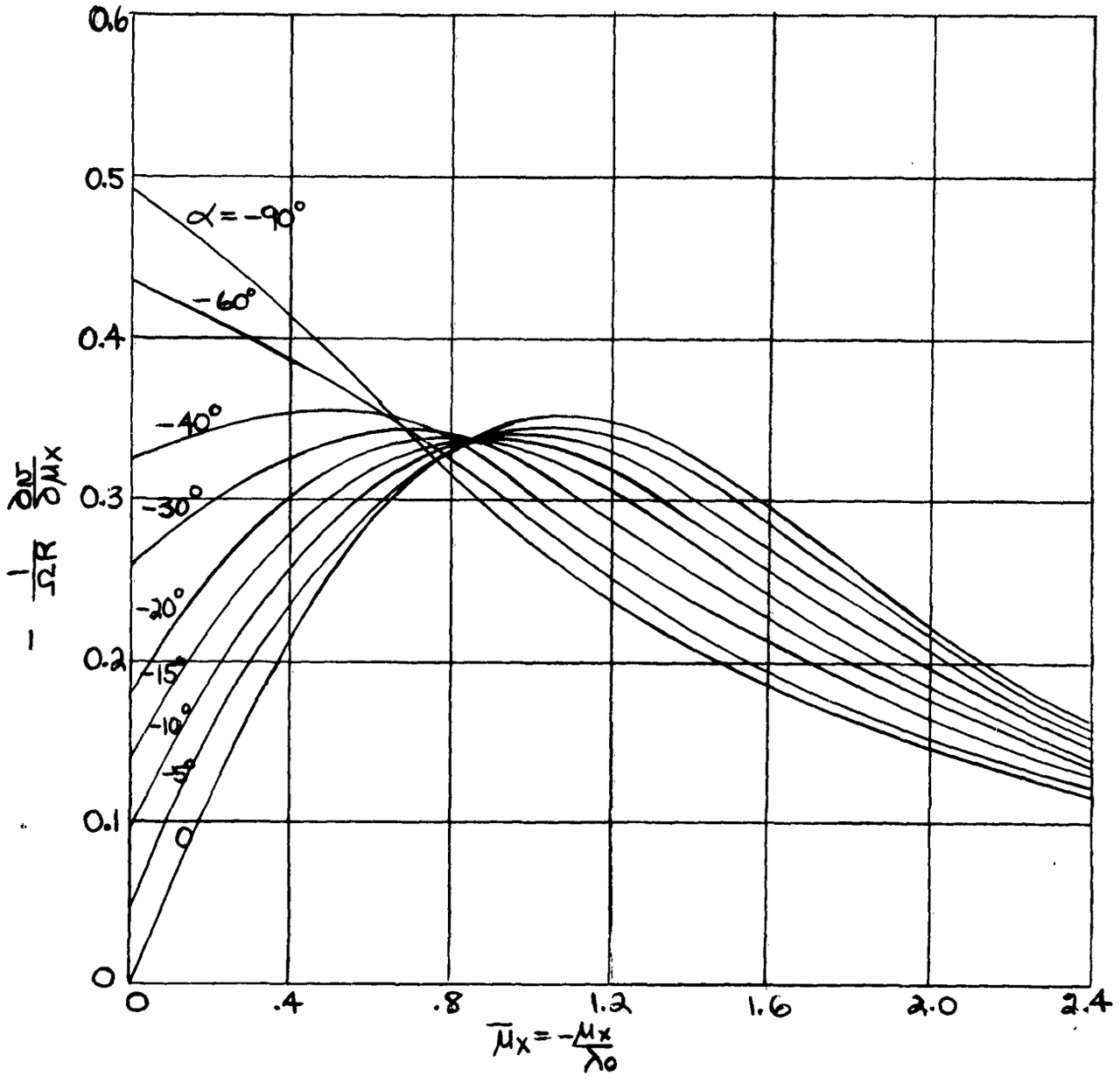
0.6
0.5
0.4
0.3
0.2
0.1
0
α = -90°
-60°
-40°
-30°
-20°
-15°
-10°
-5°
0
0
.4
.8
1.2
1.6
2.0
2.4
$\frac{1}{\Omega R}\frac{\partial \Gamma}{\partial \mu_x}$
$\bar{\mu}_x = -\frac{\mu_x}{\lambda_0}$

Figure 31

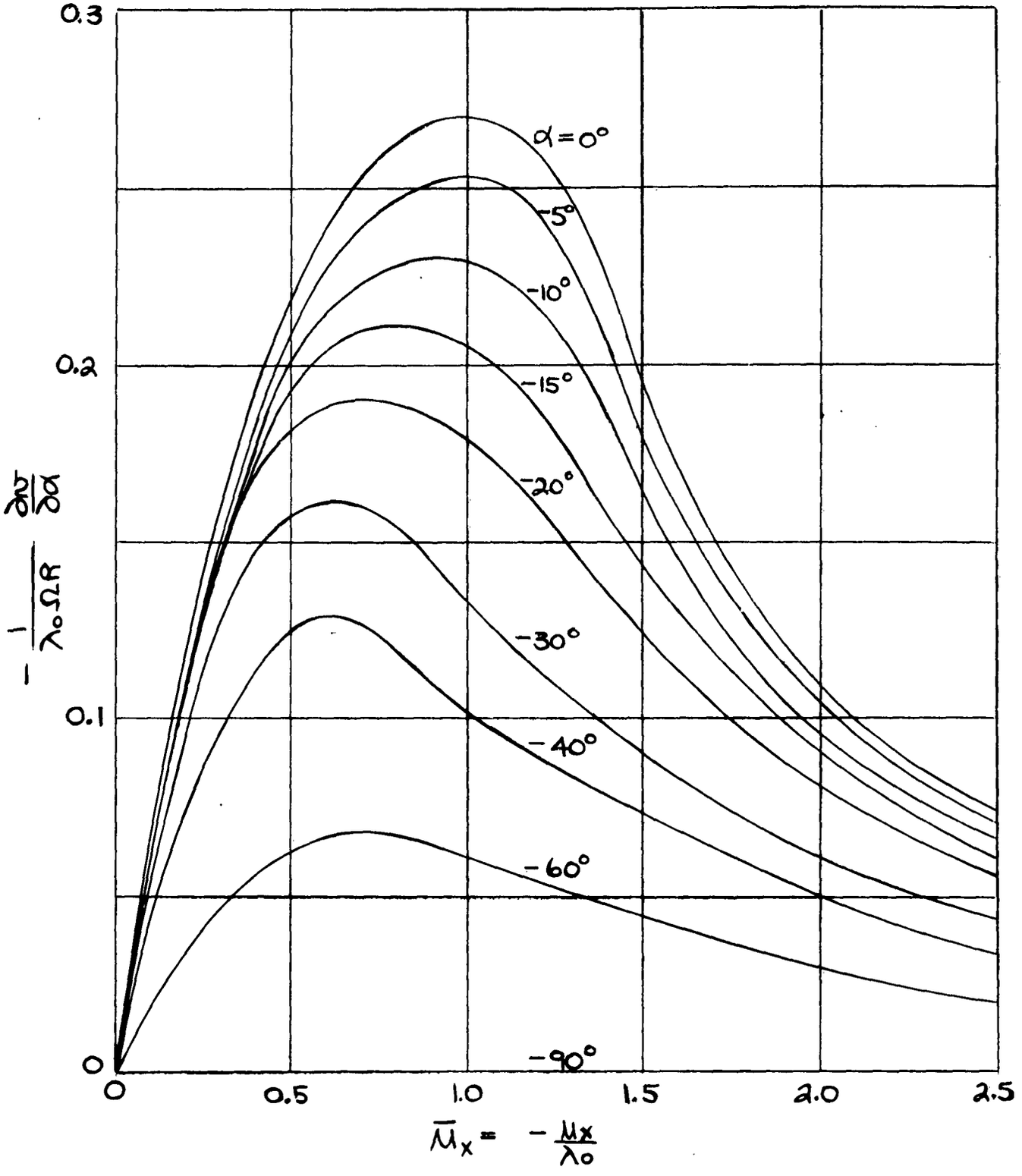
0.3
0.2
0.1
0
0
0.5
1.0
1.5
2.0
2.5
$-\frac{1}{\lambda_0 \Omega R}\frac{\partial v}{\partial \alpha}$
$\bar{\mu}_x = -\frac{\mu x}{\lambda_0}$
$\alpha = 0°$
$-5°$
$-10°$
$-15°$
$-20°$
$-30°$
$-40°$
$-60°$
$-90°$

Figure 32

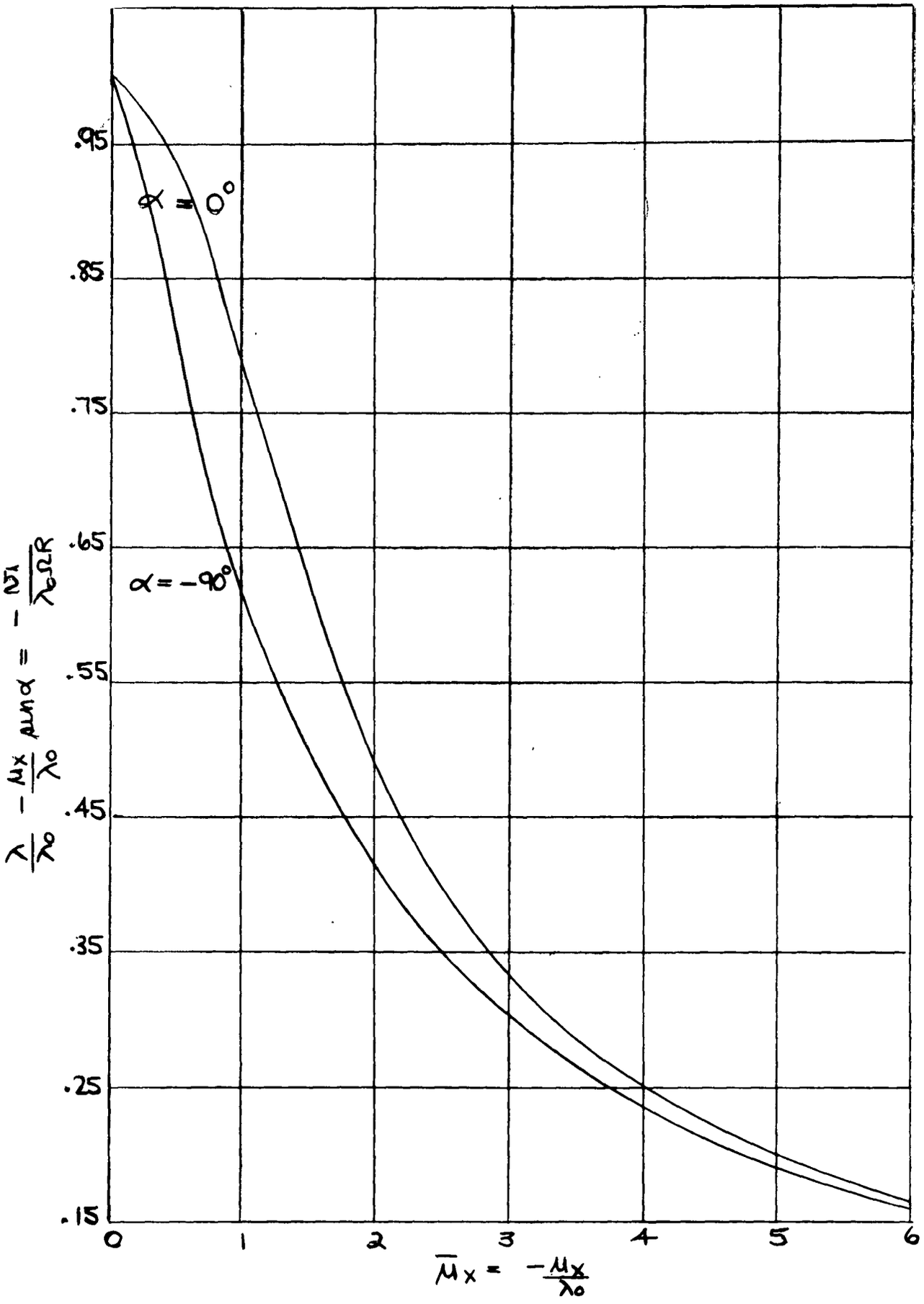
$\frac{\lambda}{\lambda_0} - \frac{\mu_x}{\lambda_0} \sin\alpha = -\frac{\dot{\Omega i}}{\lambda_0 \Omega R}$
$\alpha = 0°$
$\alpha = -90°$
.95
.85
.75
.65
.55
.45
.35
.25
.15
0
1
2
3
4
5
6
$\bar{\mu}_x = -\frac{\mu_x}{\lambda_0}$

Figure 33

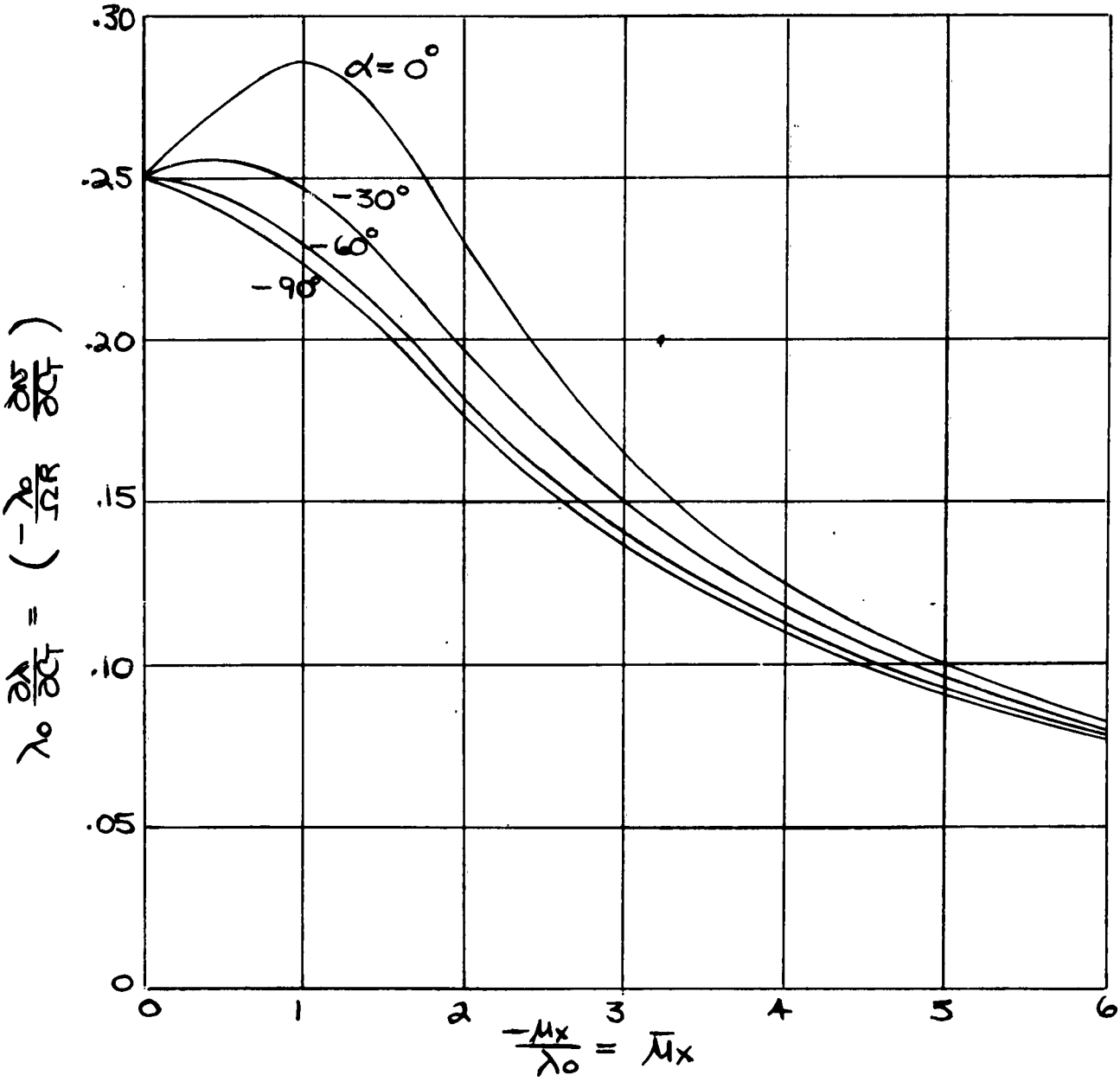
.30
.25
.20
.15
.10
.05
0
0
1
2
3
4
5
6
α = 0°
-30°
-60°
-90°
$\lambda_0 \frac{\partial \bar{\nu}}{\partial C_T} = \left(-\frac{\lambda_0}{\Omega R}\frac{\partial \nu}{\partial C_T}\right)$
$\frac{-\mu_x}{\lambda_0} = \bar{\mu}_x$

Figure 34

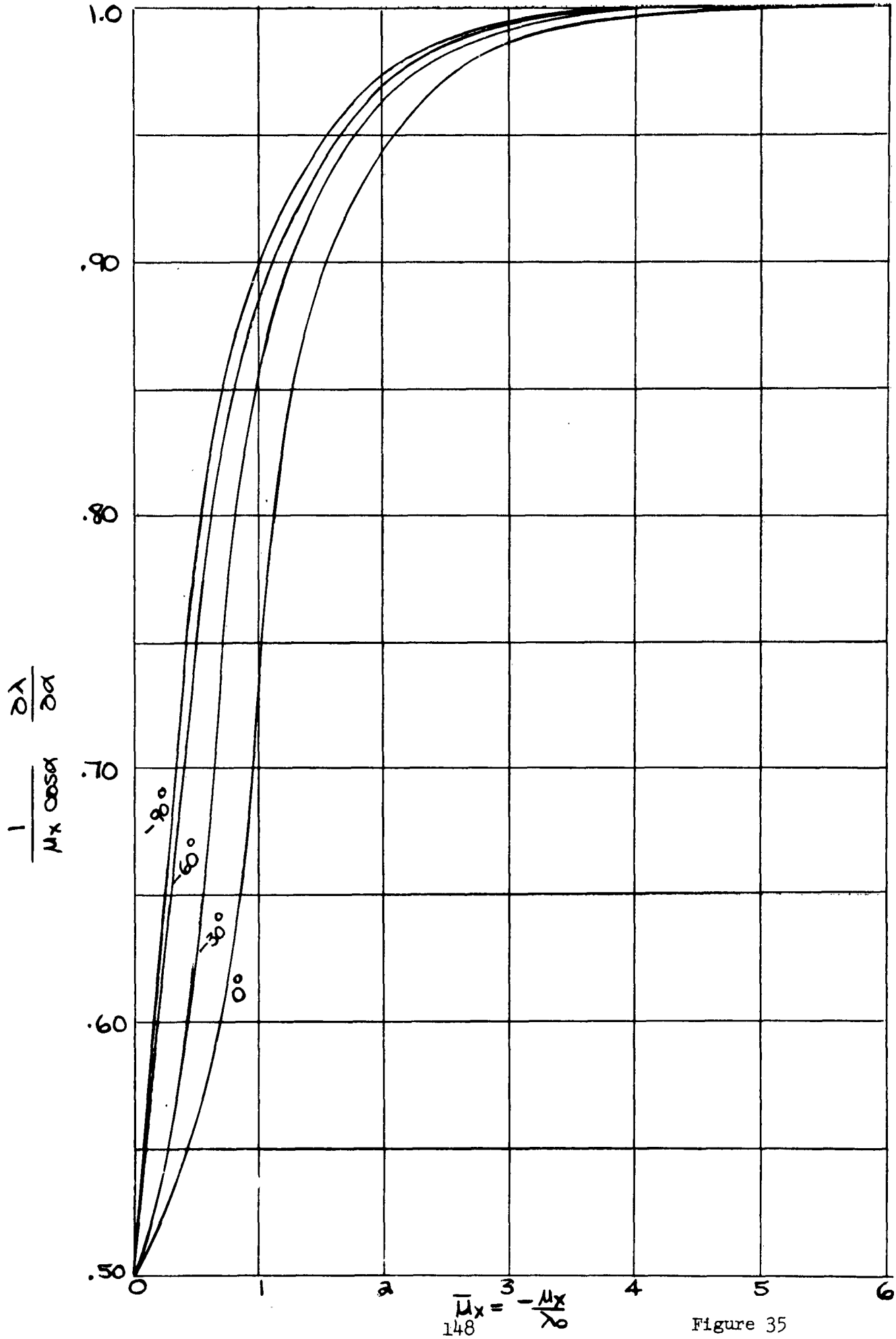
1.0
.90
.80
.70
.60
.50
0
1
2
3
4
5
6
-90°
-60°
-30°
0°
$\frac{1}{\mu_x \cos\alpha} \frac{\partial\lambda}{\partial\alpha}$
$\bar{\mu}_x = -\frac{\mu_x}{\lambda_0}$

Figure 35

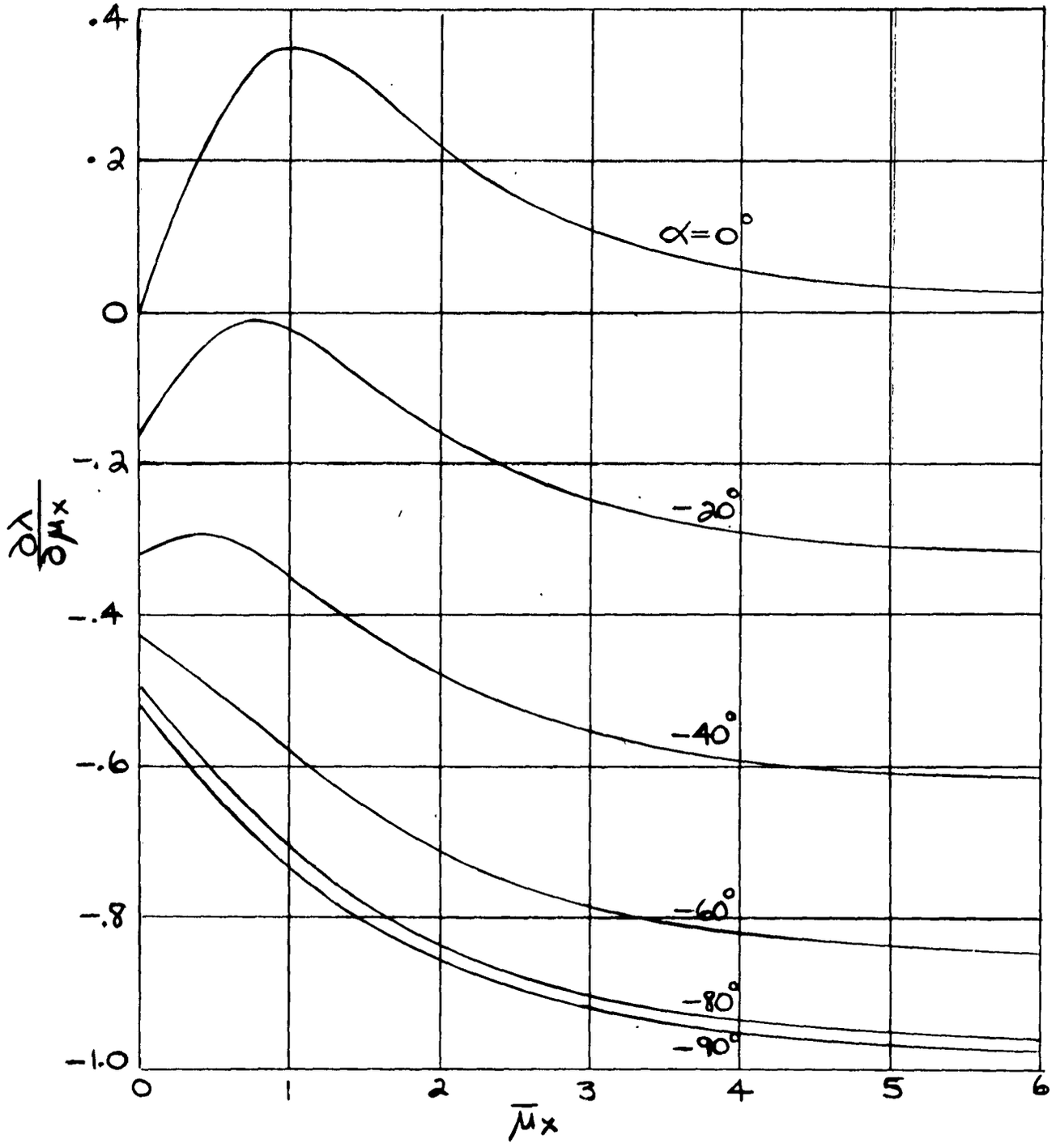
.4
.2
0
-.2
-.4
-.6
-.8
-1.0
$\frac{\partial C_l}{\partial \mu_x}$
$\alpha = 0°$
-20°
-40°
-60°
-80°
-90°
0
1
2
3
4
5
6
$\bar{\mu}_x$

Figure 36

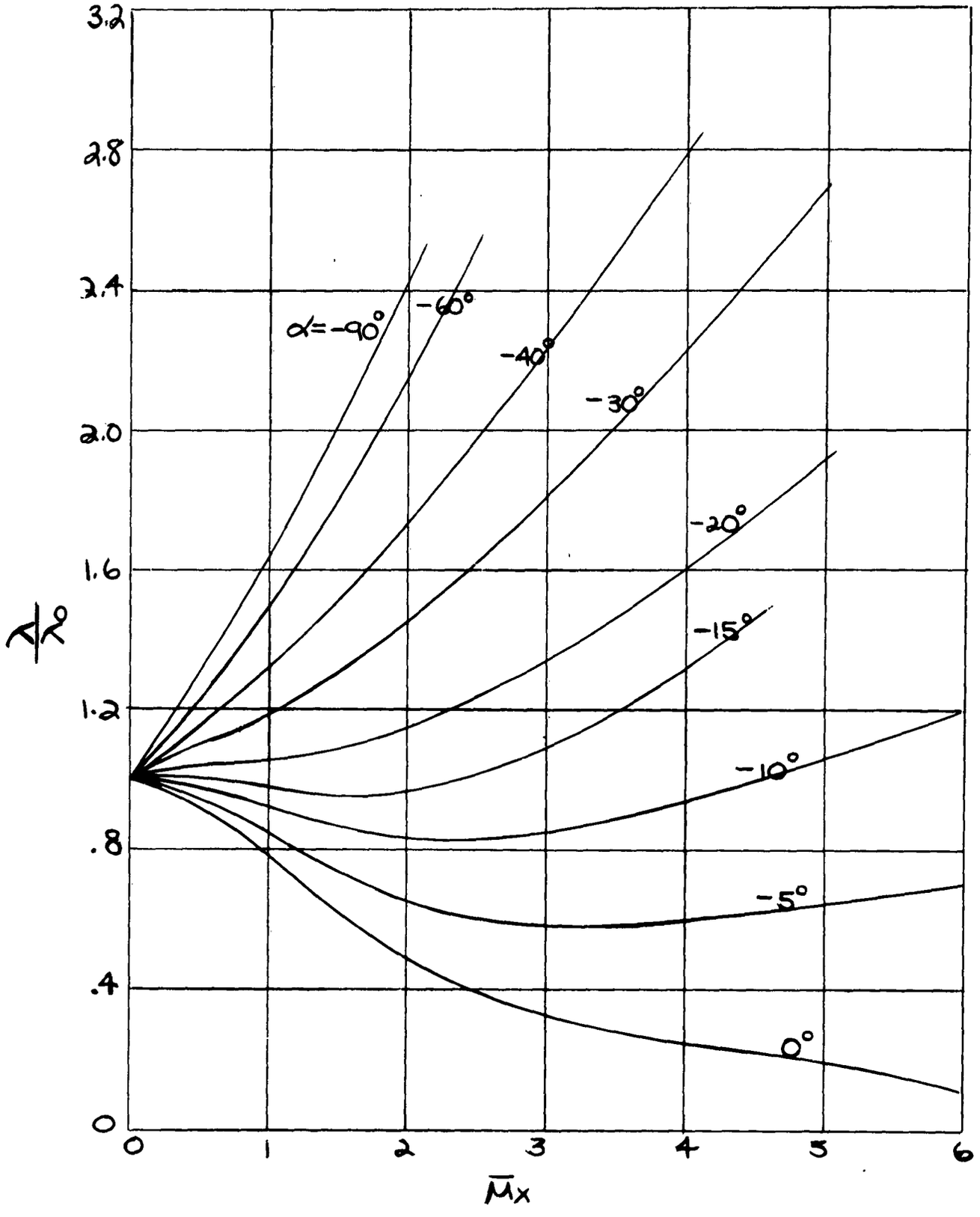
3.2
2.8
2.4
2.0
1.6
1.2
.8
.4
0
0
1
2
3
4
5
6
$\frac{T}{T_0}$
$\bar{M}_x$
$\alpha = -90°$
-60°
-40°
-30°
-20°
-15°
-10°
-5°
0°

Figure 37

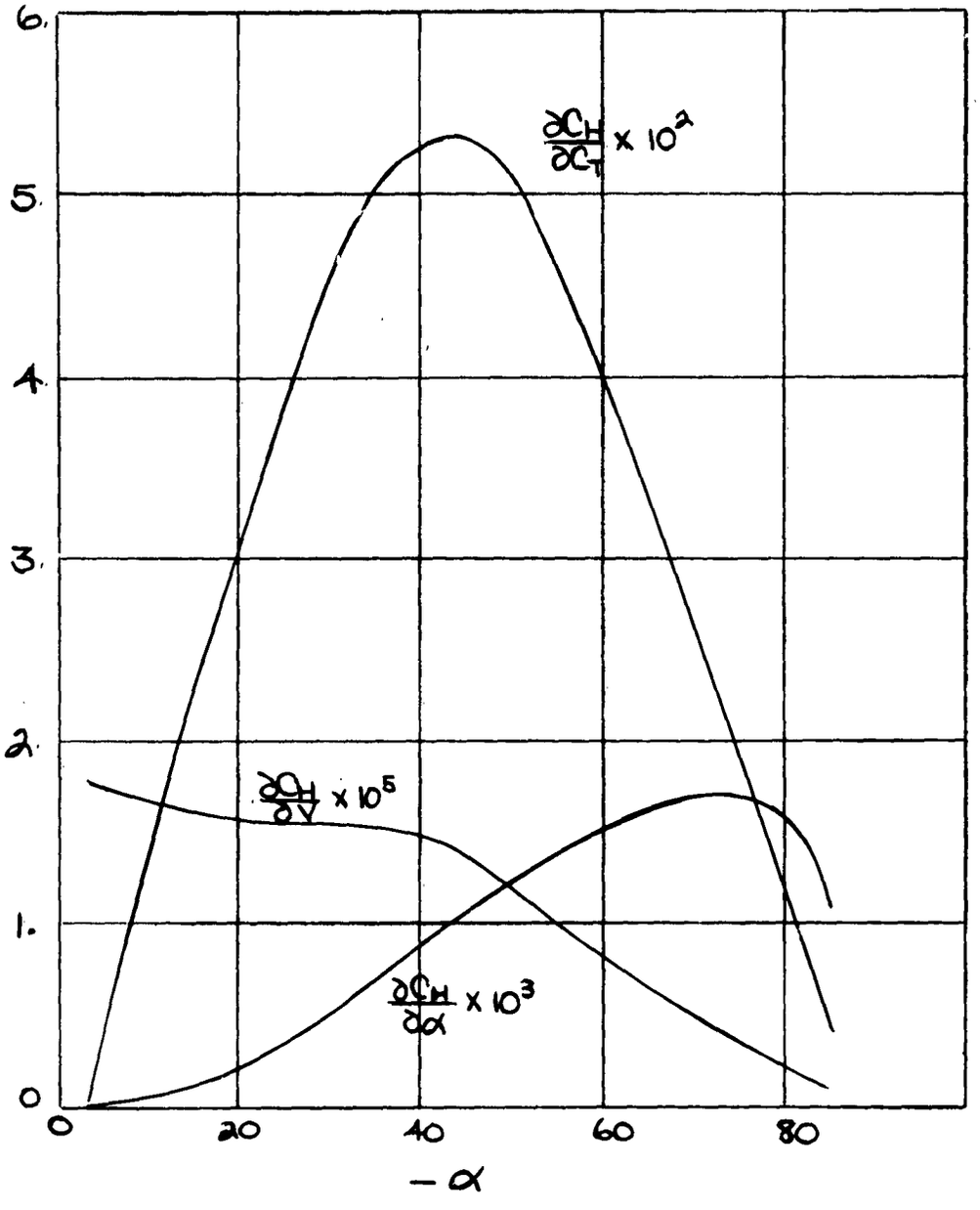
6.
5.
4.
3.
2.
1.
0
0
20
40
60
80
$-\alpha$
$\frac{\partial C_H}{\partial C_T} \times 10^2$
$\frac{\partial C_H}{\partial V} \times 10^5$
$\frac{\partial C_H}{\partial \alpha} \times 10^3$

Figure 38

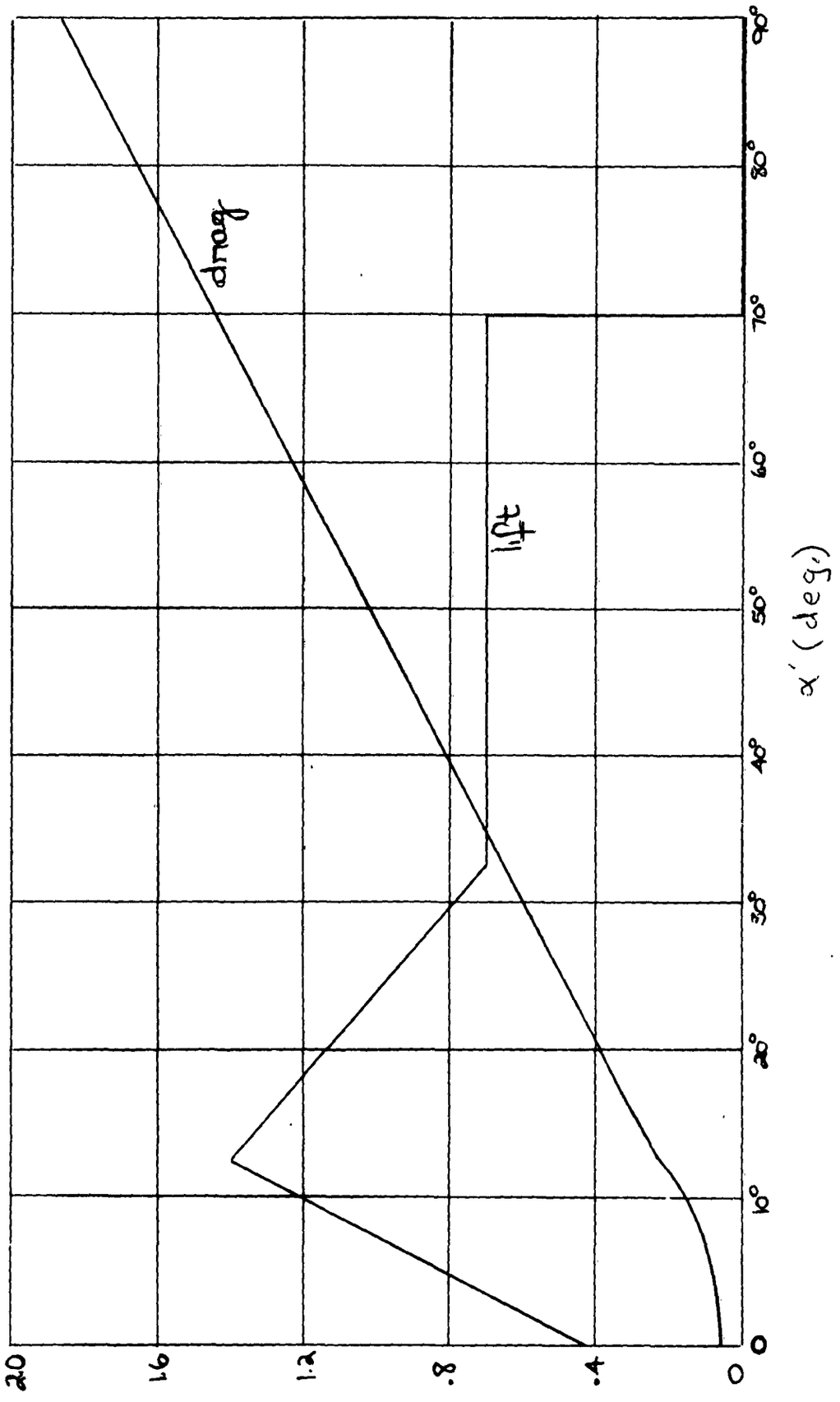

Figure 39

Appendix D

VALUES OF PARAMETERS

1	2	3	4	5	6	7	8	9	10
i_w	α	Φ	α'	V	V_R	μ_x	$-\lambda$	$-\lambda_s$	$-\lambda_o$
87	-3	87	0	0	139.0	0	.0988	.1976	.0988
75	-15	65	10	26.3	136.7	.0374	.0972	.1847	.0962
65	-25	48	17	46.8	140.0	.0665	.1043	.1804	.0965
55	-35	33	22	67.5	146.0	.0960	.1200	.1850	.0961
45	-45	22	23	84.7	151.5	.1203	.1372	.1892	.0928
35	-55	12.5	22.5	100.5	148.3	.1430	.1550	.1927	.0819
25	-65	6	19	116.5	152.3	.1660	.1760	.2018	.0718
15	-75	1.0	13	133.5	142.5	.1900	.1895	.1971	.0630
5	-85	.23	4.77	148.3	155.0	.2110	.2150	.2199	.0195

Appendix D

VALUES OF PARAMETERS

11	12	13	14	15	16	17	18	19	20
$\frac{2}{V_R}\frac{\partial V_R}{\partial \mu_x}$	$\frac{2}{V_R}\frac{\partial V_R}{\partial \alpha}$	$\frac{2}{V_R}\frac{\partial V_R}{\partial C_T}$	$\frac{\partial \phi}{\partial \mu_x}$	$1-\frac{\partial \phi}{\partial \alpha}$	$\frac{\partial \phi}{\partial C_T}$	$\frac{\partial \lambda}{\partial \mu_x}$	$\frac{\partial \lambda}{\partial \alpha}$	$\frac{\partial \lambda}{\partial C_T}$	$\frac{\partial C_H}{\partial V}$
0	0	51.3	-4.96	0	0	-.025	0	-2.54	.17813 x 10 - 4
-1.13	-.0497	54.2	-5.15	.02	5.08	-.020	.0206	-2.70	.16250 x 10 - 4
0	-.0968	50.6	-4.57	.13	8.08	-.100	.0420	-2.64	.15749 x 10 - 4
2.40	-.2960	45.5	-3.75	.34	8.95	-.275	.0674	-2.60	.15359 x 10 - 4
4.31	-.2880	42.0	-2.58	.48	7.99	-.450	.0790	-2.42	.13601 x 10 - 4
6.11	-.2320	39.4	-1.71	.65	7.10	-.630	.0784	-2.44	.99266 x 10 - 5
6.90	-.1103	36.8	- .975	.77	4.88	-.765	.0690	-2.30	.66779 x 10 - 5
7.89	-.0750	42.4	- .475	.85	3.18	-.875	.0490	-2.22	.37137 x 10 - 5
9.00	-.0071	41.7	0	.96	1.74	-.995	.0184	-2.30	.68468 x 10 - 6

Appendix D
VALUES OF PARAMETERS

21	22	23	24	25	26	27	28	29	30
$\frac{\partial C_H}{\partial \alpha}$	$\frac{\partial C_H}{\partial C_T}$	$C_{L_{SO}}$	$C_{D_{SO}}$	$\frac{\partial C_{LS}}{\partial \alpha}$	$\frac{\partial C_{DS}}{\partial \alpha}$	$\sin i_w$	$\cos i_w$	$\sin \alpha$	$\cos \alpha$
0	0	.42	.06	0	0	.999	.052	-.052	.999
.00011853	.022538	1.20	.16	.08	.025	.965	.259	-.259	.965
.00034184	.038079	1.24	.32	- .26	.162	.906	.423	-.423	.906
.00069486	.050647	1.06	.42	- .68	.426	.820	.574	-.574	.820
.0010988	.053142	1.02	.45	- .96	.60	.707	.707	-.707	.707
.0013550	.043660	1.05	.44	-1.30	.815	.574	.820	-.820	.574
.0015787	.032923	1.18	.36	-1.54	.965	.423	.906	-.906	.423
.0017387	.020514	1.38	.24	-1.70	1.06	.259	.965	-.965	.259
.0010990	.0044366	.80	.08	3.84	1.20	.087	.995	-.995	.087

Appendix D
VALUES OF PARAMETERS

31	32	33	34	35	36	37	38	39	40
$\sin\phi$	$\cos\phi$	M	C_T	$\frac{2C_T}{\sigma}$	$\frac{\Omega R}{V_R}$	$\frac{V}{V_R}$	$\frac{V}{V_R^2}$	$\left(\frac{\Omega R}{V_R}\right)^2$	$\left(\frac{V}{V_R}\right)^2$
.999	.052	0	.0195	.0303	5.05	0	0	25.5	0
.907	.423	.0361	.0185	.0287	5.14	.193	.0014	26.4	.0372
.743	.670	.0603	.0186	.0288	5.00	.334	.00238	25.0	.1120
.545	.840	.0787	.0185	.0287	4.81	.463	.00317	23.2	.2140
.374	.927	.0853	.0172	.0267	4.64	.560	.00368	21.6	.3140
.216	.977	.0820	.0134	.0208	4.73	.680	.00456	22.4	.4630
.105	.994	.0703	.0103	.0160	4.60	.765	.00500	21.2	.5850
.017	.999	.0493	.0079	.0122	4.93	.936	.00660	24.3	.8760
.004	1.000	.0184	.00076	.0012	4.53	.950	.00618	20.6	.9025

Appendix D

VALUES OF PARAMETERS

41	42	43	44	45	46	47	48	49	50
θ	a_1	X_a	Z_a	$C_{z\alpha}$	C_{zv}	C_{zc_T}	$C_{x\alpha}$	C_{xv}	C_{xc_T}
.240	0	-.00619	.3029	0	-.0030607	-78.0354	0	-.0016941	-17.52
.232	.01534	.03192	.3010	- .029204	-.003616	-80.05	-.0694	-.000382	- 5.058
.244	.026683	.06212	.2976	.18876	-.004798	-75.228	.1448	-.000593	- 4.029
.266	.037016	.08992	.2928	.57789	-.005244	-68.461	.2684	-.002454	+ 5.226
.285	.04138	.1144	.2864	.80131	-.0058224	-63.858	.1547	-.003907	13.949
.304	.04118	.1352	.2788	1.03179	-.007848	-64.967	.0030	-.004993	27.583
.312	.03378	.1510	.2703	1.1561	-.01002	-61.565	-.0871	-.004603	38.050
.322	.02366	.1619	.2610	1.2748	-.016617	-75.794	-.0953	-.003601	52.795
.327	.008134	.1674	.2512	-4.17866	-.009876	-37.881	-.4812	-.002430	57.267

Appendix D

VALUES OF PARAMETERS

51	52	53	54	55	56	57	58	59	60
$\frac{\partial C_z}{\partial \alpha}\Big\|_{\mu x}$	$\frac{\partial C_z}{\partial V}\Big\|_{\alpha}$	$\frac{2}{V_R}\frac{\partial V_R}{\partial \alpha}\Big\|_{\mu x}$	$\frac{2}{V_R}\frac{\partial V_R}{\partial V}\Big\|_{\alpha}$	$\frac{\partial \Phi}{\partial \alpha}\Big\|_{\mu x}$	$\frac{\partial \Phi}{\partial V}\Big\|_{\alpha}$	$C_{z\alpha}$	$\frac{\partial C_x}{\partial \alpha}\Big\|_{\mu x}$	$\frac{\partial C_x}{\partial V}\Big\|_{\alpha}$	$l \sin \beta$
0	-.00191	0	-.0003239	1.0	-.00706	-1.527	- .0002	-.00816	.104
- .3018	-.00888	.1428	-.0018759	.998	-.00736	-1.578	- .0223	-.01479	.223
- .496	+.01232	.27345	-.0012558	.929	-.0067	-1.505	- .0715	-.00081	.330
- .480	+.01349	.24204	.0002917	.7658	-.00596	-1.384	- .0809	-.00467	.447
- .378	.01236	.31310	.0012622	.6343	-.004603	-1.285	- .2226	-.00782	.572
- .1110	.01077	.32559	.00232	.4505	-.003586	-1.3413	- .5206	-.01199	.716
.237	.00743	.35993	.00240	.2924	-.002374	-1.27	-1.023	-.01365	.859
.518	.0042	.31553	.001305	.1793	-.00142	-1.4528	-1.648	-.01746	.996
-4.3077	-.0020	.13499	.001875	.04593	-.000457	-1.2279	-1.236	-.01698	1.12

Appendix D

VALUES OF PARAMETERS

61	62	63	64	65	66	67	68	69	70
V_T	$\frac{l}{c}$	η	t	$C_{M\ddot{\theta}}$	$C_{M\dot{\theta}}$	$C_{M\alpha}$	C_{Mv}	$C_{x\dot{\theta}}$	$C_{x\theta}$
5	.848	88°	7.7°	-.205	-.0819	- .00302	+.0119	.0101	-1.53
45	.846	78	25°	-.197	-.1102	- .1994	+.01165	.0164	-1.57
73	.846	70	27°	-.188	-.1733	- .4390	-.00138	.0207	-1.51
98	.842	61	27°	-.173	-.1863	- .5912	+.00043	.0209	-1.38
118	.854	54	23	-.161	-.1902	- .7907	+.00019	.0205	-1.29
129	.831	45	20	-.167	-.2021	-1.011	.00148	.0265	-1.35
142	.821	38	18	-.159	-.1986	-1.275	.00195	.0336	-1.28
141	.800	30	17	-.181	-.2095	-1.537	.00316	.0507	-1.46
155	.770	23	10	-.153	-.1829	-1.108	.00422	.0598	-1.23

Appendix D

VALUES OF PARAMETERS

71	72	73	74	75	76	77	78	79	80
$C_{x_{\dot{V}}}$	$C_{z_{\dot{\theta}}}$	$C_{z_{\dot{\alpha}}}$	$\frac{\partial \epsilon}{\partial \alpha}\Big\|_V$	$\frac{\partial C_H}{\partial V}\Big\|_\alpha$	$\frac{\partial C_H}{\partial \alpha}\Big\|_V$	$q_R S$	$\bar{c} q_R S$	ℓ	(MH)
-.051	.0039	0	.033	$.178 \times 10^{-4}$	0	2.07×10^3	$.985 \times 10^4$	4.03	
-.049	1.28	-1.28	.183	$.161 \times 10^{-4}$	.0002	2.00×10^3	$.95 \times 10^4$	4.02	.2885
-.047	2.18	-2.18	.206	$.148 \times 10^{-4}$	.00062	2.10×10^3	1.00×10^4	4.02	1.0431
-.043	2.91	-2.91	.164	$.119 \times 10^{-4}$	.00129	2.28×10^3	1.08×10^4	4.00	1.8098
-.040	3.37	-3.37	.123	$.0744 \times 10^{-4}$	.00186	2.45×10^3	1.16×10^4	4.06	2.7366
-.042	4.18	-4.18	.015	$.0285 \times 10^{-4}$	.001975	2.35×10^3	1.12×10^4	3.95	4.2474
-.043	4.58	-4.58	-.099	$.0004 \times 10^{-4}$	.0020	2.47×10^3	1.17×10^4	3.90	5.791
-.045	6.05	-6.05	-.190	$-.0109 \times 10^{-4}$	.001928	2.17×10^3	1.03×10^4	3.80	9.193
-.038	5.67	-5.67	.815	$-.0047 \times 10^{-4}$	.00111	2.57×10^3	1.22×10^4	3.66	7.070

Appendix D

VALUES OF PARAMETERS

81	82	83	84	85	86	87	88	89	90
(S.M.)	E	A	B	$\frac{\partial C_H}{\partial \theta}$	x_R	z_R	λ''	C_{L_S}	$\frac{\partial C_{M_{CF}}}{\partial \theta}$
		0	0	-.000123	.022	.846	-.8	.084	-.056
- .00529	-.00831	-.01235	-.01004	-.000150	.174	.825	-.646	.425	-.058
.00609	+.00920	-.01926	-.02116	-.000154	.294	.792	-.52	.595	-.055
.00819	+.01130	-.02165	-.026085	-.000062	.403	.739	-.430	.604	-.051
1.00970	-.01251	-.02170	-.02936	.000098	.500	.695	-.352	.661	-.0475
1.0107	.01449	-.02932	-.041297	.000285	.582	.590	-.256	.781	-.049
1.0099	.01271	-.03131	-.04553	.000500	.645	.500	-.188	.958	-.0466
1.0081	.01183	-.04928	-.06933	.000845	.689	.401	-.0512	1.31	-.0535
- .0204	-.02509	-.03297	-.07961	.001153	.710	.298	-.04	.77	-.045

Appendix D
VALUES OF PARAMETERS

91	92	93	94	95	96	97	98	99	100
$\frac{\partial C_{Zs}}{\partial \alpha}\Big\|_V$	$\frac{\partial C_{Zs}}{\partial V}\Big\|_\alpha$	$\frac{\partial C_{Xs}}{\partial \alpha}\Big\|_V$	$\frac{\partial C_{Xs}}{\partial V}\Big\|_\alpha$	$\frac{\partial C_{Z\delta}}{\partial \alpha}\Big\|_V$	$\frac{\partial C_{Z\delta}}{\partial V}\Big\|_\alpha$	$\frac{\partial C_{X\delta}}{\partial \alpha}\Big\|_V$	$\frac{\partial C_{X\delta}}{\partial V}\Big\|_\alpha$	$\frac{\partial C_{Zt}}{\partial \alpha}\Big\|_V$	$\frac{\partial C_{Zt}}{\partial V}\Big\|_\alpha$
0	-.000629	0	-.000367	0	.00041	0	-.00145	-.00123	-.000036
-.004290	-.00318	-.06533	.00106	-.2923	.00004	.0613	-.00139	-.0963	-.000263
-.06786	-.00393	-.224749	.00166	-.5398	.00127	.1983	-.00188	-.2445	-.000353
-.073027	-.00385	-.3379	.00167	-.7589	.00361	.4162	-.00358	-.4051	-.000370
-.201303	-.002069	-.49336	.00183	-.7748	.00521	.5966	-.00592	-.5509	-.000369
-.361055	-.003692	-.6665	.00101	-.6873	.00638	.7392	-.00977	-.6884	-.000379
-.511224	-.003280	-.8652	.00107	-.4810	.00568	.7157	-.01218	-.8003	-.000333
-.595581	-.002076	-.8336	.00151	-.3238	.00471	.6393	-.10724	-.8962	-.000226
-.179985	-.001490	-.0849	.00019	-.0908	.00151	.2125	-.01690	-.8978	-.000164

Appendix D

VALUES OF PARAMETERS

101	102	103	104	105	106	107	108	109	110
$\frac{\partial C_{MCF}}{\partial \alpha}\Big\|_V$	$\frac{\partial C_{MCF}}{\partial V}\Big\|_\alpha$	$\frac{\partial C_{LS}}{\partial V}\Big\|_{\alpha,CT}$	$\frac{\partial C_{DS}}{\partial V}\Big\|_{\alpha,CT}$	$\frac{\partial C_{LS}}{\partial C_T}$	$\frac{\partial C_{DS}}{\partial C_T}$	$\frac{\partial C_{LS}}{\partial \alpha'}\Big\|_0$	$\frac{\partial C_{DS}}{\partial \alpha'}$	$\frac{\partial C_T}{\partial \alpha}\Big\|_V$	OR $\frac{\partial C_T}{\partial V}\Big\|_\alpha$
0	.001076	.0317	0	0	0	4.5	0	0	-.00443
.008681	.001028	.0330	.0092	-22.9	- 6.35	4.5	1.25	.00355	-.00345
.025404	.000934	-.0130	.0081	16.16	-10.1	-2	1.25	.00732	-.01742
.049200	.000806	-.0107	.0067	17.9	-11.2	-2	1.25	.01182	-.04824
.070866	.000619	-.0074	.0046	16.0	-10.0	-2	1.25	.01431	-.08152
.098988	.000487	-.0049	.0030	14.2	- 8.9	-2	1.25	.01415	-.11372
.110603	.000292	-.0028	.0017	9.76	- 6.1	-2	1.25	.01278	-.14167
.147992	.000164	-.0014	.0008	6.36	- 4.0	-2	1.25	.00921	-.16447
.128905	.000072	0	0	- 7.83	- 1.0	4.5	.58	.00341	-.18426

Appendix D

VALUES OF PARAMETERS

l_{11}	l_{12}	l_{13}	l_{14}
C	D	$\frac{\partial C_{Lo}}{\partial \alpha'}\Big\|_0 (1-\lambda'')$	$\frac{\partial C_{Ls}}{\partial \alpha}$
		.9	0
-.01420	-.02475	1.59	.003
-.04921	.00394	- .96	- .078
-.07895	-.00179	-1.14	- .267
-.11300	-.0149	-1.30	- .475
-.18638	-.04524	-1.49	- .820
-.26018	-.0784	-1.64	-1.16
-.4339	-.1669	-1.90	-1.56
-.2868	-.1596	+4.3	4.1

ALART PROGRAM
Technical Report
Distribution List

	ADDRESS	NO. OF COPIES
1.	Chief of Transportation Department of the Army Washington 25, D.C. ATTN: TCACR	2
2.	Commander Wright Air Development Division Wright-Patterson Air Force Base, Ohio ATTN: WCLJA	2
3.	Commanding Officer U.S. Army Transportation Research Command Fort Eustis, Virginia ATTN: Research Reference Center ATTN: Aviation Directorate	 4 3
4.	U.S. Army Representative HQ AFSC (SCR-LA) Andrews Air Force Base Washington 25, D.C.	1
5.	Director Air University Library ATTN: AUL-8680 Maxwell Air Force Base, Alabama	1
6.	Commanding Officer David Taylor Model Basin Aerodynamics Laboratory Washington 7, D.C.	1
7.	Chief Bureau of Naval Weapons Department of the Navy Washington 25, D.C. ATTN: Airframe Design Division ATTN: Aircraft Division ATTN: Research Division	 1 1 1
8.	Chief of Naval Research Code 461 Washington 25, D.C. ATTN: ALO	1

	ADDRESS	NO. OF COPIES
9.	Director of Defense Research & Development Room 3E - 1065, The Pentagon Washington 25, D.C. ATTN: Technical Library	1
10.	U.S. Army Standardization Group, U.K. Box 65, U.S. Navy 100 FPO New York, New York	1
11.	National Aeronautics & Space Administration 1520 H Street, N.W. Washington 25, D.C. ATTN: Bertram A. Mulcahy Director of Technical Information	5
12.	Librarian Langley Research Center National Aeronautics & Space Administration Langley Field, Virginia	1
13.	Ames Research Center National Aeronautics & Space Agency Moffett Field, California ATTN: Library	1
14.	Armed Services Technical Information Agency Arlington Hall Station Arlington 12, Virginia	10
15.	Office of Chief of Research & Development Department of the Army Washington 25, D.C. ATTN: Mobility Division	1
16.	Senior Standardization Representative U.S. Army Standardization Group, Canada c/o Director of Weapons & Development Army Headquarters Ottawa, Canada	1
17.	Canadian Liaison Officer U.S. Army Transportation School Fort Eustis, Virginia	3

	ADDRESS	NO. OF COPIES
18.	British Joint Services Mission (Army Staff) DAQMG (Mov & Tn) 1800 "K" Street, N.W. Washington 6, D.C. ATTN: Lt. Col. R.J. Wade, R.E.	3
19.	Office of Technical Services Acquisition Section Department of Commerce Washington 25, D.C.	2
20.	Librarian Institute of the Aeronautical Sciences 2 East 64th Street New York 21, New York	2
21.	U.S. Army Research & Development Liaison Group APO 79 New York, New York ATTN: Mr. Robert R. Piper	1

AD_____Accession No._____UNCLASSIFIED

Princeton University Aero. Eng. Dept., Princeton, N.J.

1. VTOL stability (longitudinal)

AN ANALYTICAL STUDY OF THE LONGITUDINAL DYNAMICS OF A TILT-WING VTOL

2. Contract No. DA44-177-TC-524

Charles R. Hargraves

Report No. 561, June 1961
169 pp. - illus.

Contract No. DA44-177-TC-524
Project No. 9-38-01-000, TK902
Unclassified Report

AD_____Accession No._____UNCLASSIFIED

Princeton University Aero. Eng. Dept., Princeton, N.J.

1. VTOL stability (longitudinal)

AN ANALYTICAL STUDY OF THE LONGITUDINAL DYNAMICS OF A TILT-WING VTOL

2. Contract No. DA44-177-TC-524

Charles R. Hargraves

Report No. 561, June 1961
169 pp. - illus.

Contract No. DA44-177-TC-524
Project No. 9-38-01-000, TK902
Unclassified Report

AD_____Accession No._____UNCLASSIFIED

Princeton University Aero. Eng. Dept., Princeton, N.J.

1. VTOL stability (longitudinal)

AN ANALYTICAL STUDY OF THE LONGITUDINAL DYNAMICS OF A TILT-WING VTOL

2. Contract No. DA44-177-TC-524

Charles R. Hargraves

Report No. 561, June 1961
169 pp. - Illus.

Contract No. DA44-177-TC-524
Project No. 9-38-01-000, TK902
Unclassified Report

An analysis of the stability characteristics of a tilt-wing VTOL aircraft is made. General equations for aircraft are derived and charts are given which enable one to quickly estimate the required stability derivatives.

Numerical calculations for a typical tilt-wing VTOL transition are made and an extensive discussion of the effect of important derivatives and parameters on stability characteristics is given.

An analysis of the stability characteristics of a tilt-wing VTOL aircraft is made. General equations for aircraft are derived and charts are given which enable one to quickly estimate the required stability derivatives.

Numerical calculations for a typical tilt-wing VTOL transition are made and an extensive discussion of the effect of important derivatives and parameters on stability characteristics is given.

An analysis of the stability characteristics of a tilt-wing VTOL aircraft is made. General equations for aircraft are derived and charts are given which enable one to quickly estimate the required stability derivatives.

Numerical calculations for a typical tilt-wing VTOL transition are made and an extensive discussion of the effect of important derivatives and parameters on stability characteristics is given.

An analysis of the stability characteristics of a tilt-wing VTOL aircraft is made. General equations for aircraft are derived and charts are given which enable one to quickly estimate the required stability derivatives.

Numerical calculations for a typical tilt-wing VTOL transition are made and an extensive discussion of the effect of important derivatives and parameters on stability characteristics is given.